

**THE CHROMATIN REMODELER AND TUMOR SUPPRESSOR CHD5
PROMOTES EXPRESSION AND PROCESSING OF TRANSCRIPTS
DURING DEVELOPMENT OF THE ZEBRAFISH NEURAL SYSTEM**

by

Erin Sorlien

A Dissertation

Submitted to the Faculty of Purdue University

In Partial Fulfillment of the Requirements for the degree of

Doctor of Philosophy



Department of Biochemistry

West Lafayette, Indiana

May 2019

THE PURDUE UNIVERSITY GRADUATE SCHOOL
STATEMENT OF COMMITTEE APPROVAL

Dr. Joseph Ogas

Department of Biochemistry

Dr. Scott Briggs

Department of Biochemistry

Dr. Ann Kirchmaier

Department of Biochemistry

Dr. Emily Dykhuizen

Department of Medicinal Chemistry and Molecular Pharmacology

Approved by:

Dr. Andrew Mesecar

Head of the Graduate Program

This dissertation is dedicated to my parents and sisters, to my grandparents and family, to my friends and Nemo and Gracie:

Thank you for seeing me through this journey and for your unending support in taking on the next stages of my career.

ACKNOWLEDGMENTS

I sincerely thank my friends, colleagues and my teammates, without whom this journey would have been far less rewarding. To Rachel and Michael Graham, I cannot thank you enough for the laughs, the help, and the friendship throughout these years. To Shaina Riciputi and Erin Rhody, you have been both friends and teammates, and I sincerely look forward to our future adventures together! To the lovely friends who have made board game nights, dog parties, sports, meals, beer and our shows an incredibly fun addition to my time here! To all the members of the soccer community I have had the privilege to play with, and to my IM teams across sports, thank you all for the t-shirts and great memories.

I acknowledge the very helpful guidance of my thesis committee: Emily Dykhuizen, Ann Kirchmaier, Scott Briggs, and my adviser Joe Ogas. Thank you to each of you for the contributions you have made to this work, and to helping me grow into a thoughtful scientist. I would like to extend a special thank you to Emily, for sharing your lab space, and lab members expertise in training me in cell culture work- this has been a very rewarding collaboration for me. I also wish to thank the members of the Chromatin Club, past and present, for helping me develop my speaking skills and contributions to my projects over the years together.

To my lab mates, both past and present, your help and companionship in B017 will never be forgotten. To Brett Bishop, thank you for initiating the labs zebrafish work. To Ben Carter, your guidance and patient teaching is something I will be forever grateful for, and your continued friendship is as invaluable. I really couldn't thank you enough. To Mary Witucki, you were such a wonderful student to mentor, and friend to me throughout all the years of my Ph.D.- I sincerely look forward to watching your successes as you continue your career. To Ellen Denning and Taylor Sabato, you have contributed excellent work to these projects and you have my best wishes for the wonderful careers you will build. To Jiaxin and Kirsten, thank you for your companionship and help, and good luck going forward with the work in the Ogas lab!

Lastly, I would like to thank additional members of the Department: especially the guidance provided by Dr. Beth Tran, who has graciously led the founding of the Graduate Student Organization and been a thoughtful mentor to me in leading our Graduate/Postdoc Seminar. Also, to Dr. Fred Gimble, I am grateful for your guidance in developing my leadership skills and for many thoughtful conversations about my work. I would also like to acknowledge Dr. Clint Chapple, you have added so much fun and mentorship to my time at Purdue, and I am grateful incredibly grateful for your support.

TABLE OF CONTENTS

LIST OF TABLES	7
LIST OF FIGURES	8
LIST OF ABBREVIATIONS	10
ABSTRACT	12
CHAPTER 1. INTRODUCTION: CHD REMODELERS IN MULTICELLULAR EUKARYOTES: COMPARING AND CONTRASTING THE CONTRIBUTIONS OF CHD PROTEINS IN CHROMATIN-BASED PROCESSES.....	16
1.1 Abstract	16
1.2 Introduction	16
1.3 Phylogenetic analysis of CHD remodelers in plants and animals	18
1.4 CHD proteins are regulated, ATP-driven motors, that remodel nucleosomes	19
1.5 CHD proteins contribute to a diverse set of <i>in vivo</i> remodeling activities	22
1.6 Conclusions	29
CHAPTER 2. EFFICIENT PRODUCTION AND IDENTIFICATION OF CRISPR/CAS9-GENERATED GENE KNOCKOUTS IN THE MODEL SYSTEM DANIO RERIO	35
2.1 Introduction	35
2.2 Protocol	37
2.3 Representative Results	49
2.4 Discussion	54
CHAPTER 3. TRANSCRIPTOMICS REVEALS A ROLE FOR THE CHROMATIN REMODELER CHD5 IN NEUROGENESIS IN THE DEVELOPING ZEBRAFISH BRAIN	61
3.1 Introduction	61
3.2 Experimental Results	63
3.3 Discussion	74
CHAPTER 4. CHD5 PROMOTES SPLICING DURING BRAIN DEVELOPMENT IN ZEBRAFISH EMBRYOS	77
4.1 Introduction	77
4.2 Experimental Results	78
4.3 Discussion	91

CHAPTER 5. ESTABLISHMENT OF MOUSE EMBRYONIC STEM CELL KNOCKOUT LINES TO MODEL THE CONSEQUENCE OF LOSS OF CHD5 ON NEURAL DIFFERENTIATION	94
5.1 Introduction.....	94
5.2 Experimental Results	95
5.3 Discussion.....	100
CHAPTER 6. ONGOING PROJECTS.....	102
6.1 Introduction.....	102
6.2 Genetic interaction models to reveal a role for <i>chd5</i> in promoting tumorigenesis.....	105
6.3 Chemical-genetic screen of zebrafish lacking the chromatin remodeler <i>chd5</i>	108
6.4 Homologous recombination strategy to engineer a dominant-negative allele of <i>Chd5</i> in zebrafish.....	112
CHAPTER 7. FUTURE DIRECTIONS	118
7.1 Characterization of transcriptome phenotypes associated with loss of <i>chd5</i>	118
7.2 Characterization of neural differentiation of mESCs that lack <i>Chd5</i>	120
REFERENCES	123
VITA.....	156

LIST OF TABLES

Table 2.1 Table of materials to perform CRISPR/Cas9 experiments in zebrafish by this protocol.	57
Table 3.1 Overlap of developmentally identified genes in long-pec compared to 5-day whole embryos (White et al. 2017) overlaps strongly with the genes that are differentially expressed in our WT brain transcriptome analysis.....	68
Table 3.2 Predicted activated pathways enriched in wild-type DEGs list from 2- to 5-days.	70
Table 3.3 Predicted inhibited pathways enriched in wild-type DEGs list from 2- to 5-days.	70
Table 3.4 Upstream regulator analysis predicts transcriptional networks are largely inhibited in the absence of Chd5 at 5-days old.	73
Table 4.1 Summary of differentially spliced features and by direction of change (increase or decrease) calculated using JunctionSeq.....	79
Table 4.2 Known splicing factors exhibit differential expression in <i>chd5</i> ^{-/-} brains at 2-day and 5-day compared to WT embryos.....	82
Table 4.3 Known polyadenylation genes are not differentially expressed in the absence of <i>chd5</i> in developing zebrafish brains, as determined at 2- or 5-days compared to WT.....	86
Table 4.4 GO biological processes that are associate with decreased novel features in the 2-daySE comparison.....	87
Table 4.5 GO biological processes that are associate with decreased novel features in the 5-daySE comparison.....	88
Table 4.6 We observe a large number of changes occurring in the 3' UTR using the observed changes in all differentially utilized features in <i>chd5</i> mutants compared to WT.	89
Table 4.7 Features that specifically change in the 3' UTR of genes in our mutant embryos exhibits significant overlap at 2-day and 5-day.....	89
Table 5.1 Guide RNA sequences targeting murine Chd5.....	96
Table 6.1 Zebrafish embryos lacking <i>chd5</i> exhibit increased sensitivity to epigenetic inhibitors compared to wild-type embryos treated continuously from 1-3 days.....	110
Table 6.2 Chd5 knockout fish exhibit a dose-dependent response to JQ1 treatment at 3-days..	111
Table 6.3 High efficiency of homologous recombination strategy employing piggyBac to target zebrafish genes.....	115

LIST OF FIGURES

Figure 2.1 Zebrafish embryos exhibit a pigment defect when injected with a sgRNA targeting <i>tyrosinase</i> at the one-cell stage.	50
Figure 2.2 <i>In vitro</i> transcription of sgRNA using synthesis kit.	51
Figure 2.3 Comparison of the health of 24 hpf injected embryos.	52
Figure 2.4 Heteroduplex mobility assay of sgRNA-Cas9 microinjected zebrafish embryos.	52
Figure 2.5 Heteroduplex mobility assay of gDNA extracted from the tail of an adult CRISPR-injected zebrafish.	53
Figure 2.6 Heteroduplex mobility assay of single embryos generated by breeding a F0 CRISPR-injected zebrafish to a wild-type fish to identify germline transmitted indels.	53
Figure 2.7 Heteroduplex mobility assay of adult F1 zebrafish tail clips.	54
Figure 3.1 Loss of <i>chd5</i> does not result in overt developmental defects in zebrafish embryos in contrast to morpholino injection which causes off-target effects.	65
Figure 3.2 Quality assessment of RNA-seq data.	66
Figure 3.3 Changes in gene expression during development in WT embryos enriches for numerous neurogenic programs.	69
Figure 3.4 Summary of differentially expressed genes.	71
Figure 3.5 <i>Chd5</i> regulates numerous metabolic activities during brain development by GO/KEGG pathway analysis.	72
Figure 3.6 <i>In situ</i> analysis of genes that mark sympathetic ganglion cells.	74
Figure 4.1 MA Plots for each comparison (WT5v2-day, 2-daySE and 5-daySE) showing the differential exon, junction or novel feature usage plotted as the fold change as a function of the gene expression level (mean normalized coverage).	80
Figure 4.2 The differential splicing events identified in brains that are missing <i>chd5</i> show a striking overlap comparing the 2-day to 5-day splice changes.	81
Figure 4.3 Bar graph showing the proportion of splicing events (exons, splice site and novel splice sites) that map to the indicated regions of the gene for increased (upper graph) or decreased (lower graph) usage.	83
Figure 4.4 DNA content analysis shows that the enrichment of A/T nucleotides is highest in junctions and novel features, compared to exons, indicated novel features are most likely noncoding features of the genome.	85
Figure 4.5 Novel splicing features are enriched in the 3' UTR of genes at both 2-day and 5-day in the <i>chd5</i> mutant embryos.	86

Figure 4.6 Gene profile plot for Neurexin1b shows significantly differentially used features calculated by JunctionSeq at 2-day and 5-day.....	90
Figure 4.7 Representative Gviz plot to examine splicing/termination defects observed in our <i>chd5</i> knockout embryos compared to WT, at both 2- and 5-days.	91
Figure 5.1 Western blot analysis of clonal cell populations to identify possible knockout lines. 97	
Figure 5.2 CRISPR/Cas9 induced mutations in <i>CHD5</i> result in formation of premature stop codons in the coding sequence to create gene knockouts.	98
Figure 5.3 Quantitative PCR shows a reduction of <i>CHD5</i> transcript in mouse ESCs, consistent with nonsense mediated decay caused by deleterious mutations to the gene.	98
Figure 5.4 <i>CHD5</i> -KO cells fail to express markers of neural differentiation compared to WT. 100	
Figure 6.1 <i>Chd5</i> is preferentially expressed in the neural tissues of adult zebrafish.....	104
Figure 6.2 <i>Chd5</i> is not required to observe morpholino phenotypes, indicating likely off-target effects of this knockdown approach to study <i>chd5</i>	104
Figure 6.3 Tumor-free survival is decreased in zebrafish containing both <i>p53</i> and <i>chd5</i> alterations compared to <i>p53</i> mutation alone.....	106
Figure 6.4 Loss of <i>chd5</i> results in increased cell death in zebrafish embryos treated with roscovitine.	109
Figure 6.5 Representative images of (+)-JQ1 treated embryos.	110
Figure 6.6 Schematic of CRISPR-based homologous recombination strategy to promote gene replacement using a two-step method.....	114
Figure 6.7 Putative homologous recombination events are easily scored by GFP fluorescence.114	
Figure 6.8 PCR verification of homologous recombination at <i>tyrosinase</i> and <i>chd5</i>	116
Figure 6.9 Constitutive expression of PiggyBac is observed in zebrafish carrying the transgene.	117
Figure 7.1 HPLC sample chromatogram showing identification of neurotransmitter standards.	119

LIST OF ABBREVIATIONS

5-hmC	5-hydroxymethylcytosine
5-mC	5-methylcytosine
AS	alternative splicing
ATP	Adenosine triphosphate
BP	Base pair
CAS9	CRISPR-Associated protein 9
CD	Chromodomain
CDS	Coding sequence
CHD5	Chromodomain/helicase/DNA-binding protein 5
CNS	Central nervous system
CRISPR	Clustered regularly interspaced short palindromic repeats
DA	Dopamine
DBD	DNA-binding domain
DBH	Dopamine beta hydroxylase
DEG	Differentially expressed gene
DPF	Days post fertilization
DSB	Double-strand break
DSE	Differential splicing event
EB	Embryoid body
ESC	Embryonic stem cell
GFP	Green fluorescent protein
GO	Gene ontology
H3K27me3	Trimethylation of histone H3 at lysine 27
HDR	Homology directed repair
HMA	Heteroduplex mobility assay
HPF	Hours post fertilization
HPLC	High-performance liquid chromatography
ISH	In situ hybridization
MPNSTs	Malignant peripheral nerve sheath tumors

mRNA	Messenger RNA
NGS	Next-generation sequencing
NHEJ	Nonhomologous end joining
NPC	Neural precursor cell
NuRD	Nucleosome remodeling and deacetylase complex
pA	Polyadenylation
PAM	Protospacer adjacent motif
PBAC	PiggyBac transposase
PCR	Polymerase chain reaction
PHD	Plant-homeodomain
PKL	Pickle
PRC2	Polycomb Repressive Complex 2
PTM	Post-translational modification
qRT-PCR	Quantitative real-time PCR
RA	Retinoic acid
SE	Splice event
SGC	Sympathetic ganglion cell
sgRNA	Single-guide RNA
Snf2	Sucrose nonfermenting 2
TH	Tyrosine hydroxylase
UTR	Untranslated region
WT	Wild type

ABSTRACT

Author: Sorlien, Erin, L. PhD

Institution: Purdue University

Degree Received: May 2019

Title: The Chromatin Remodeler and Tumor Suppress Chd5 Promotes Expression and Processing of Transcripts During Development of the Zebrafish Neural System

Committee Chair: Joseph Ogas

Vertebrate neurogenesis is a multistep process that coordinates complex signaling pathways and chromatin-based regulatory machinery to generate highly specialized cells (Hsieh and Zhao 2016; Urban and Guillemot 2014; Alunni and Bally-Cuif 2016; Yao and Jin 2014; Schmidt, Strahle, and Scholpp 2013). Epigenetic factors play a fundamental role in underwriting neurogenesis in part by contributing to control of gene expression in differentiating neurons. A mechanistic understanding of the epigenetic machinery underlying neurogenesis in vertebrates is necessary both to fully understand biogenesis of neural tissue in this subphylum as well as to develop effective therapeutic strategies to treat diseased or damaged neural tissue.

An example of an epigenetic factor that is important for both neuronal differentiation and disease states is *CHD5*, a vertebrate-specific member of the CHD family of ATP-dependent chromatin remodeling proteins. Chromodomain / Helicase / DNA-binding (CHD) proteins play a variety of roles in vertebrate development, and misregulation or loss of CHD proteins has been linked to numerous diseases (Mayes et al. 2014; Marfella and Imbalzano 2007; Bartholomew 2014). *CHD5* is expressed primarily in neural tissue, where it is thought to contribute to neurogenesis, and has been strongly linked to tumor suppression (Thompson et al. 2003; Vestin and Mills 2013). Loss of *CHD5* plays a significant role in development of neuroblastoma, a devastating tumor that is a leading cause of cancer-related death in children (Jiang, Stanke, and Lahti 2011; Maris and Matthay 1999). Consistent with the disease phenotype associated with loss of *CHD5*, reduced expression of *CHD5* impairs differentiation of neuronal cells (Egan et al. 2013b). However, ablation of *CHD5* in mice surprisingly resulted in no detectable defects in brain development (Li et al. 2014; Zhuang et al. 2014). A subsequent report revealed that mice conditionally ablated for *CHD5* in neural tissue exhibit symptoms consistent with an autism spectrum disorder (Pisansky et al. 2017). Much remains to be learned about the role of *CHD5* in these processes to clarify these observations.

Further, Chd5 is unique among the family of Chd remodelers in that it provides a biochemical basis for crosstalk between the critical epigenetic marks H3K27me3 and DNA methylation. Chd5 and the closely related remodelers Chd3 and Chd4 are all components of the Mi-2/NuRD histone deacetylase complex that plays a critical role in mediating transcriptional repression in response to DNA methylation in mammals (Allen, Wade, and Kutateladze 2013). Only *CHD5* is preferentially expressed in neural tissue, however, and only Chd5 remodelers have biochemical evidence of direct interaction with H3K27me3, which plays a critical role in enabling proper expression of transcriptional programs during neurogenesis (Egan et al. 2013b). Chd5 is thus unique among CHD remodelers in that it is biochemically linked to both DNA methylation and H3K27me3 in addition to being preferentially expressed in neural tissue.

With regards to mechanism, much remains to be learned regarding how Chd5 remodelers contribute to gene expression and tumor suppression. However, the data to date do not show extensive transcript phenotypes and it is not clear how the biochemical action of *CHD5* contributes to the neurological phenotypes ascribed to altered expression of *CHD5*. Therefore, it is critical to determine a suitable context to study the role of *CHD5* in these processes. Identification of *CHD5*-dependent genes in neurons is likely to generate insight into how loss of *CHD5* contributes to tumorigenesis, in particular with regards to development of neuroblastoma. Regulatory pathways that drive neurogenesis have been found to be extensively conserved between humans and zebrafish. Therefore, we have turned to the power of the zebrafish model system to characterize how loss of Chd5 alters brain development during embryogenesis.

Importantly zebrafish development, and neurogenesis in particular, occurs largely over the first 5-days of development. Zebrafish are born outside of the mother, which can produce large clutches of several hundred embryos per week, providing us with an accessible context to study the role of *chd5*, the zebrafish homolog of human *CHD5*. The central nervous system of the zebrafish develops rapidly, and shares many of the organization features of the mammalian brain (Kalueff, Stewart, and Gerlai 2014). In particular, neuroblastoma arises from a population of cells known as sympathetic ganglion cells that are derived from the neural crest (Pei et al. 2013). These cells are conserved in vertebrates, and several models to study how these cells transform into neuroblastoma exist in zebrafish (Zhu et al. 2017; Morrison et al. 2016; Zhu and Thomas Look 2016). However, our understanding of the mechanisms controlling ganglion cell differentiation is incomplete and requires further investigation to understand how epigenetic and transcriptional

mechanisms contribute to development of these cells and how failure of these processes leads to cancer. The neural crest undergoes a series of differentiation steps to form mature sympathetic neurons that are guided by bone morphogenic protein signaling, and transcription changes (Ernsberger and Rohrer 2018). These cells express key enzymes for synthesizing dopamine and norepinephrine to control the sympathetic system throughout the central nervous system (Ernsberger and Rohrer 2018).

To address these questions about *Chd5*, we have used CRISPR/Cas9 to generate *chd5*^{-/-} zebrafish that are protein nulls as determined by western blot. These *chd5*^{-/-} fish are phenotypically indistinguishable from wild-type fish under standard growth conditions as was previously observed for mice lacking *CHD5* (Zhuang et al. 2014; Li et al. 2014). By using zebrafish, we are able to perform transcriptome analyses to identify *Chd5* target genes at stages much earlier than has previously been performed in mice because we can harvest large amounts of the tissue of interest from the readily accessible embryos. We have therefore undertaken RNA-seq analysis of isolated brains from wild-type and *chd5*^{-/-} fish to identify *chd5*-dependent genes in predominantly differentiating (2-day old) and substantially differentiated (5-day old) neural tissue. These data provide a substantively different perspective from previous studies that examine the role of *CHD5* in gene expression of differentiated SY-SH5Y cells (Egan et al. 2013a) or in the forebrain of 8-week-old mice (Pisansky et al. 2017). (Jiang, Stanke, and Lahti 2011). One role we identified from this data, is the promotion of development of sympathetic ganglion cells (detailed below), illuminating for the first time a role for *chd5* in promoting differentiation of cells directly involved in neuroblastoma.

We observe not only extensive changes in gene expression, but also identify a novel role for *Chd5* in enabling proper splicing during this critical window of neurogenesis in the zebrafish brain. We are further exploring the role of *CHD5* in these processes by creating comparable cell culture-based models of loss of *CHD5* to determine the conservation of molecular phenotypes observed in zebrafish. Furthermore, this model enables us to leverage the extensive biochemical tools available in cell culture to examine alterations to the chromatin that are difficult to interpret from studies of complex tissues such as the brain.

Herein I will describe the research progress we have made to understand the role of *Chd5* in gene expression and splicing in zebrafish, as well as ongoing work to engineer mouse embryonic stem cells as an additional model to study the transcriptional consequences of loss of *CHD5*.

Critically, the addition of the cell culture model will greatly enable biochemical characterization of the changes that are leading in particular to the changes in gene expression and splicing and will provide us with a context to test for a direct role of CHD5 in these processes. In addition, this thesis will detail the results from ongoing projects using the zebrafish model system, including: development of models in zebrafish to study the tumor suppressive role of Chd5, phenotypes observed using a targeted chemical-genetic screen, and advancement in developing new tools in zebrafish to engineer specific genomic modifications that will greatly expand the power of this vertebrate model.

CHAPTER 1. INTRODUCTION: CHD REMODELERS IN MULTICELLULAR EUKARYOTES: COMPARING AND CONTRASTING THE CONTRIBUTIONS OF CHD PROTEINS IN CHROMATIN-BASED PROCESSES

1.1 Abstract

Chromatin remodeling proteins are critical regulators of chromatin structure in eukaryotes that dynamically alter nucleosomes in an ATP-dependent fashion. Their ability to alter histone protein-DNA contacts to achieve distinct remodeling outcomes enables fundamental DNA-based processes such as replication, repair, and transcription. These factors share a common characteristic SNF2-like helicase domain and can be further distinguished by sequence homology within this domain as well as by additional distinct sequence motifs. Work in yeast and animal systems reveals that Chromodomain/*Helicase/DNA-binding* (CHD) family of remodelers have been harnessed to achieve a wide range of functional outcomes. Work in plant systems indicates that related remodelers have distinct chromatin-based roles that nonetheless have been harnessed for related developmental outcomes. Further characterization of this family of remodelers in both plants and animals will shed light on how these remodelers have been differently harnessed by evolution in each kingdom and suggest new roles for previously characterized factors.

1.2 Introduction

Compaction of DNA by histone proteins and other factors has enabled the evolution of genomes of considerable complexity and size (Cavalier-Smith 2005; Vinogradov 2005). The resulting nucleoprotein complex provides a platform on which DNA-templated processes such as replication, repair and transcription are carried out. Proteins that are structurally related to eukaryotic histones are found in Archaea and likely share a common ancestor (Mattioli et al. 2017; Sandman and Reeve 2006; Malik and Henikoff 2003; Talbert and Henikoff 2010). Although Archaeal histone-DNA complexes share significant structural similarities, eukaryotes evolved a distinct nucleosomal structure based on four distinct histone proteins. The nucleosome is the fundamental repeating unit of eukaryotic chromatin, and consists of an octameric core of two H2A-H2B and two H3-H4 heterodimers around which is wrapped ~145-147 base pairs (bp) of DNA in 1.65 left-handed superhelical turns. The four core histones are small basic proteins that each

contain the highly conserved histone fold dimerization motif and an unstructured N-terminal tail. The core histones are highly conserved across eukaryotes (Malik and Henikoff 2003); however, there has also been diversification of H2A and H3 genes into histone variants that typically differ in relatively few amino acids and yet have profound effects on DNA-templated processes when incorporated into chromatin (Talbert and Henikoff 2017, 2010; Li and Fang 2015; Henikoff and Smith 2015; Macadangdang et al. 2014).

ATP-dependent chromatin remodelers enable exchange of histone variants and facilitate many additional aspects of chromatin homeostasis. Chromatin structure in eukaryotes is tightly controlled by a variety of proteins that interact in some form with histones, including histone chaperones, posttranslational histone modifiers, as well as ATP-dependent chromatin remodelers (Chen et al. 2017). These remodelers are ubiquitously found in eukaryotes, and related enzymes are found in some eubacteria and archaea (Bhattacharyya, Mattioli, and Luger 2018; Reeve 2003; Eichler and Adams 2005). Chromatin remodelers contain helicase-like domains that harness the energy generated by ATP hydrolysis to dynamically alter nucleosome structure (Flaus et al. 2006). These factors can modify nucleosomes in a non-covalent fashion by assembly or disassembly, as well as by shifting their position or by switching out histone subunits (Clapier and Cairns 2009; Zhou et al. 2016; Narlikar, Sundaramoorthy, and Owen-Hughes 2013). Biochemical characterization suggests that these domains primarily act as translocases that reposition the DNA in 1 bp increments relative to the nucleosome and thereby generate the forces necessary to alter histone-DNA contacts and drive nucleosome remodeling (Singleton, Dillingham, and Wigley 2007). Although altering chromatin structure as defined by nucleosome composition/position is often a primary function of these remodelers, they may also affect interactions between non-histone proteins and DNA (McBride and Kadoch 2018; Sokpor et al. 2017; St Pierre and Kadoch 2017; Lorch and Kornberg 2017; Torrado et al. 2017). In addition, ATP-dependent remodelers often contribute to or are affected by chromatin structure that is defined by covalent modification of DNA and histones, which includes a particularly extensive set of modifications in the case of histones (Prakash and Fournier 2018; Talbert and Henikoff 2010).

The substrate and product of a given remodeling reaction is dictated by the interplay between a catalytic Snf2 ATPase domain that powers the remodeling action and flanking domains that contribute to both substrate specificity and the outcome of the remodeling reaction (Bartholomew 2014). The sequence/presence of these domains also can be used to delineate

different chromatin remodelers into five broad families: namely, SWI/SNF, ISWI, INO80, ATRX, and CHD remodelers, which are the focus of this review (Flaus et al. 2006). Different families of remodelers are associated with distinct types of remodeling events, which is most strongly associated with the sequence of the ATPase domain (Flaus et al. 2006). There is typically a gap, however, in connecting the remodeling activities of these various factors as defined in vitro or using chromatin-based assays to specific biological outcomes of interest. The success of this type of undertaking is particularly confounded by structurally complex dynamic nature of chromatin, which renders identification and subsequent generation of the relevant in vitro substrate for a remodeler in a given biological process challenging at best. Further, processes of interest such as transcription are dynamic and dependent on many different factors, making it difficult to tease out the contribution of any specific component, but perhaps especially those factors that contribute to the dynamic nature of the template.

This review examines the contributions of CHD remodelers to chromatin-based processes in both animals and plants. Extensive diversification of CHD remodelers has taken place independently in plant and animals as well as within each kingdom. This single family of chromatin remodelers facilitates a diverse set of nucleosome-based transitions that contribute in varied ways to fundamental biological processes. As a result, comparative functional analyses of related remodelers in different biological contexts helps to reveal the range of specific contributions made by CHD remodelers to DNA-templated processes as well as to much more emergent biological traits such as differentiation and development.

1.3 Phylogenetic analysis of CHD remodelers in plants and animals

Phylogenetic analysis of SF2-domain containing proteins from more than 1300 proteins identifies 24 distinct subfamilies in total (Flaus et al. 2006). Members of these subfamilies can also often be distinguished by the presence of additional domains of sequence homology in addition to the conserved residues of the ATPase domain. Biochemical characterization of a number of these domains reveals that they contribute to a range of properties of remodelers, including regulation of the ATPase domain, recognition of histones, protein-protein interactions, and DNA contacts (Bartholomew 2014).

The name of the CHD subfamily of remodelers is derived from an acronym of the domains commonly found in these remodelers: a tandem Chromo domain in the N-terminus, a SWI/SNF2

ATPase/Helicase domain, and a DNA binding domain that is found C-terminal to the ATPase domain (Marfella and Imbalzano 2007). Phylogenetic analysis of CHD remodelers separates them further into subfamilies I, II, and III that are also distinguished by the presence of additional domains (Hall and Georgel 2007; Sims and Wade 2011). Subfamily I and II contain a DNA-binding domain that contains both a SANT and a SLIDE domain, and subfamily II additionally includes tandem PHD zinc finger domains (Woodage et al. 1997; Bienz 2006). Members of subfamily III are distinguished by the presence of a BRK domain in the C-terminal region.

Phylogenetic analysis of selected CHD remodelers in plants and animals reveals that members of subfamilies I and II are found in both kingdoms whereas subfamily III is specific to animals (Ho et al. 2013b; Hall and Georgel 2007). In plants, members of subfamily II segregate into two separate clades, denoted by the Arabidopsis proteins PKL and PKR1. Members of these two clades are also distinguished by a distinct domain architecture: the PHD domain of PKL-related proteins in plants are immediately adjacent to the chromodomains as observed in animal members of subfamily II, whereas the PHD domains of PKR1-related CHD remodelers of plants are often closer to the N-terminus of the protein than the chromodomains and so distinct from animal members of subfamily II. The existence of CHD remodelers belonging to subfamilies I and II strongly suggests that members of these subfamilies were present in the last common ancestor of plants and animals and thus that there was a common ancestral role for each subfamily.

1.4 CHD proteins are regulated, ATP-driven motors, that remodel nucleosomes

Biochemical characterization of CHD1 strongly informs our understanding of the ATP-dependent activities of CHD proteins.

Biochemical characterization of yeast CHD1 has provided a great deal of insight into how ATPase domains work with chromodomains and DNA-binding domain to determine remodeling reaction. The basic movement of the nucleosome entails sliding the histone octamer without dissociation. This involves the disruption of numerous histone-DNA contacts, that are stabilized by the positive residues on histones and the negatively charge phosphate backbone of the DNA (Luger et al. 1997). Few of these contacts are highly specific and while the wrapped state is favorable, DNA unwrapping can occur transiently (Polach and Widom 1995; Anderson and Widom 2000).

Characterization of the translocation of nucleosome DNA during remodeling showed for SWI/SNF-type remodelers, DNA was shifted in a continuous manner in 1-2 bp increments (Harada et al. 2016; Sirinakis et al. 2011). CHD1 has been demonstrated to evenly reposition nucleosomes on DNA and is able to shift the nucleosome bidirectionally in short bursts of multiple base pairs (Qiu et al. 2017). This remodeling is similar to that observed for ISWI translocation that occurs in a step-wise manner beginning with a 7-bp step, followed by 3-bp subsequent steps- all which are comprised of the characteristic 1-bp substep (Deindl et al. 2013).

The core of the translocase domain consist of two RecA-like lobes that they are highly dynamic in relation to one another, and that bind ATP and nucleic acids (Hauk and Bowman 2011). The crystal structure of yeast Chd1 bound to a ubiquitylated nucleosome, a histone post-translation modification (PTM) that is present where Chd1 is found in vivo, has recently been reported (Sundaramoorthy et al. 2018). Chd1 makes few contacts with histones, relying primarily on contact with the H3 alpha helix and the H4 tail (Sundaramoorthy et al. 2018). Additionally, the ATPase domain makes contacts with DNA to create a closed confirmation within the motor. Binding of ATP further drives this closure and movement of the second RecA lobe to catalyze the translocation in a ‘ratcheting’-like conformational change (Farnung et al. 2017).

Through these studies it has become clear that the domains of CHD remodelers work together to both recognize the nucleosomal substrate and DNA to determine the outcome of the remodeling reaction. Chd1 additionally contacts extranucleosomal DNA through the DNA-binding domain (DBD) located C-terminally to the helicase. Crystallographic structures have been mapped for yeast Chd1 DBD in complex with DNA (Sharma et al. 2011). The DBD of Chd1 does not show strong sequence preference and has been shown to contribute to the affinity of Chd1 for the nucleosome (McKnight et al. 2011). The DNA binding domain of CHD1 is highly similar to that of ISWI and consists of a SANT-SLIDE domain (Ryan et al. 2011; Sharma et al. 2011). This similarity is particularly interesting in light of the role that both domains are thought to play sensing the length of DNA external to the nucleosome that is available for sliding the nucleosome. Deletion of a small region between the ATPase domain and the DNA-binding domain of yeast CHD1 largely abrogates nucleosome sliding but only minimally affects nucleosome binding and nucleosome-stimulated ATPase activity (Patel et al. 2011).

Characteristic of the CHD family, CHD1 contains tandem chromodomains (CD) N-terminal to the helicase (Hargreaves and Crabtree 2011; Marfella and Imbalzano 2007). Crystallography of

the CD and helicase of CHD1 has demonstrated that the CD inhibits DNA-binding of the ATPase motor to prevent ATPase activity, and this interaction is required to distinguish between DNA and nucleosomes (Hauk et al. 2010). Deletion or mutation of the chromodomain results in a dramatic increase in the ability of DNA to stimulate the ATPase activity of comparable remodeler constructs that possess the chromodomain. This type of regulation, termed gating, negatively regulates the ATPase motor in the absence of the proper substrate to change the chromodomain conformation upon binding to the desired nucleosomal substrate or other binding partners (Qiu et al. 2017).

Subfamily II CHD proteins contribute distinct biochemical actions.

Subfamily II CHD proteins are comparatively less well characterized compared to the biochemical studies of CHD1. Subfamily II contains the CHD3 (sometimes called Mi2 α), CHD4 (also called Mi2 β) and CHD5 remodelers, and are defined by the additional presence of tandem PHD domains located N-terminally to the CD domains. *In vitro* characterization of subfamily II members shows that like subfamily I, these proteins reposition mononucleosomes to the center of a fragment of DNA (Hall and Georgel 2007). CHD5, however, in the same type of assay, loosens the DNA around the nucleosome without repositioning the nucleosome. Thus, CHD5 contains a unique activity compared to other animal subfamily II members (Quan and Yusufzai 2014).

Similar to CHD1 remodelers, the multidomain structure of these proteins cooperates to drive the specific remodeling actions. Substantial insight has been gained from structural studies of CHD4 and is likely to inform our understanding of how CHD3 and CHD5 work. Notably, it has been shown that the ATPase motor of CHD4 is structurally similar to CHD1. The domains of CHD4 have been studied individually and in the intact protein. The CDs have been shown to contact DNA, and both the CDs and PHDs have been shown to bind histone tails (Morra et al. 2012). Further characterization of the CHD4 PHD domains show the highest affinity for H3 tails that are unmodified at Lys4 but methylated at Lys9 (Mansfield et al. 2011; Musselman et al. 2009). Additionally, it was shown that the N-terminal PHD and CD modules associated tightly with the ATPase to occlude the ATPase activity (Watson et al. 2012; Morra et al. 2012; Morra et al. 2016). This conformational change induced upon binding a nucleosome to stimulate ATPase activity in CHD4 is thus similar to that observed for CHD1 and may therefore represent a common mechanism used to control remodeler actions.

In animals, CHD remodelers in subfamily II, unlike subfamily I members, often work in concert with other epigenetic regulators in multisubunit complexes. Perhaps the best characterized of these is the Mi-2/NuRD complex (Torchy, Hamiche, and Klaholz 2015; Allen, Wade, and Kutateladze 2013). This complex incorporates an ATP-dependent chromatin remodeler as well as a histone deacetylase. Incorporation of a subfamily II member into Mi-2/NuRD increases the efficiency of deacetylation by the histone deacetylase by 2-fold compared to a histone deacetylase alone (Xue et al. 1998a). In addition, however, CHD 3/4 proteins from animal systems also have been shown to be in another complex with a histone acetyltransferase, p300 (Williams et al. 2004). These complexes illustrate that the remodeling activity of members of this subfamily can be harnessed to promote either transcriptional inactivation or activation depending on the presence or absence of additional chromatin machinery.

1.5 CHD proteins contribute to a diverse set of *in vivo* remodeling activities

In vitro biochemical properties of CHDs provide rational for understanding the in vivo remodeling products.

How these activities relate to the emergent roles of CHD1 to regulate chromatin states is an important consideration to study the *in vivo* outputs of these proteins. Both the CHD1-related and SWI/SNF remodeling proteins contain domains that recognize specific chemical moieties on histones, and this in turn can affect their localization *in vivo*, as well as their activity *in vitro* (Swygert and Peterson 2014). Studies in *Saccharomyces* shows that Chd1 can assemble nucleosomes *in vivo*. Characterization of sliding defective versions of yeast and *Drosophila* CHD1 reveal that these proteins can promote nucleosome assembly in an ATP-dependent fashion but do not properly space them (Torigoe et al. 2013). Thus, these studies indicate that CHD1 remodelers promote chromatin assembly via two distinct ATP-dependent activities: nucleosome assembly followed by nucleosome sliding. The further implication is that identification of one activity for a CHD remodeler does not preclude identification of another. Additional factors, such as transcription factors, bind to chromatin and have been shown to influence the remodeling outcome of Chd1. To generate evenly spaced nucleosomal arrays Chd1 can slide nucleosomes bidirectionally, but this directionality choice depends on DNA availability and barriers posed by proteins bound to nucleosomes (Nodelman et al. 2016).

In this light, it is important to note that the chromodomains of different members of subfamily I differ in their affinity for modification states of the histone tail of histone H3. The chromodomains of human CHD1 exhibits much higher affinity for H3K4me3 than the chromodomains of either yeast CHD1 or *Drosophila* (Morettini et al. 2011; Sims et al. 2005). Biochemical characterization of the other CHD remodeler in subfamily I in humans, CHD2 revealed that although the chromodomains do have a higher affinity for H3K4me3 than yeast, the affinity is 30-fold less than that of the chromodomains of CHD1 (Flanagan et al. 2007; Kim, Jo, et al. 2018). These observations suggest that evolving the ability to discriminate between different modification states of histones by the chromodomains of CHD remodelers may similarly alter the preferred substrate of these remodelers during evolution.

Subfamily I remodelers are commonly associated with chromatin assembly and transcription activation.

Characterization of both yeast and animal CHD1 remodelers *in vivo* indicate that these remodelers play a role in both chromatin assembly and activation of transcription and that, in fact, the two roles may be intertwined. With regards to assembly of chromatin, these remodelers have been linked to incorporation of a centromere-specific variant of histone H3 at the centromeres of fission yeast and some animal systems. In fission yeast, the CHD1 gene HRP1 is necessary for loading the centromere-specific histone variant CENP-A onto centromeres (Walfridsson et al. 2005). Further, CHD1 localizes to centromeres throughout the cell cycle in both DT40 cells from chickens and HeLa cells from humans, and knockdown of CHD1 in HeLa cells results in reduction of CENP-A at centromeres (Okada et al. 2009). In *Drosophila*, however, CHD1 does not localize to centromeres in either *Drosophila* embryos or S2 cells and knockdown of CHD1 does not affect levels of CenH3CID at centromeres (Podhraski et al. 2010). Thus these remodelers are not thought to play a universal conserved role in building centromeric chromatin, and have in fact been proposed to act indirectly at these regions by promoting disassembly of nucleosomes containing H3 during the transcription of noncoding RNA at the centromeres (Choi et al. 2011).

In addition, CHD1 proteins have been shown to be necessary for assembly of chromatin containing the histone variant H3.3 in a transcription-independent fashion in animal systems. *Drosophila* lacking CHD1 are defective in incorporation of H3.3 into chromatin of the male pronucleus, revealing a critical role for CHD1 in replication-independent nucleosome assembly

(Konev et al. 2007). Although H3.3 is incorporated into transcriptionally active regions of the genome in a replication-independent manner in animals, it is important to note that early *Drosophila* embryos are not transcriptionally active thus revealing that CHD1 proteins have at least one role in chromatin assembly that is not immediately linked to gene expression. In addition, CHD2 has been shown to contribute to differentiation of muscle cells in mice by promoting deposition of H3.3 at myogenic loci prior to differentiation. This deposition occurs prior to expression of these loci, indicating that this deposition is also not dependent on transcription, and is likely to be necessary for subsequent transcriptional activation (Harada et al. 2012).

CHD1-mediated nucleosome assembly, disassembly, and spacing have all been shown to contribute to transcription. Rather than primarily disrupting chromatin like SWI/SNF remodelers to enable transcription of genes, CHD1 remodelers both clear and preserve chromatin structure during transcription. In this way, CHD1 remodelers act to both reset and preserve epigenetic status in transcribed genes in both yeast and animal systems. In budding yeast, CHD1 is recruited to actively transcribed genes via the nucleosome free region based on ChIP-seq of uncrosslinked (native) chromatin, from which it is then transferred to the gene body (Zentner, Tsukiyama, and Henikoff 2013). In the gene body, CHD1 is necessary for regeneration of nucleosome structure after passage of RNA Pol II (Zentner, Tsukiyama, and Henikoff 2013; Smolle et al. 2012). Loss of CHD1 results in increased nucleosome turnover in transcribed regions, leading to increased acetylation of H4 and decreased H3K36me3 in transcribed regions of the genome and ultimately to increased intragenic and cryptic transcription (Zentner, Tsukiyama, and Henikoff 2013; Smolle et al. 2012; Radman-Livaja et al. 2012).

CHD1 functions with ISWI remodelers to reset chromatin after transcription in budding yeast. Loss of both ISWI remodelers and CHD1 in this organism results in a profound defect in nucleosome positioning, in particular losing phasing of nucleosomes downstream of +1 nucleosome at the transcription start site (Gkikopoulos et al. 2011). Analyses of fission yeast lacking one or both members of CHD subfamily I, HRP1 and HRP3, similarly reveal a role for these remodelers in nucleosome positioning and suppression of cryptic transcription in this organism (Shim et al. 2012; Pointner et al. 2012; Hennig et al. 2012; Touat-Todeschini, Hiriart, and Verdel 2012).

Characterization of histone dynamics in both *Drosophila* and budding yeast reveals that CHD1 plays a similar role at transcribed loci in both of these model systems (Radman-Livaja et

al. 2012). In addition, these studies also reveal that CHD1 acts in a polar fashion: although CHD1 suppresses nucleosome turnover and preserves chromatin structure in the 3' region of transcribed genes, it also promotes nucleosome turnover in the 5' region of genes (Radman-Livaja et al. 2012; Smolle et al. 2012). Similarly, HRP remodelers have been shown to promote nucleosome turnover near the transcription start site in fission yeast (Walfridsson et al. 2007).

A recent paper by Skene and colleagues demonstrates the relevance of many of these findings to mammals (Skene et al. 2014). The investigators used ChIP-seq in which micrococcal nuclease was used to digest crosslinked chromatin to increase the resolution of their analysis of nucleosome and CHD1 position as well as CATCH-IT (covalent attachment of tags to capture histones and identify turnover) to examine nucleosome turnover in mouse embryonic fibroblasts (MEFs) (Deal, Henikoff, and Henikoff 2010). Their studies revealed that Chd1 acts to suppress nucleosome turnover in the 3' regions of genes of MEFs as previously observed in other systems. Further, their analyses revealed that CHD1 plays a critical role in eviction of nucleosomes flanking the transcription start site as well as facilitating efficient escape of RNA polymerase II from the promoter. It is worth noting that the demonstration that CHD1 plays a major role in evicting promoter nucleosomes relies primarily on use of a dominant negative version of CHD1 that is catalytically inactive, K510R-Chd1, rather than reduction of CHD1 expression in an effort to prevent masking of any CHD1-dependent role by factors that act redundantly with CHD1.

These studies further suggest that the nucleosome that is proximal to the transcription start site acts as a barrier to escape of RNA polymerase II from the promoter in mammalian cells and that CHD1 removes this barrier. The observation that CHD1 promotes turnover of 5' nucleosomes in *Drosophila* as well as budding and fission yeast (Radman-Livaja et al. 2012; Smolle et al. 2012; Walfridsson et al. 2007), and suggests that CHD1 may generally play such a role in clearing promoter nucleosomes in transcribed genes in eukaryotes (albeit redundantly with ISWI in budding yeast (Gkikopoulos et al. 2011)). In this regard, however, it is important to keep in mind that the transcription start site in metazoans is in the nucleosome depleted regions approximately 50 bp upstream of the +1 nucleosome (Mavrich et al. 2008; Schones et al. 2008) as opposed to the just within the +1 nucleosome in budding yeast (Rhee and Pugh 2012). Thus, the potential role of the +1 nucleosome as a barrier to RNA pol II elongation and the contribution of CHD1 to removing this barrier are likely to be unique to metazoans.

Vertebrate Subfamily I also contain the CHD2 protein.

Vertebrates are unique in that they have two remodelers in the Subfamily I of CHDs. Analysis of the other CHD1-related remodeler found in mammals and other vertebrates, CHD2, indicates that it plays a redundant, although not identical role to CHD1 in mammalian cells (Siggens et al. 2015). Comparative analysis of ChIP-seq data from CHD1 and CHD2 and the chromatin states delineated (Ernst et al. 2011). Ernst et al. revealed that enrichment of CHD1 and CHD2 at a locus is best predicted by the presence of RNA Pol II machinery, suggesting that these remodelers are co-recruited with transcription machinery. A similar relationship was observed between CHD1 and RNA Pol II (Skene et al. 2014). Enrichment of CHD1 and CHD2 is also observed at highly transcribed enhancers, revealing that recruitment of these remodelers are not restricted to coding transcripts and suggesting that they may contribute to epigenetic regulation of these enhancers (Ernst et al. 2011). 60% of CHD1 and CHD2 sites of enrichment overlapped, raising the prospect of functional redundancy at these loci. Examination of highly expressed genes, however, revealed important differences in distribution of the two remodelers: CHD1 enrichment mirrored the distribution of H3K4me_{2/3} enrichment whereas CHD2 enrichment was strongest at nucleosome depleted regions. Given that the chromo domains of CHD1 have a higher affinity for H3K4me_{2/3} than CHD2 (Flanagan et al. 2007), the authors speculate that the remodelers are initially recruited in concert with the RNA pol II complexes where the subsequent interaction with the chromatin template is directed by the respective affinities of the chromo domains.

In further support of these overlapping roles, functional characterization of CHD1 and CHD2 using siRNA in K562 cells, a human immortalized myelogenous leukemia cell line, reveals both distinct and overlapping roles for these two remodelers. Knockdown of CHD1 reduced DNase I hypersensitive sites at the transcription start sites of highly expressed genes whereas CHD2 did not (Siggens et al. 2015). Analysis of H3 and H3.3 using ChIP at selected sites reveals that knocking down CHD2 significantly increases H3 occupancy at transcription start sites. Although knockdown of CHD1 did not result in a significant increase in H3 occupancy, knockdown of CHD1 and CHD2 elevated H3 occupancy above knockdown of CHD2 alone suggesting some degree of redundancy. Knockdown of CHD2 but not CHD1 led to a strong decrease in H3.3 enrichment at the transcription start sites that were examined. Overall these data are thus consistent with roles in nucleosome turnover and deposition of H3.3 that have previously been identified for CHD1 remodelers in other organisms. In particular, these data support a role

for CHD1 remodelers in evicting promoter proximal nucleosomes as was observed in studies using the dominant negative version of CHD1 (Skene et al. 2014).

Plant remodelers in subfamily I: AT contains CHD1 (PKR3/CHR5) also contains CHD2

Unlike the lethality observed in mice, mutation of *PKR3/CHR5* has an extremely modest effect on plant growth and development (Shen et al. 2015). This suggests that this remodeler plays a minor role in transcription, if any, or another possibility is that ISWI remodelers (of which there are three in Arabidopsis (Flaus et al. 2006), function redundantly with PKR3/CHR5 as observed in *S. cerevisiae* (Tsukiyama et al. 1999). When plant CHD proteins were added to the phylogenetic analysis, the subsequence analysis indicates that the PKR3 proteins are the plant homologs of CHD1. At present, the *in vitro* biochemical activity of PKR3 has yet to be examined. Determination that PKR3 exhibits assembly activity similar to CHD1 in animals would demonstrate conservation of this important activity within this subfamily. We have found that loss of *PKR3* results in no obvious phenotype in Arabidopsis (unpublished data). If PKR3 plays a similar role as animal CHD1 proteins, the phenotype of *pk3* plants suggests that one or more other remodeler's function redundantly with PKR3 in promoting incorporation of H3.3 into chromatin.

Plant CHD1 remodelers have been much less extensively characterized than their fungal and animal counterparts. Characterization to date, however, are consistent with similar roles for CHD1 remodelers in transcription in plants as they do in animals. Mutation of the CHD1 remodeler PKR3/CHR5 in Arabidopsis results in no obvious shoot phenotype other than a weak long hypocotyl phenotype (Shen et al. 2015). However, more detailed analysis of a potential role in seed development revealed several modest defects in gene expression, indicating that PKR3/CHR5 plants a positive role in transcription during at least this stage of development. Further, the authors obtained ChIP data suggesting that nucleosome occupancy was decreased at one of the affected loci, although interpretation of these data is slightly confounded due to analysis of a developmental sample (siliques) comprised of diverse tissues with multiple expression states of the locus of interest. Nevertheless, the data are consistent with CHD1 remodelers playing a role at transcribed genes in plants that is similar to that observed in animal and fungal systems.

Subfamily II remodelers in plants and animals exhibit conserved and divergent roles.

Similar to CHD1, CHD3 and CHD4 also slide nucleosomes, but they additionally have important roles in histone deacetylation and acetylation, often as part of multi-subunit remodeler complexes (Xue et al. 1998b). In particular, the Subfamily II CHD remodelers are members of the repressive NuRD complex. Along with gene repression, subfamily II members can also activate gene expression as a result of incorporation in a complex containing the histone acetyltransferase p300. This complex activates genes important for T-cell differentiation, suggesting that subfamily II members are utilized by different complexes in different contexts (Williams et al. 2004). Vertebrates have diversified the Subfamily II family, acquiring the additional member CHD5. Similar to other members of Subfamily II, CHD5 appears to play roles in both activating and repressing gene expression (Pisansky et al. 2017; Quan et al. 2014; Egan et al. 2013a).

The only CHD remodeler that has been reported to be biochemically characterized from plants is PICKLE, a subfamily II member (Ho et al. 2013a). Like animal subfamily II members, PKL mobilized nucleosomes into the center of a DNA template (Ho et al. 2013a). Intriguingly, unlike animal subfamily II members, several observations strongly suggest that PKL primarily exists as a monomer. These data suggest that plant members of subfamily II primarily act outside the context of a complex unlike animal subfamily II members. However, this scenario raises the possibility that the animal subfamily II members may also play an undiscovered role as monomers.

PICKLE promotes the repressive histone modification H3K27me3 and is necessary for repression of a wide range of H3K27me3-enriched genes (Zhang et al. 2012; Zhang et al. 2008). Intriguingly, PKL is also necessary for expression of H3K27me3-regulated genes, suggesting that PKL acts to both repress genes in the tissues where they are supposed to be off and activate genes where they are to be expressed. The mechanism by which PKL contributes to both activation and repression of H3K27me3-regulated genes is unknown (Aichinger et al. 2009; Zhang et al. 2012). Although PKL promotes H3K27me3 there is no evidence of biochemical interaction of PKL with the members of the PRC2 complex in Arabidopsis (Ho et al. 2013a). It is intriguing to note that PKL plays a role that is remarkably similar to that of the animal subfamily II member CHD5. Both proteins function to repress H3K27me3 targets and activate tissue specific genes important for development (Zhang et al. 2012; Egan et al. 2013a). This perceived overlap of function is interesting because characterization of this shared role may illuminate a remodeling activity that is universal to all subfamily II members.

Recently, PKL was shown to act as a maturation factor to convert prenucleosomes into nucleosomes (Carter et al. 2018). This finding suggests that PKL may act after deposition of H3K27me3 to promote retention of this mark. This function has also been reported for CHD1 (Fei et al. 2015), but not for CHD5 in our hands (data not shown). This data is consistent with models that ascribe CHD1 function to retention of H3K36me3, a mark found across transcribed genes (Radman-Livaja et al. 2012; Smolle et al. 2012; Venkatesh et al. 2012).

1.6 Conclusions

CHD proteins exhibit a variety of biochemical properties in plants and animals.

Members of the CHD family of ATP-dependent remodelers have been shown to possess a variety of different biochemical activities. Importantly, through these analyses present here, it is clear that many of these chromatin remodeling proteins can achieve more than one biochemical output. For example, one activity of CHD1 remodelers is the spacing of nucleosomes, and another is the assembly of nucleosomes containing H3.3, which appears intrinsically linked to transcriptional activation. The same remodeler can contribute to both activation and repression of expression, suggesting that a remodeling activity is not inherently linked to a specific transcriptional outcome.

Importantly, what we measure *in vitro* is likely to be only an approximation of what these proteins do *in vivo*, particularly in the context with other remodeling factors. With regards to identification of *in vivo* roles, analysis of remodelers in both plant and animals is likely to generate novel insights. Identification of kingdom-specific clades raises the prospect of additional or redundant roles for those remodelers. Further, identification of new roles in one kingdom raises the prospect of related remodelers playing a similar role in the other kingdom. For example, the prospect that PKL primarily acts as a monomer in plants raises the possibility that CHD3/4/5 proteins can act similarly in animals. Similarly, establishing a connection between epigenetic pathways in one kingdom establishes precedent for similar relationships in the other. Multicellularity evolved separately in plants and animals, and yet ATP-dependent chromatin remodelers play a critical role in enabling the tissue-specific expression that underwrites development in both kingdoms. We are just beginning to characterize the *in vitro* and *in vivo* activities of remodelers in plants. These studies are likely to substantially increase our knowledge of how remodelers contribute to chromatin structure and gene expression in both kingdoms.

CHD proteins contain conserved domains that contribute to the biochemical outcomes of remodeling.

The targeting of CHD proteins to the genome is through interactions either between DNA or specific post-translational modifications on histone tails. Both subfamily I and II members are targeted to the nucleosome through their chromodomains and PHD zinc fingers. Subfamily (Morris 2014 CHD4 paper says mouse like *Drosophila* with regards to role of remodelers in genome) I members have been shown to preferentially associate with tails of histone H3 containing either di- or trimethylated H3K4 via their chromodomains (Flanagan et al. 2005; Sims et al. 2005; Okuda, Horikoshi, and Nishimura 2007). The targeting of subfamily I members to H3K4me2 or H3K4me3 is proposed to explain how subfamily I members are targeted to the promoters to activate transcription (Hennig et al. 2012; Pointner et al. 2012). Subfamily II members CHD4 and CHD5, in contrast, preferentially associate with tails of histone H3 with unmethylated H3K4, and CHD4 does not bind to nucleosomes in which H3K4me3 is present (Musselman et al. 2012; Oliver et al. 2012). CHD5 is targeted in a similar fashion as CHD4. Both PHD zinc fingers of CHD5 bind to unmodified H3K4 and are required for targeting of CHD5 to the genome (Paul et al. 2013b; Oliver et al. 2012). The chromodomains of CHD5 are also sufficient to bind to H3K27me3 and associates with genes enriched for H3K27me3 *in vivo* (Egan et al. 2013a).

The chromodomains of subfamily I and II along with the PHD zinc fingers of subfamily II members play another role in addition to associating with the correct substrate: they act as a gate to ensure that ATP hydrolysis occurs only upon proper targeting of the proteins (Morra et al. 2012; Hauk et al. 2010). Upon correct targeting with a nucleosome, the chromo domains and PHD zinc fingers undergo a conformational change that allows the ATPase domain to be freed up (Hauk et al. 2010; Morra et al. 2012). Upon the conformational change of the ATPase domain, ATP is able to be hydrolyzed and the CHD protein is able to remodel the nucleosome.

Although subfamily I proteins appear to act as monomers, they are recruited to the genome in concert with different complexes (Pray-Grant et al. 2005; Tran et al. 2000; Tai et al. 2003). Animal subfamily II members, in contrast to subfamily I members, commonly exist as integral members of multisubunit complexes (Xue et al. 1998b; Allen, Wade, and Kutateladze 2013). The data suggest that each individual subfamily II member plays a role in these complexes independently, and these proteins are not found together within these complexes (Hoffmeister et

al. 2017; Nitarska et al. 2016; Bode et al. 2016). Targeting of the Mi2/NuRD complex occurs in two predominant ways. The first is through protein-protein interaction of a protein outside of the Mi2/NuRD complex. An example of targeting the Mi2/NuRD complex is through the c-jun transcription factor (Zhu et al. 2009; Aguilera et al. 2011). The Mi-2/NuRD complex can also be targeted through the various forms of DNA methylation. The Mi2/NuRD complex contains MBD2 which bind to methylated DNA (Ramirez et al. 2012; Gunther et al. 2013). The Mi2/NuRD complex also contains MBD3, which binds to hydroxymethylated DNA, which is abundantly present in neurons and pluripotent cells (Yildirim et al. 2011; Kriaucionis and Heintz 2009; Tahiliani et al. 2009).

As mentioned previously, PICKLE, a plant subfamily II member acts as a monomer (Ho et al. 2013a). However, PICKLE has been shown to interact with the transcription factors PIF3 and BZR1 *in vivo* to regulate genes important for photomorphogenesis, suggesting that PKL is also recruited by protein-protein interactions (Jing and Lin 2013; Jing et al. 2013; Zhang et al. 2014). These transcription factors play a role in promoting the expression of genes important for the skotomorphogenic response (Jing et al. 2013). To date, animal subfamily II members have not been shown to act outside of a complex to perform its biochemical function, as observed in PICKLE. This could mean that animal subfamily II members play a yet undiscovered role outside of the various complexes. In addition to activating expression of H3K27me3-regulated genes, PKL is also targeted to actively transcribed genes like *ACT7* (Zhang et al. 2012). Loss of PKL, however, does not appear to affect expression of these genes (unpublished data). The observation that PKL acts as a prenucleosome maturation factor provides a new biochemical explanation for how PKL promotes retention of H3K27me3 marks and contribute to gene expression (Carter et al. 2018).

Subfamily III members are targeted to the genome through protein-protein interactions as well. CHD7 has been shown to associate with members of the pBAF SWI/SNF complex in neural crest cells (Bajpai et al. 2010), suggesting that CHD7 requires members of the pBAF complex to properly target within these cells. CHD8 has been shown to interact with an insulator protein, CTCF, and a transcription factor, beta-catenin (Ishihara, Oshimura, and Nakao 2006; Thompson et al. 2008). Both of these proteins repress gene transcription, which in turn suggests that CHD8 contributes to transcriptional repression of developmentally regulated genes. CHD8 also exhibits a unique activity by forming a trimeric complex with histone H1 and p53 that inhibits transactivation by p53 (Nishiyama et al. 2009).

CHD proteins contribute to numerous transcriptional effects.

The effect CHD proteins have on transcription depends on the remodeler and context. Subfamily I members are strongly associated with active transcription in yeast and animals (Persson and Ekwall 2010; Biswas, Dutta-Biswas, and Stillman 2007). In yeast, CHD1 is targeted to genes through the C-terminal domain of RNA polymerase II and is not targeted through H3K4me3, as their animal counterparts (Biswas, Dutta-Biswas, and Stillman 2007; Simic et al. 2003). However, Chd1 is likely to function differently to activate transcription in yeast because yeast do not have a gene encoding for histone variant H3.1 (Gaspar-Maia et al. 2009). The ability of CHD1 to act as a transcriptional activator in animals is consistent with its ability to assemble nucleosomes containing H3.3 (Radman-Livaja et al. 2012). In animals, CHD1 activates expression of genes important for pluripotency and plays a role in keeping cells in a pluripotent state (Gaspar-Maia et al. 2009). CHD1 is also required for the activation of genes important for induction of pluripotent stem cells from somatic cells. The plant specific subfamily I member, PKR3 (CHR5), has been shown to associate with the promoters, and similar to CHD1 is required to reduce nucleosome turnover at the transcriptional start site (Shen et al. 2015).

Animal subfamily II members, however, play an important role in repression of tissue specific genes. As an example, CHD5 is a member of a Mi-2/NuRD complex in mammals and targets to genes enriched for the repressive mark H3K27me3 (Potts et al. 2011; Quan et al. 2014; Egan et al. 2013a). However, CHD5 is also necessary for the activation of genes that are required for neuronal differentiation revealing that CHD5 can both repress and activate expression (Egan et al. 2013a). In animals, repression of tissue-specific genes is often mediated by DNA methylation (Lande-Diner and Cedar 2005; Reddington, Pennings, and Meehan 2013). As noted above, the Mi-2/NuRD complex couples DNA methylation with histone deacetylation and subsequent transcriptional repression. CHD remodelers thus contribute to repression of a wide spectrum of genes as a result of incorporation in this complex. Not only does the Mi-2/NuRD repress genes marked with DNA methylation, it also facilitates gene repression by the repressive H3K27me3 histone modification. The CHD4 containing Mi2/NuRD complex has been shown to facilitate recruitment of PRC2 components to its target genes by promoting deacetylation of H3K27Ac (Reynolds et al. 2012). As a result of deacetylation, the PRC2 complex is able to deposite

H3K27me3 (Reynolds et al. 2012). In addition to the Mi2/NuRD complex promoting H3K27me3, CHD5 was also shown to associate with and promote H3K27me3 (Egan et al. 2013a).

It remains to be determined if the role of PKL at genes such as *ACT7*, if any, is related to its role in promoting expression of H3K27me3-regulated loci. The subfamily II member in *Drosophila*, CHD3, targets to heat shock genes during treatment with heat (Murawska et al. 2011). Not only is CHD3 recruited to heat shock genes, but CHD3 plays a role in promoting expression of these genes (Murawska et al. 2011). Understanding the role that *Drosophila* CHD3 plays in gene activation may shed light on the role PKL plays at *ACT7* and vice versa.

Relative to the other CHD subfamilies, little is resolved regarding the biochemical action of these enzymes. The CHD6 ATPase domain was shown to be stimulated by DNA, which is a biochemical characteristic of ATP-dependent remodelers (Lutz, Stoger, and Nieto 2006). Recombinant CHD8 exhibits nucleosomal stimulated ATPase activity, and is able to mobilize a mononucleosome into a central position on a strand of DNA, as observed with other CHD proteins (Thompson et al. 2008). Taken together, these data suggest that animal specific subfamily III members are also likely to mobilize nucleosomes.

Subfamily III member, CHD7, has been extensively studied due to its role in human disease, especially the CHARGE syndrome (Pauli et al. 2012; Sperry et al. 2014). CHARGE syndrome is a developmental disorder that affects the face structure and causes mental retardation in the patients (Hsu et al. 2014). Characterization of the role of CHD7 in CHARGE has revealed that it plays a role in neuronal differentiation (Feng et al. 2013; Bajpai et al. 2010). CHD7 promotes transcription of both *Sox4* and *Sox 10* transcription factors leading to differentiation of neurons (Feng et al. 2013). CHD7 also interacts with components of the pBAF complex and activates genes important for neural crest migration and differentiation (Bajpai et al. 2010). CHD8, in contrast, represses genes that are in the beta-catenin signaling pathway (Thompson et al. 2008). These observations demonstrate that subfamily III members can either activate or repress transcription, much like remodelers belonging to subfamily II.

There has been extensive biochemical and functional characterization of CHD remodelers in yeast and animal systems, and there is a growing body of literature associated with plant remodelers. CHDs in these distinct biological contexts illustrates the malleability with which chromatin directs such emergent properties as transcription. The presence of related CHD remodelers in plant and animals implies the existence of these remodelers in the last common

ancestor of both kingdoms and thus also to shared ancestral functions. By comparing and contrasting the contributions of related remodelers in each kingdom, we may therefore gain insight into how these remodelers contribute to fundamental chromatin-based processes in each. This review highlights the common activities that suggest conserved roles for these remodelers as well as identify potential areas for investigation in one kingdom based on discoveries in the other. Herein, we will compare and contrast the current understanding of the biochemical and functional roles of CHD remodelers from subfamilies I and II in plants and animals, and briefly touch on the animal-specific subfamily III.

CHAPTER 2. EFFICIENT PRODUCTION AND IDENTIFICATION OF CRISPR/CAS9-GENERATED GENE KNOCKOUTS IN THE MODEL SYSTEM DANIO RERIO

2.1 Introduction

The conservation of molecular machinery across eukaryotes underlies the power of using model organisms for research. Many of these model systems facilitate the use of reverse-genetic approaches such as targeted gene knockouts to characterize the contribution of a gene product to a biological or disease process of interest. Gene disruption techniques in organisms such as zebrafish have historically relied on targeted introduction of frameshift mutations that result from imprecise repair of double-strand breaks (DSBs)(Urnov et al. 2010; Hsu and Zhang 2012). When a DSB is introduced into the genome, the DNA lesion is repaired through one of two pathways that are universally present in nearly all cell types and organisms: non-homologous end joining (NHEJ) and homology-directed repair (HDR)(Shrivastav, De Haro, and Nickoloff 2008; Chapman, Taylor, and Boulton 2012). The imprecise nature of the NHEJ machinery frequently produces insertions and/or deletions (indels) of various lengths(Lieber 2010; Bee et al. 2013; Betermier, Bertrand, and Lopez 2014; Chang et al. 2017; Davis and Chen 2013). Introduction of frameshift mutations in the coding sequence of a gene can produce a premature stop codon, which often renders the gene nonfunctional.

Early genome engineering strategies in zebrafish to promote indels included meganucleases, zinc-finger nucleases, and transcription activator-like effector nucleases, all of which utilized DNA-protein interactions to target a nuclease to a specific genomic target where it introduced a DSB(Ata, Clark, and Ekker 2016; Sertori et al. 2016; Varshney, Sood, and Burgess 2015; Liu et al. 2014; Xiao et al. 2013; Dahlem et al. 2012). However, these technologies are often difficult to apply due to the laborious and complex engineering needed to generate a nuclease that targets the DNA sequence of interest. Unlike previous strategies, CRISPR-based gene editing does not rely on protein-DNA interactions for targeting. Instead, the CRISPR-associated (Cas) endonuclease is directed via an RNA guide that uses nucleotide base-pairing interactions to target a genomic site of interest(Ran, Hsu, Wright, et al. 2013; Enriquez 2016; Sander and Joung 2014; Jinek et al. 2012; Garneau et al. 2010; Gasiunas et al. 2012). Due to the simplicity of designing a RNA guide with the desired base pairing interactions for targeting it is relatively easy to target the Cas endonuclease

to the desired locus. The type II CRISPR system in particular has been widely developed for genome editing applications due to several advantageous features including use of a single multidomain Cas nuclease (Cas9) that requires interaction with DNA to stimulate endonuclease activity and use of a single guide RNA (sgRNA) to target it to the cognate DNA sequence (Sander and Joung 2014). The sequence requirements necessary for targeting of the cognate sgRNA are well understood (Jinek et al. 2012), and the desired sgRNA is easily generated by *in vitro* transcription. The simplicity and robustness of the CRISPR/Cas9 approach greatly facilitates targeted genetic modification in zebrafish a wide variety of other organisms.

The enhanced ability to undertake targeted genome editing in zebrafish as a result of developing CRISPR-based reagents has significantly increased the opportunity to study processes emblematic of vertebrate organisms such as development of the central nervous system. The zebrafish genome contains orthologs of 70% of the protein-coding genes found in the human genome as well as 84% of genes associated with diseases in humans (Howe et al. 2013). Zebrafish development exhibits several key qualities that enhance its use in reverse genetic studies: the embryos are laid in large clutches, develop externally from the mother making them amenable to genetic manipulation by microinjection, and adult zebrafish sexually mature by 3 months of age, allowing for rapid propagation of desired lines (Ota and Kawahara 2014).

Numerous protocols are available that describe a variety of approaches to generate and identify CRISPR-derived indels in zebrafish (Samarut, Lissouba, and Drapeau 2016; Yu et al. 2014; Talbot and Amacher 2014; Prykhozhij, Rajan, and Berman 2016; Burger et al. 2016; Varshney et al. 2016; Xie et al. 2016; Vejnar et al. 2016). However, many of these procedures are time intensive, require access to expensive equipment, and can be challenging for labs with limited expertise. The steps described herein provide a simple, robust, and economical CRISPR/Cas9 strategy to engineer zebrafish knockout lines. This protocol describes the use of a highly efficient kit to synthesize sgRNAs using DNA oligonucleotides (oligos), similar to other approaches that have been previously described (Gagnon et al. 2014). The described protocol includes two steps in particular that greatly simplify analysis of CRISPR-mutated lines: step-by-step use of the PCR-based heteroduplex mobility assay (HMA) (Ota et al. 2013) to easily determine the presence of genome modifications, and sequencing analysis of heterozygous zebrafish to rapidly and easily determine the nature of multiple indels in an economical fashion. In addition, step-by-step instructions are included for robust selection, reliable production, and injection of guide RNAs.

The steps provided here exemplify a robust, relatively inexpensive protocol that enables laboratory personnel with a range of expertise to contribute to the identification of gene knockouts in zebrafish.

2.2 Protocol

This study was carried out in strict accordance with the recommendations in the Guide for the Care and Use of Laboratory Animals of the National Institutes of Health. The protocol was approved by the Purdue Animal Care and Use Committee (PACUC number 08-031-11).

1. Design of Template-Specific Oligos for Guide RNA Production

1.1. Select the target region of interest to be modified in the coding region of the gene. This should be close to the 5' end of the gene to generate a truncated protein, but not so close such that a subsequent in-frame start codon enables production of a protein with a modest N-terminal truncation.

Note: One way to preclude this possibility is to scan the downstream coding region of the gene for an in frame start codon. In addition, using a guide RNA that targets the middle of a large exon, can help to identify PCR primers for subsequent scoring of the resulting indel.

1.2. Identify potential guide sites in the genomic region of interest using a guide RNA selection program (see Table of Materials)(Montague et al. 2014; Haeussler et al. 2016; Oliveros et al. 2016). Set the browser data to *Danio rerio* and the protospacer adjacent motif (PAM) sequence to 5'-NGG-3'.

Note: Ideal gRNA sequences contain a 5'-G in the first position of the gRNA for efficient T7 *in vitro* transcription. If no acceptable guide is found with a G at the 5' position, the 5' base of another guide can be altered to a G or a G can be added onto the 5' end of the guide RNA, but this may reduce cutting efficiency(Cho et al. 2014). To maximize the cutting efficiency, an optimal guide sequence has 40-80% GC content (higher is better), and contains a G at the 20th position, adjacent to the PAM, but is not required(Wang et al. 2014). An example of an ideal

targeting sequence: 5'- G (N)₁₈ G -3' -NGG in which the PAM is underlined. In addition to examining the results from the guide RNA selection program to identify optimal guide RNAs as described above, care should be taken to avoid guide RNAs with predicted strong off-target effects which greatly complicate downstream analysis. In particular, guide RNAs with predicted off-target effects that fall within coding regions should be excluded, and the total off-target sites predicted should be minimized.

1.3. From the output of the guide RNA design tool, exclude the PAM sequence (5'- NGG -3'), it is not used for targeting but comprises the recognition sequence for Cas9 cleavage.

1.4. To the remaining 20 nucleotides (nts), add the T7 promoter sequence and the overlap sequence (region complementary to a scaffold oligo used to synthesize full length sgRNAs supplied in the recommended *in vitro* transcription kit) in the order indicated below to obtain a 54 nt oligo:

T7 promoter sequence: 5'- TTCTAATACGACTCACTATA -3'

Guide RNA sequence 5'- G (N)₁₈ G -3'

Overlap sequence: 5'- GTTTTAGAGCTAGA -3'

1.5. Identify PCR primers that flank the predicted cut site (Cas9 cleaves 3 nt upstream of the PAM sequence) at a distance of 50-150 base pairs (bp) each from the cut using web-based software (see Table of Materials).

Note: These will be used in a later step for measurement of cutting efficiency. If no suitable primers are identified using these constraints, another guide RNA site may need to be considered.

1.6. Order 54 nt oligonucleotides to produce the guide RNA and PCR primers for analysis of the target sites (see Table of Materials).

Note: As an optional positive control, it may be helpful to produce a sgRNA targeting a gene necessary for production of pigment to verify the performance of this protocol using an easily

scored visual phenotype (see Figure 2.1 for representative results). A common target is the gene tyrosinase, using the oligo (guide RNA sequence is underlined)(Jao, Wente, and Chen 2013):

5'-

TTCTAATACGACTCACTATAGGACTGGAGGACTTCTGGGGGTTTTAGAGCTAGA -
3'.

2. Preparation of CRISPR-reagents for Embryo Microinjection

2.1. Order commercially available Cas9 protein (see Table of Materials).

Note: Injection of Cas9 mRNA can also be used to generate indels in zebrafish(Ota et al. 2014; Hisano, Ota, and Kawahara 2014), however zebrafish embryo microinjection with Cas9 protein has been shown to be more efficient(Kotani et al. 2015; Gagnon et al. 2014).

2.1.1. Suspend the Cas9 protein in the supplied buffer to generate a 1 mg/mL solution. Store the solution in injection-ready aliquots in PCR tubes at -80 °C to minimize the number of freeze-thaw cycles. To generate a 5 µL injection solution, 2 µL of 1 mg/mL Cas9 solution is used, therefore the Cas9 can be aliquoted in 2 µL aliquots using PCR strip-tubes.

2.2. Synthesize the sgRNA using the sgRNA *in vitro* transcription kit (see Table of Materials). Perform the *in vitro* transcription as per the manufacturer's instructions.

Note: Maintain RNase-free technique during all synthesis, clean-up and injection solution preparation steps. For example, use disposable gloves and change them frequently, use tubes and tips that are certified RNase-free, and clean surfaces and pipettes with commercially available solutions to decontaminate labware (see Table of Materials).

2.3. Purify the synthesized sgRNA using an ammonium/acetate precipitation using RNase-free technique.

Note: Alternatively, sgRNAs can be purified using a variety of commercially available column-based RNA clean up kits for a relatively modest cost.

2.3.1. Add 25 μ L of 5 M ammonium acetate and vortex to mix thoroughly.

Note: Ammonium acetate solution is commercially available (see Table of Materials), or a 5 M solution can be made in house by adding 385.4 mg of molecular grade ammonium acetate to 1 mL of RNase-free water and stored at -20 °C.

2.3.2. Add 150 μ L of 200-proof nuclease-free ethanol to each sample. Place the reaction in a -80 °C freezer for a minimum of 20 min.

Note: The samples can be stored overnight at -80 °C, but will not significantly increase the total RNA yield.

2.3.3. Centrifuge the samples at maximum speed (>16,000 x g) in a 4 °C microcentrifuge for 20 min.

2.3.4. Remove the supernatant carefully by slowly pipetting off the liquid, ensuring the RNA pellet is not disturbed.

2.3.5. Add 1 mL of 70% ethanol (created by diluting nuclease-free ethanol in RNase-free water) and gently mix the tube by inverting it several times to wash residual salt from the tube.

2.3.6. Repeat the centrifugation step for 7 min.

2.3.7. Remove the supernatant by first pipetting off most of the solution using a P1000 pipette, then use a P200 pipette to remove as much solution as possible without perturbing the pellet. Dry the RNA pellet in a clean space, such as a laminar flow hood or a bench top being careful to avoid RNase contamination, for 15 min or until no more liquid drops are visible in

the tube.

2.3.8. Resuspend the pellet in 30 μL of RNase free water, quantify the product (for example using a spectrophotometer) and aliquot the solution for long-term storage in a $-80\text{ }^{\circ}\text{C}$ freezer.

Note: Typical concentrations range from 800-2500 $\text{ng}/\mu\text{L}$.

2.4. (OPTIONAL) Verify that full-length RNA has been generated using urea/PAGE. Alternatively, use an agarose gel to verify that the RNA is intact.

Note: However, if using an agarose gel a larger amount of gRNA must be run to visualize the RNA, and the length cannot be accurately determined. When analyzing the efficiency of target cutting after injection of the reagents into the fish, if there is no or little cutting the sgRNA should be checked for degradation.

2.4.1. Cast an 8% polyacrylamide gel in TBE with 40% polyacrylamide (19:1) and 8 M urea using RNase-free technique for the solutions and equipment (Summer, Gramer, and Droge 2009).

Note: Commercially available materials can be used to clean equipment (see Table of Materials).

2.4.2. After the gel has completely solidified (approximately 30 min), equilibrate the gel by placing it in TBE running buffer and performing electrophoresis for 30 min at 5 V/cm.

2.4.3. Mix 300-500 ng of sgRNA with an equal volume of 2x RNA gel loading dye (see Table of materials). Using a P1000, clear the wells of any debris by pipetting running buffer in each well several times. Load the solution(s) and run the gel at 10 V/cm for 2.5 h.

Note: A marker lane here is useful to visual the length of the RNA but is not required, generally it is readily apparent if full length RNA has been synthesized (see Figure 2.2).

2.4.4. Visualize the bands using a nucleic acid stain (see Table of Materials).

Note: sgRNA bands should appear as a single band, whereas smearing indicates RNA degradation, (see Figure 2.2 for example).

3. Microinjection of CRISPR-components into Zebrafish Embryos

3.1. Set up breeding tanks the night prior to injecting by placing the number of desired males and females (typically 2 females and 1 or 2 males) in a breeding tank with a divider in place (Nasiadka and Clark 2012).

3.2. Prepare a microinjection plate with 1.5% agarose in 1x E3 media (see Table of Materials) with 0.01% methylene blue (a fungicide) by pouring 35 mL of the melted agarose into a 10 cm petri dish and gently lay a plastic mold to create wedge-shaped troughs into the solution, tapping the mold to eliminate air bubbles.

3.3. Allow the agarose to set, and store the dish with a small amount of media and wrapped in paraffin film to prevent the plate from drying out at 4 °C.

Note: Injection plates are reusable for several weeks, until the wells become deformed or dry or the plate begins to grow mold.

3.4. On the morning of injecting, thaw purified sgRNA and Cas9 protein on ice. Remember to handle all materials with gloves to prevent RNase contamination and to use RNase-free tips and tubes.

3.5. Generate a 5 µL injection solution by combining Cas9 protein and the sgRNA in a 2:1 ratio of Cas9: sgRNA to obtain final concentrations of 400 pg/nL Cas9 protein and 200 pg/nL sgRNA. Incubate the Cas9/sgRNA solution at room temperature for 5 min to allow the Cas9

and sgRNA to form a ribonucleoprotein complex. Add 0.5 μ L of 2.5% wt/vol phenol red solution (see Table of Materials), and RNase-free water to a final volume of 5 μ L.

Note: The ionic strength of the solution has been shown to affect the solubility of the Cas9/sgRNA complex, therefore addition of KCl may increase the cutting efficiency of sgRNAs that exhibit low indel formation (Burger et al. 2016).

3.6. Make an injection needle by pulling a 1.0 mm glass capillary using a micropipette puller using the manufacturers recommended settings (see also Table of Materials). Cut the tip of the freshly-made needle using a new razor blade or forceps to obtain an angled opening that will easily pierce the chorion and yolk sac.

3.7. Place the needle in a micromanipulator attached to a microinjector with the air source turned on. Under a light microscope using the magnification suitable for the calibration determined for the particular apparatus, adjust the injection pressure until the needle consistently ejects a 1 nL solution into a petri dish filled with mineral oil.

Note: The quality of the needle is critical. Practice producing a needle and injecting into the yolk sac of embryos until this skill is mastered before attempting further experiments (Rosen, Sweeney, and Mably 2009).

3.8. Remove the divider and allow the fish to breed for approximately 15 min.

Note: Longer breeding times will produce more embryos, however the injection should be completed while the embryos are at the 1-cell stage to maximize the chance that Cas9 cutting will occur early and therefore decrease genetic mosaicism. Embryos can be injected at later stages (2-4 cell stages), but this may possibly decrease the germline transmission rate of the modified allele.

3.9. Collect the eggs using a strainer and rinse them into a 10 cm petri dish using 1x E3 media with 0.0001% methylene blue. Examine the health of the eggs under the light microscope, removing any unfertilized eggs and debris.

3.10. Set aside 10-15 embryos as an uninjected control in a separate, labeled petri dish.

3.11. Using a transfer pipette, gently line up the eggs on the injection plate warmed to room temperature.

3.12. Under a dissecting microscope at 2.5X magnification, inject 1 nL of the solution into the yolk sac of each embryo to inject a total of 400 pg of Cas9 protein and 200 pg of sgRNA.

Note: To increase cutting if desired/necessary, increase the final concentration of Cas9 protein to 800 pg/nL and of sgRNA to 400 pg/nL in the injection solution, however this may also increase off-target cutting and/or decrease embryo health. Cutting efficiency may also be increased by injecting directly into the cell (Xu 1999), however injection into the yolk sack is technically less demanding and gives sufficient cutting to produce fish with high germline transmission (>70% of offspring containing a modified allele).

3.13. Return the injected embryos to a properly labeled Petri dish and cover them with 1x E3 media with 0.0001% methylene blue and put them in an embryo incubator set to 28 °C.

3.14. At 24 hours post fertilization (hpf), inspect the health of the injected embryos, removing dead or abnormally developing individuals and change the media (see Figure 2.3 for example). Check the rate of survival against the uninjected control.

Note: When targeting a nonessential gene, less than 10% lethality is expected relative to the uninjected control. If elevated levels of lethality are observed in the guide-injected populations compared to the uninjected control, it may indicate that the targeted gene is essential for development, or off-target effects are leading to failed development. Reducing

the amount of injected CRISPR-reagents may be necessary or generation of a new sgRNA with reduced off-target effects.

3.15. Return the embryos to the incubator and continue growing the embryos to 72 hpf, changing the media daily to maintain embryo health.

4. Analysis of Efficiency of Indel Formation using a Heteroduplex Mobility Assay

4.1. Collect two sets of five embryos from the injected plates grown to 72 hpf into microcentrifuge tubes and collect one set of five embryos from an uninjected control.

4.2. Anesthetize the embryos by adding 0.004% MS-222 (tricaine) and wait 2 min.

4.3. To extract the genomic DNA (gDNA), gently pipette the media off each embryo set and add 45 μ L of 50 mM NaOH. Incubate the embryos at 95 $^{\circ}$ C for 10 min.

4.4. Remove embryos from the heat source and cool to room temperature. Add 5 μ L of 1 M Tris-HCl pH=8, and vortex the samples vigorously (5-10 s). Centrifuge the solution at max speed ($>16,000 \times g$) in a room temperature microcentrifuge for 3 min. Transfer the supernatant to a clean, labeled tube and store the gDNA at -20 $^{\circ}$ C DNA for up to 6 months.

Note: DNA fragments of approximately 900 bp and smaller will be generated through use of this protocol.

4.5. Set up a 50 μ L PCR reaction using 2 μ L of the prepared gDNA from each sample (including an uninjected control) per the instructions included with the polymerase, using the previously designed primers flanking the predicted cut site.

4.6. Purify the PCR products using a PCR clean up kit (see Table of Materials), elute the samples in 30 μ L of water or elution buffer and quantify the DNA using a spectrophotometer.

4.7. Reanneal all 30 μ L of each purified PCR product by placing the tubes in a floatable rack in a boiling water bath (approximately 150 mL in a 500 mL beaker). After 3 min, turn off the heat source and allow the solutions to cool to room temperature, about 1 h.

Note: This step first denatures the DNA and then allows the strands to reanneal randomly to generate possible heteroduplex bands, or mismatched double-strand DNA that contains polymorphisms created by CRISPR-mutagenesis and therefore have an altered electrophoretic mobility compared to homoduplexes. Last cycle of PCR or ramp-down program in thermocycler can also be used to reanneal products (Yin, Maddison, and Chen 2016; Yin, Jao, and Chen 2015), but use of boiling bath may yield improved resolution of heteroduplex products.

4.8. Add 5 μ L of 6X loading dye (see Table of Materials) to the reannealed PCR solutions.

4.9. Cast a 15% polyacrylamide/TBE gel using 30% polyacrylamide (29:1). After the gel has set, place it into an electrophoresis apparatus with TBE running buffer. Using a P1000, clear the wells of any debris such as residual salts or gel fragments that can obstruct the wells by gently pipetting buffer up and down into the wells several times.

4.10. Load 500 ng of the reannealed PCR products, loading a control (sample from uninjected fish) next to each set of sgRNA samples. Run the gel at 150 V for 2.5 h or until the dye front is at the bottom of the gel.

4.11. Visualize the bands using a nucleic acid stain (e.g. ethidium bromide or SYBR green (see Table of Materials)).

4.12. Examine the band pattern for each control and CRISPR-injected pool of embryos.

Note: Appearance of multiple bands that run slower in the injected versus uninjected lanes indicates formation of novel heteroduplex products (see Figure 2.4 for an example). The presence of novel heteroduplex DNA indicates insertions and/or deletions (indels) were

generated by the CRISPR-injection. Reduction in the homoduplex band intensity in the injected solutions of approximately 50% or greater is generally sufficient to result in sufficient germline transmission. Additionally, extra bands are sometimes identified in the uninjected fish, and should not be considered heteroduplex bands when observed in the injected fish.

4.13. Choose the injections with highest cutting efficiencies relative to the uninjected control for each target, embryos from these injections can be used to grow up fish to look for indels causing premature stop codons.

Note: For highly efficient cutting (reduction in the homoduplex band by approximately >50% intensity), screening 20-30 adult fish should be sufficient to obtain germline transmission. For sgRNAs that generate less cutting, more adult fish may be needed to increase the likelihood of identifying fish that exhibit germline transmission of modified alleles containing a premature stop codon. If indel formation is not observed it may be necessary to redesign the sgRNA to a different region of the gene. If no heteroduplex band formation is observed, the sgRNA may have been degraded, and the sgRNA quality should be verified using a urea/PAGE gel.

5. Identification and Propagation of Knock-out Lines

5.1. To identify a potential founder parent fish, perform tail clips of the adult F0 fish (grown to approximately 2.5-3 mo) to identify presence of indels. Anesthetize the fish in 0.62 mM tricaine (see Table of Materials for recipe), then use a clean, sharp razor blade to remove approximately 1/2-3/4 of the tail fin.

5.2. Place the tail in 45 μ L of 50 mM NaOH, and return the fish to a recovery tank. Perform the gDNA extraction as described (4.2-4.4). Once the fish resumes normal swimming behavior, place the fish back on flowing system water until the nature of the indel is identified.

Note: It is critical to ensure that individual fish are identifiable, and can be appropriately matched to the results of the tail clips.

5.3. As described (Step 4.5-4.9), perform a HMA on the tail clip gDNA to determine if the fish was modified by the CRISPR injection (Figure 2.5). To identify a founder fish, breed the adults that exhibit heteroduplex bands from tail gDNA to wild-type fish. Collect the embryos and grow them to 72 hpf.

5.4. At 72 hpf, collect 10 embryos and place each embryo in an individual tube. Perform a genomic DNA extraction as described above (Step 4.2-4.4) using 11.25 μ L of 50 mM NaOH and 1.25 μ L of 1 M Tris pH=8.

5.5. Repeat the PCR and electrophoresis to identify heteroduplex bands as described above (Step 4.7-4.13) to determine if indel alleles have been passed on to this generation (Figure 2.6).

5.6. Based on the percent transmission observed in single embryos using the heteroduplex mobility assay (HMA), grow an average of 20-30 embryos obtained by the cross for each CRISPR-lines of interest to adulthood.

Note: Number may be increased or decreased depending on the frequency of germline transmission.

5.7. Perform tail clips of the adult F1 fish to identify presence of indels as described (Step 5.1-5.2). As described (Step 4.5-4.11), perform a HMA on the tail clip gDNA to determine if the fish carries an indel (Figure 2.7).

5.8. For fish that contain a heteroduplex band, prepare the DNA for sequencing analysis using the following steps (5.8.1-5.8.2).

5.8.1. Perform PCR using new primers to amplify a 300-600 bp PCR product centered around

the cut site.

5.8.2. Use a PCR purification kit to clean up the DNA, and elute in 30 μ L. Examine the DNA on an agarose gel to ensure a single band is present.

Note: Some heteroduplex banding may be present on the agarose gel and appears as a small smear or double band just above the PCR product at the expected size.

5.9. If one to three indels are analyzed, sequence the PCR products using Sanger sequencing and determine the sequence of the indel using a bioinformatics tool(Hill et al. 2014).

Otherwise, determination of sequence of multiple PCR products using NGS analysis (See Table of Materials) is more economical.

5.10. Determine if a premature stop codon has been obtained by analyzing the sequence using a bioinformatics tool (see Table of Materials).

5.11. Place fish containing desired mutant allele into a new tank with appropriate label.

5.12. Design PCR primers for specific indel alleles for future genotyping needs. These primers should span the mutated sequence and not amplify the wild-type sequence.

5.13. In-cross heterozygous zebrafish to generate a segregating population that will contain 25% knock-out lines.

2.3 Representative Results

The experimental approaches described in this protocol allow for efficient, cost-effective production of zebrafish knock-out lines using CRISPR/Cas9 technology. The following figures have been included in this article to facilitate interpretation and troubleshooting of the results obtained using this protocol. Following successful production and microinjection of CRISPR-reagents, the zebrafish embryos can be analyzed for overt phenotypes and for indel formation using HMA. A helpful control to visualize the success of the CRISPR-experiment is the use of the

sgRNA described in Step 1.5 to target the pigment-producing gene tyrosinase. Cas9-induced indel formation at tyrosinase results in loss of pigmentation and is easily scored by 48 hpf (Figure 2.1). Another helpful control to ensure that preparation of the CRISPR-reagents for injection has been successful, is to verify that full-length (120 nt) sgRNA has been synthesized using a denaturing polyacrylamide gel (Figure 2.2, Lane 1 and 2). If the RNA has been degraded it may appear as a smear, for example Lane 3 (Figure 2.2) shows degraded RNA that is not suitable for injection.

To analyze the indel formation frequency of genes targeted by CRISPR-Cas9 that do not result in overt phenotypes such as tyrosinase, HMA analysis is a simple and reliable method. sgRNA/Cas9 injected embryos analyzed using HMA results in the formation of heteroduplex bands, and reduction of the intensity of the homoduplex band (Figure 2.4). Presence of heteroduplex bands is further utilized in this protocol to identify potential founder fish from the microinjected embryos and as adults (Figure 2.4 and 2.5), to analyze the germline transmission efficiency of a founder (Figure 2.6), and to verify presence of an indel in a heterozygous F1 fish (Figure 2.7). The heterozygous fish that contain an indel are candidates for NGS to identify the nature of the indel and to determine if a premature stop codon is present in the coding region of the target gene.

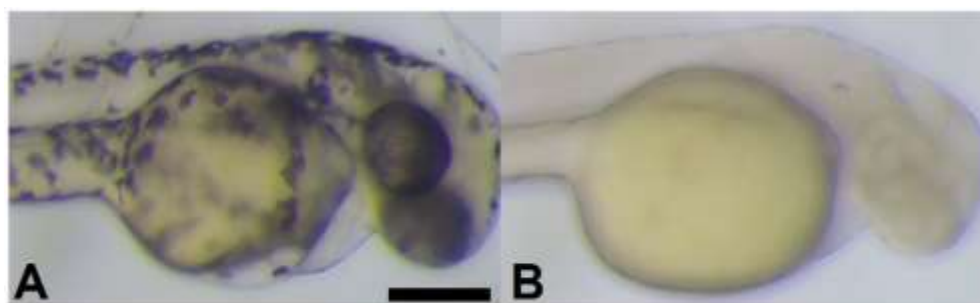


Figure 2.1 Zebrafish embryos exhibit a pigment defect when injected with a sgRNA targeting *tyrosinase* at the one-cell stage.
(A) Wild-type, uninjected embryo at 48hpf and (B) injected embryo at 48hpf.

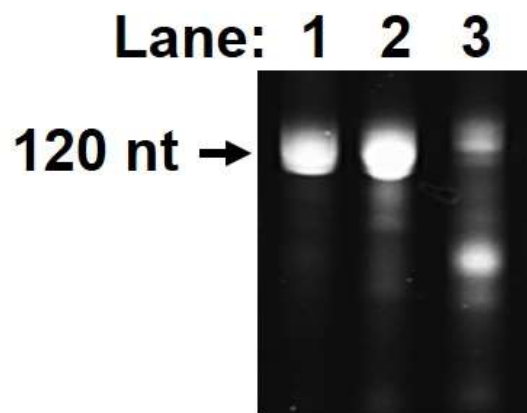


Figure 2.2 *In vitro* transcription of sgRNA using synthesis kit. Oligos were synthesized using *in vitro* transcription according to the sgRNA synthesis kit instructions. 500 ng of RNA was run on a urea/PAGE gel as described. sgRNA loaded in lanes 1 and 2 show a band corresponding to the full length, intact 120 nt RNA. The sgRNA in lane 3 shows a degraded RNA sample that is not suitable for injection.

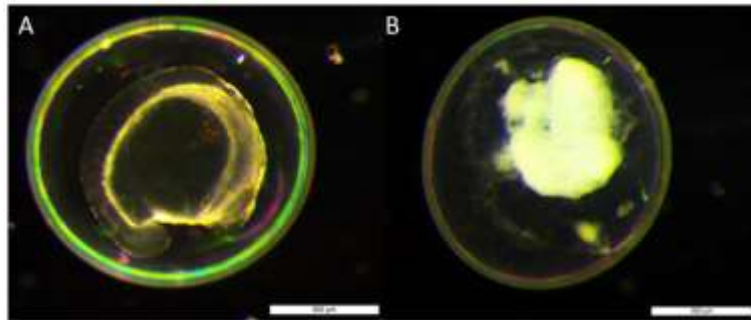


Figure 2.3 Comparison of the health of 24 hpf injected embryos. A living embryo (A) developed to 24 hpf, is easily identified compared to an embryo that aborted development (B). Embryos that resemble (B) or have drastically altered features to (A), such as spinal curvature or altered head and eye development should be removed from dish.



Figure 2.4 Heteroduplex mobility assay of sgRNA-Cas9 microinjected zebrafish embryos. Pools of 5 embryos per sample were collected at 72 hpf and gDNA was extracted. Heteroduplex analysis was performed as described, samples were loaded equally with 500 ng of DNA. Lanes: M= 100 bp marker, 1= uninjected control, 2= injection sample 1, 3= injection sample 2. Expected band size= 98 bp.

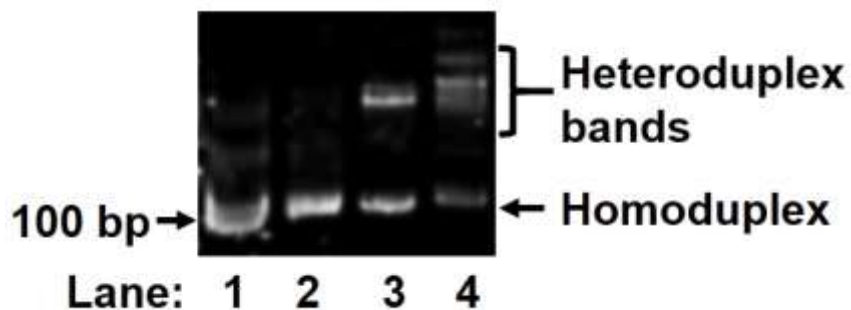


Figure 2.5 Heteroduplex mobility assay of gDNA extracted from the tail of an adult CRISPR-injected zebrafish.

Embryos that were injected with an sgRNA and Cas9 protein were grown to adulthood (3 months). Fish B and C exhibit heteroduplex bands and were subsequently bred to identify germline transmitted indels, fish A was not used in subsequent analysis because it does not exhibit a positive heteroduplex band. Lanes: 1= wild-type control, 2= Fish A, 3= Fish B, 4= Fish C. Expected band size= 98 bp.

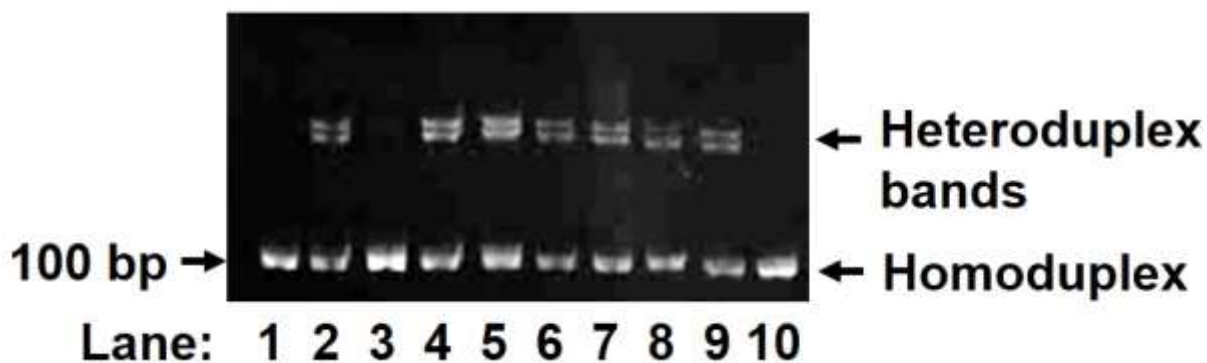


Figure 2.6 Heteroduplex mobility assay of single embryos generated by breeding a F0 CRISPR-injected zebrafish to a wild-type fish to identify germline transmitted indels. Zebrafish were mated, and the F1 embryos grown for 72 h. Single embryos were collected and heteroduplex analysis performed as described. Lanes: 1= wild-type control, 2-10= a single F1 embryo per lane. This gel shows that 7 out of 10 embryos show a positive heteroduplex band, indicating a germline transmission rate of 70% of the indel. Expected band size= 98 bp.

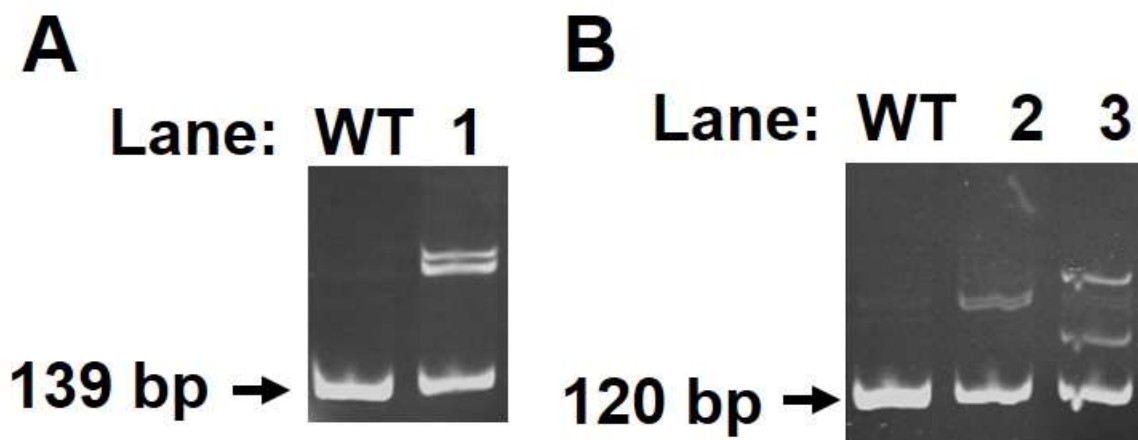


Figure 2.7 Heteroduplex mobility assay of adult F1 zebrafish tail clips.

Adult F1 fish were scored by HMA to identify indels. Fish that exhibited a positive heteroduplex band were PCR amplified and submitted for wide sequencing analysis to determine the nature of the mutation. (A) Lanes: 1= wild-type control, 2= fish A (4 bp deletion, 1 bp mismatch). (B) These F1 fish were identified from the same founder, and yet show different heteroduplex patterning, indicating germline transmission of multiple modified alleles from a single founder. Lanes: 1= wild-type control, 2= fish B (4 bp insertion, 7 bp mismatch), 3= fish C (4 bp deletion, 4 bp mismatch). Each of these indels created a premature stop codon in the coding sequence of the target gene, as determined by NGS.

2.4 Discussion

This protocol describes the production of gene knockouts in the zebrafish vertebrate model system using CRISPR-Cas9 technology. A number of protocols have previously been described to undertake CRISPR-mediated genome engineering in zebrafish (Cong et al. 2013; Dahlem et al. 2012; Hwang et al. 2015; Gonzales and Yeh 2014; Yu et al. 2014; Talbot and Amacher 2014). This protocol builds on previous efforts by combining a number of simple yet reproducibly consistent experimental techniques, in particular HMA and next generation sequencing of multiple heterozygous fish, to create a straightforward, economical, and experimentally robust protocol for CRISPR-mediated mutagenesis in zebrafish that is appropriate for labs staffed with personnel with a range of training and experience and also teaching labs.

Recommendations for design and synthesis of guide RNAs are included in this protocol. A major consideration in guide RNA design is the minimization of off-target effects. Several prediction algorithms have been developed to allow CRISPR-users to access computation tools with use-friendly graphical interfaces that predict both the activity of the on-target guide and the

chance of off-target effects(Haeussler et al. 2016; Montague et al. 2014; Oliveros et al. 2016). A specific advantage of the zebrafish system is lowered rates of off-target effects because the Cas9 is injected into the embryos and therefore expression is transient, which has been shown in mice to result in decreased off-target effects(Iyer et al. 2015). Nevertheless, off-target effects have been demonstrated to occur in zebrafish(Hruscha et al. 2013). One way to control for off-target effects is to phenotype founder zebrafish that have been generated by two independent guide RNAs that target the same gene, as these guides would be very likely to affect different off-target sites. An alternative method to minimize off-target effects that is not described in this protocol is the use of a mutated Cas9 that generates single strand breaks at the target DNA, which are repaired highly efficiently. Pairing DNA nicks within proximity of one another that are complementary to the opposite strands results in effective indel formation at the desired locus and minimizes off-target effects(Shen et al. 2014; Ran, Hsu, Lin, et al. 2013).

In addition to having different rates of off-target effects, different sgRNAs can have different rates of mutagenesis of the desired target(Wang, Yang, et al. 2013; Ren et al. 2014; Fu, Reyon, and Joung 2014). This protocol uses HMA to analyze the efficiency of mutagenesis of a given sgRNA using heteroduplex band formation(Ota et al. 2013; Ota et al. 2014). Heteroduplex bands are created by hybridization of PCR-generated DNA strands that contain mismatches, and can be easily resolved using gel electrophoresis. Unlike other methods commonly used to measure indel formation, such the T7 endonuclease assay or high resolution melt analysis(Yu et al. 2014; Talbot and Amacher 2014), HMA does not require an expensive enzyme to cut mismatched DNA, and does not require complicated analysis of PCR melt curves. Importantly, using HMA to verify high rates of indel formation in the injected population also enables the investigator to minimize the number of fish needed for subsequent production of knock-out lines, which reduces the cost of identifying a mutation with the desired characteristics.

The relative ease of generating CRISPR-based indels enables creation of multiple alleles of multiple genes at once. Web-based software is available for analysis of single mutations from heterozygous fish using Sanger sequencing of PCR products(Hill et al. 2014). In the case where three or more CRISPR-mutated alleles are analyzed, next generation sequencing (NGS) to characterize the nature of the indel is likely to be more cost effective to characterize the nature of the indel as this approach allows a pool of up to 50 different alleles to be characterized at once (see

Table of Materials)(Bell et al. 2014; Jung et al. 2017; van Dijk et al. 2014). Such economy of scale would likely be particularly useful in an undergraduate laboratory setting.

In summary, this protocol provides step-by-step directions for reproducibly generating high quality CRISPR-reagents (in particular sgRNA) such that fewer adult fish need to be created and analyzed to successfully identify the mutant alleles of interest, which also reduces the time and cost of generating the desired lines. Importantly, this protocol has been designed such that it can be applied by laboratories with limited resources to produce mutant zebrafish in an affordable manner. Furthermore, we have found that this approach is suitable for undergraduates and thus expands the opportunities for education and training of undergraduate students interested in hands-on experience in CRISPR-based genome editing.

Table 2.1 Table of materials to perform CRISPR/Cas9 experiments in zebrafish by this protocol.

Name of Material	Company	Catalog No.	Comments/Description
CRISPOR			sgRNA analysis software. http://crispor.tefor.net/
Breaking-Cas			sgRNA analysis software. https://omictools.com/breaking-cas-tool
ChopChop			sgRNA analysis software. https://chopchop.rc.fas.harvard.edu/
Primer 3			PCR primer design. http://bioinfo.ut.ee/primer3-0.4.0/
Rnase free technique			http://genomics.no/oslo/uploads/PDFs/workingwithrna.pdf
RNase-free water	Any brand		Synthesis of guide RNAs. Thermo Fisher and Qiagen both carry suitable water.
Rnase-free ethanol	Any brand		Molecular biology grade ethanol is Rnase free. Fischer, VWR sell suitable ethanol.
Cas9 Protein	PNA Bio	CP01	Cas9 protein with nuclear localization signal.
Target specific oligos	Integrated DNA Tech. (IDT)		Synthesize guide RNAs.
Primers flanking gRNA cut site	Integrated DNA Tech. (IDT)		Use for heteroduplex analysis, 100-300 bp product.
Primers flanking gRNA cut site	Integrated DNA Tech. (IDT)		Use for sequencing CRISPR-alleles, 300-600 bp product recommended.
EnGen sgRNA Synthesis Kit	New England BioLabs	E3322	<i>In vitro</i> transcribe guide RNAs.
10X TBE	Thermo Fisher	B52	RNase-free buffer for electrophoresis of nucleic acids.
6X Load Dye	New England BioLabs	B7025S	Loading DNA for electrophoresis.
5M Ammonium acetate	Thermo Fisher	AM9071	Clean up reagent for purification of guide RNAs.
Ethanol (200 proof, nuclease-free)	Any brand		Clean up reagent for purification of guide RNAs. Molecular grade materials are RNase free.

Table 2.1 continued

RNase away	Thermo Fisher	10328011	Eliminates RNase contamination from surfaces, equipment, glassware.
DNA Ladder, 100 bp	New England BioLabs	N0467S	Molecular weight standards for gel electrophoresis of DNA.
DNA Ladder, 1 kb	New England BioLabs	N0552S	Molecular weight standards for gel electrophoresis of DNA.
RNA Ladder	New England BioLabs	N0364S	Single strand RNA marker to verify that full length sgRNA has been synthesized
TEMED	Thermo Fisher	17919	Casting polyacrylamide gel.
Ammonium persulfate (APS)	Sigma-Aldrich	A3678	Casting polyacrylamide gel.
40% Polyacrylamide (19:1)	BioRad	161-0154	Casting denaturing polyacrylamide gel.
Urea	Sigma-Aldrich	U5378-100G	Casting denaturing polyacrylamide gel.
RNA Gel Loading Dye (2x)	Thermo Fisher	R0641	Loading guide RNA onto denaturing gel for electrophoresis.
Ethidium bromide	Sigma-Aldrich	E1510-10ML	Visualization of nucleic acids.
SYBER Green	Thermo Fisher	S7563	Alternate method to ethidium bromide for detection of dsDNA in agarose or polyacrylamide gels.
Microcentrifuge	Eppendorf	5424	RNA clean up, PCR purification.
MyTaq Polymerase	Bioline	BIO-21105	For amplification of DNA using PCR.
Thermocycler	Any brand		PCR amplification.
Spectrophotometer	Any brand		NanoDrop or related product to quantify the amount of DNA/RNA.
E3 embryo media	Made in house		Recipe: http://cshprotocols.cshlp.org/content/2011/10/pdb.rec66449
Methylene Blue	Sigma-Aldrich	M9140	Added to 1x E3 media to prevent fungal growth on embryos.
Petri dish	Thermo Fisher	FB0875711Z	Store embryos, cast injection plate.
Agarose	Denville	CA3510-8	Casting injection plate, agarose gels.

Table 2.1 continued

Microinjection mold	Adaptive Science Tools	TU-1	To create wells to hold embryos during injection.
Phenol Red	Sigma-Aldrich	P0290	Dye for visualization of injection.
Mineral Oil	Sigma-Aldrich	M5904-5ML	To calibrate needle injection volume.
Transfer pipettes	Any brand		Moving embryos.
Razor blade	Thermo Fisher	11295-10	Cutting injection needle, tail clipping adult fish.
Incubator	Any brand		Maintaining embryos at 28.5 °C.
Verticle pipette puller	David Kopf Instruments	700C	Geneate needles for injection.
Capillary tubes	Sutter Instruments	BF100-58-10	Geneate needles for injection.
Microloader tips	Eppendorf	930001007	Load solution into injection needles.
Microinjector	World Precision Instruments	PV 820	Injecting embryos.
Disecting microscope	Leica		Injecting embryos.
30% Polyacylamide (29:1)	BioRad	161-0156	Heteroduplex gel casting.
MS-222 (Tricaine)	Sigma-Aldrich	A-5040	Anesthetize zebrafish for tail clipping and gDNA extraction from embryos.
Microwave	Any brand		Casting injection plate, agarose gels.
Scale	Any brand		Casting injection plate, agarose gels.
Gloves	Any brand		For all aspects of the protocol.
N2	Any brand		To expell liquid from the capillary for embryo injection.
1,000 μ L tips	Any brand		For all aspects of the protocol.
200 μ L tips	Any brand		For all aspects of the protocol.
10 μ L tips	Any brand		For all aspects of the protocol.

Table 2.1 continued

PCR strip tubes	Any brand		For all aspects of the protocol.
Micropipettes	Any brand		For all aspects of the protocol.
NGS Sequencing platform: Wideseq			External cost: \$35. Visit: https://www.purdue.edu/hla/sites/genomics/wideseq-2/
Software for sequence analysis			For Sanger sequencing of heterozygous fish: http://yosttools.genetics.utah.edu/PolyPeakParser/
Software for sequence analysis			SnapGene Viewer, Sequence Scanner for analysis of NGS sequencing.

CHAPTER 3. TRANSCRIPTOMICS REVEALS A ROLE FOR THE CHROMATIN REMODELER CHD5 IN NEUROGENESIS IN THE DEVELOPING ZEBRAFISH BRAIN

3.1 Introduction

A wide variety of cellular machinery is employed to coordinate the transcriptional changes that direct cellular differentiation. Neurogenesis is a multistep process involving complex interplay between signaling pathways and regulatory machinery that generates highly specialized cells (Hsieh and Zhao 2016; Urban and Guillemot 2014; Alunni and Bally-Cuif 2016; Yao and Jin 2014; Schmidt, Strahle, and Scholpp 2013). Differentiation is associated with both activation and repression of specific sets of genes. Much of this control is achieved through the coordinated action of conserved transcription factors and epigenetic machinery that regulate gene expression. With regards to epigenetic machinery, DNA methylation and hydroxymethylation, histone acetylation status, and histone methylation status have all been shown to contribute to gene expression and differentiation of neuronal cells (Wang et al. 2016; Hsieh and Zhao 2016; Corley and Kroll 2015; Yao and Jin 2014; Roidl and Hacker 2014; Ma et al. 2010). Another critical aspect of gene expression dynamics are chromatin remodeling factors. One such factor is the vertebrate-specific remodeler CHD5, which is preferentially expressed in neurons.

Chromodomain / Helicase / DNA-binding (CHD) proteins play a variety of roles in vertebrate development, and misregulation or loss of CHD proteins has been linked to numerous diseases (Mayes et al. 2014; Marfella and Imbalzano 2007; Bartholomew 2014). CHD5 is a vertebrate-specific member of a family of ATP-dependent chromatin remodeling proteins. *CHD5* is expressed primarily in neural tissue where it is thought to contribute to neurogenesis and has been strongly linked to tumor suppression. Spontaneous loss of *CHD5* by mutation or silencing is associated with formation of a wide range of tumors including colorectal cancer, lung cancer, and leukemia. Reduced expression of *CHD5* in a tumor is strongly correlated with a worse clinical outcome (Wu, Zhu, Li, Fu, Su, Fu, Zhang, Luo, Sun, and Dong 2012; Du et al. 2012; Wong et al. 2011a; Garcia et al. 2010). Loss of *CHD5* also plays a significant role in development of neuroblastoma, a devastating tumor that is a leading cause of death of childhood cancer patients (Jiang, Stanke, and Lahti 2011; Maris and Matthay 1999).

At present, there is little known regarding the molecular mechanisms by which CHD5 contributes to neurogenesis or tumor suppression, although some insights have been obtained by biochemical characterization of CHD5 and related remodelers, and by genome-wide analyses. The CDs of CHD5 have been shown to bind to histone H3 that carries the repressive epigenetic modification H3K27me3 (trimethylation of histone H3 at lysine 27) and are necessary for proper expression of genes enriched for this mark during differentiation of neural tissue (Egan et al. 2013b). Furthermore, CHD3-related proteins are subunits in Mi-2/NuRD complexes that play a major role in histone deacetylation and transcriptional repression in vertebrates (Wolffe, Urnov, and Guschin 2000; Quan et al. 2014; Potts et al. 2011; Allen, Wade, and Kutateladze 2013). In addition to these roles in gene repression, chromatin immunoprecipitation data shows that CHD5 associates with the transcriptional start site of actively transcribed genes (Egan et al. 2013b). These data raise the prospect that CHD5 also promotes activation of a cohort of genes involved in neural development (Egan et al. 2013b). However, much remains to be learned regarding the mechanisms by which CHD5 contributes to gene expression and tumor suppression.

In light of the biochemical properties and functional importance of Chd5 remodelers, we have developed a zebrafish model to study Chd5, the zebrafish homolog of human CHD5 (He, Jing, and Look 2017; Hayes and Langenau 2017; Drabsch, Snaar-Jagalska, and Ten Dijke 2017; Chernyavskaya, Kent, and Sadler 2016; Corallo et al. 2016; Sanchez and Amatruda 2016; Zhu and Thomas Look 2016; Lobert, Mouradov, and Heath 2016; Hwang and Goessling 2016; Phelps and Chen 2016). Epigenetic factors have been identified that play a critical role in differentiation in vertebrate neurons, and effectors and regulatory pathways have been found to be extensively conserved between humans and zebrafish. As a vertebrate-model system, zebrafish offer a powerful set of tools uniquely available in this system to characterize how Chd5 remodelers contribute to epigenetic status, gene expression, and neurogenesis in vivo. First, zebrafish embryos develop externally from the mother which makes them highly amenable to genetic alteration by microinjection (Xu 1999; Rosen, Sweeney, and Mably 2009). Second, the embryos develop rapidly and well-established protocols are available to visualize gene expression in these animals (Thisse and Thisse 2014). Furthermore, the updated zebrafish genome assembly (GRCz11) published in 2017 greatly facilitates the use of next-generation sequencing to examine the transcriptome of zebrafish.

Using the CRISPR/Cas9 suite of genetic tools we have engineered nonsense alleles in *chd5* (*chd5*^{-/-}) in zebrafish, providing us with a new model to investigate the role of *CHD5* remodelers in reprogramming the transcriptome of neural precursor cells during differentiation. As noted above, characterization of neuroblastoma cells indicates that they are derived from neural precursor cells (Pei et al. 2013). Given the evidence that *CHD5* contributes to differentiation and gene expression in neural tissue (Egan et al. 2013b; Pisansky et al. 2017; Higashi et al. 2015), we hypothesized that loss of *CHD5* contributes to development of neuroblastoma because neural precursor cells lacking *CHD5* fail to alter some aspect of their neural precursor transcriptome/epigenome. Therefore, we used next-generation sequencing (NGS) to determine the transcriptional alterations that take place in differentiating neural tissue lacking *CHD5*.

Although previous analyses provide strong support for a role of *CHD5* in neural differentiation and gene expression, analyses to date have focused on examining the consequence of loss of *CHD5* after embryogenesis and thus after the bulk of neurogenesis has taken place (Egan et al. 2013b; Potts et al. 2011). To address this gap, we undertook RNA-seq analysis of brains from wild-type and *chd5*^{-/-} zebrafish to identify *chd5*-dependent genes in predominantly differentiating (2-day old) and substantially differentiated (5-day old) neural tissue, staged in accordance with previously ascribed features (Kimmel et al. 1995). In our analysis we have identified 1522 and 1614 differentially expressed genes in 2-day and 5-day old brains compared to wild-type, respectively. These data reveal that *Chd5* has a substantially larger impact on the transcriptome of developing brains in early zebrafish embryogenesis. We further show that loss of *chd5* results in a failure of the cells that contribute to neuroblastoma, the sympathetic ganglion cells (SGCs), to acquire terminal differentiation markers, consistent with a role for *chd5* in tumor suppression in neuroblastoma. Taken together, these data support a role for *CHD5* in promoting neurogenesis by modulating transcription.

3.2 Experimental Results

Loss of *chd5* does not result in an overt developmental phenotype in zebrafish.

To characterize the contributions of *CHD5* to vertebrate development we generated protein-null alleles of *chd5* (*chd5*^{-/-}), the zebrafish ortholog of human *CHD5* (Ho et al. 2013b), using CRISPR/Cas9. Guide RNAs (gRNAs) were designed to target *chd5* upstream of characterized domains of homology, and the presence of indels was evaluated as previously

described (Figure 3.1 A) (Sorlien, Witucki, and Ogas 2018). We identified two alleles from independent gRNAs that result in polymorphisms and insertions adjacent to the predicted CRISPR cut site that create nonsense mutations in *chd5* (Figure 1A). Transmission of either of these identified *chd5*-mutant alleles was examined using PCR and was found to exhibit Mendelian inheritance (Table 3.1). Herein, we used the nonsense allele in exon 4 for subsequent analyses and designate this mutation as *chd5*^{-/-}.

Loss of *chd5* expression in fish that were homozygous for the CRISPR/Cas9-generated alleles was confirmed by western blot using polyclonal antibodies generated with a recombinant Chd5 peptide (Fig. 3.1 B). Phenotypic characterization of *chd5*^{-/-} fish revealed no obvious developmental defects under standard growth conditions (Figure 3.1 C), consistent with prior characterization of *CHD5*-knockout mice (Zhuang et al. 2014; Li et al. 2014). However, this observation is inconsistent with our knockdown studies of *chd5* using morpholinos, which may suggest that the morpholinos exhibit an off-target effect (Schulte-Merker and Stainier 2014). Also consistent with mouse knockout studies, we found that the *chd5*^{-/-} alleles were not sufficient to promote tumorigenesis (n=185 fish, aged >16 months), suggesting that *CHD5* acts in concert with other factors to suppress tumor formation or that the effect of *CHD5* in suppressing tumor formation is only observed in conditions of genotoxic stress (Li et al. 2014; Zhuang et al. 2014).

RNA-seq reveals differential gene expression in zebrafish brains with and without *chd5*.

We have previously shown that *chd5* is upregulated during development in zebrafish, and that expression of *chd5* is highest in neural tissues and sperm (Bishop et al. 2015), consistent with the observation that *CHD5* expression is restricted to neurons in mouse and humans (Egan et al. 2013b; Potts et al. 2011; Thompson et al. 2003). Previous characterization of altered *CHD5* expression in brain development of mice revealed that *CHD5* is necessary for neural differentiation and migration (Nitarska et al. 2016; Pisansky et al. 2017; Egan et al. 2013b; Hwang et al. 2018). To characterize the effect of loss of *chd5* to neurogenesis in developing zebrafish embryos, we undertook RNA-seq analysis of 2-day old and 5-day old brains. These developmentally distinct samples enable us to look across a developmental period when a significant portion of neurons are undergoing migration, differentiation and establishment of connectivity. Previous analyses confirm these critical periods in zebrafish neurogenesis, demonstrating that strong proliferation but weak differentiation is occurring at 2-days, and 5-day old brains exhibit strong differentiation (Mueller, Vernier, and Wullimann 2006). It is estimated that 2 days post fertilization (dpf) in

zebrafish neurogenesis is equitable to 10.5-days in rats, and 5 dpf is reflective of 35-42 days old in rats (Kozol 2018). We observe a similar trend of decreased expression of a number of genes that mark neural precursor cells from 2-day to 5-day, and the expression follows a similar trend in our mutant fish, consistent with our observation that the brains develop phenotypically normal (Figure 3.2).

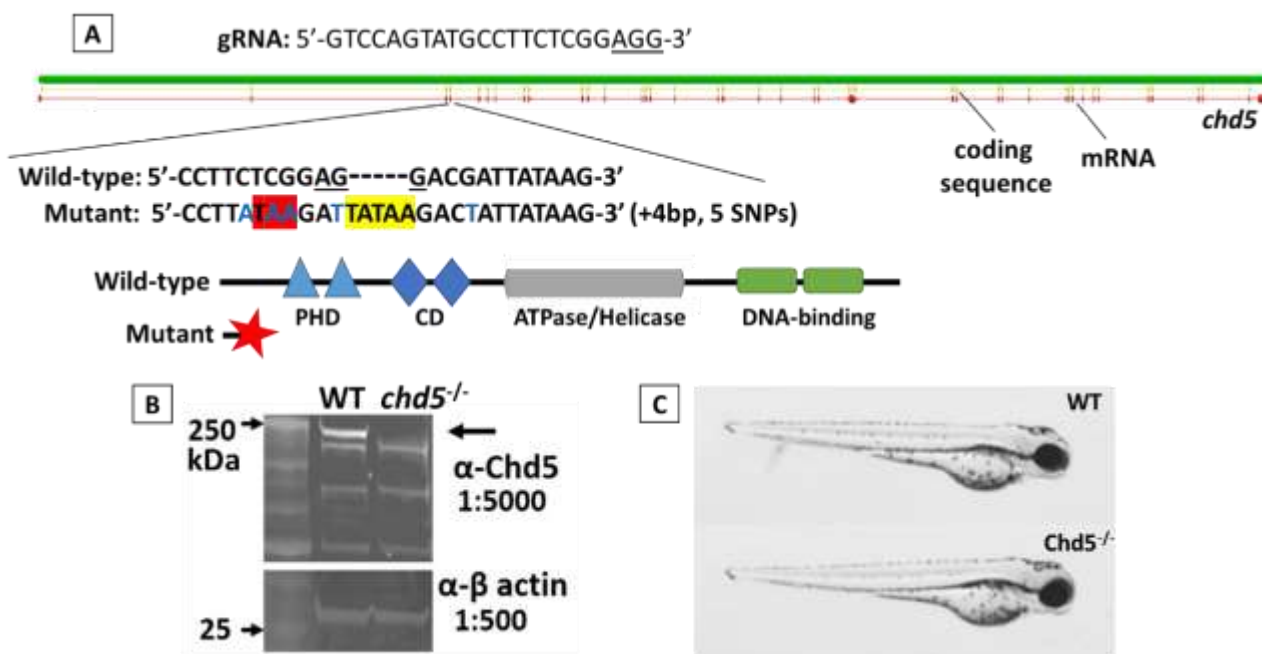


Figure 3.1 Loss of *chd5* does not result in overt developmental defects in zebrafish embryos in contrast to morpholino injection which causes off-target effects.

(A) CRISPR/Cas9 was used to generate protein-null alleles of *chd5*. The schematic of the zebrafish genomic *chd5* is shown, and the gRNA target is shown. The PAM sequence is underlined, mismatch bases are shown in blue, and insertions are highlighted. Red highlight indicates the in-frame stop codon generated by the mutations. (B) Western analysis of whole brain protein extract shows the nonsense allele created in *chd5* is a protein null. Immunoblots probed using polyclonal antibody to zebrafish Chd5 protein, and β -actin as a loading control. The band identified by the arrow (top panel) migrates near the predicted molecular weight of the Chd5 protein (227kD) and is absent in the *chd5*^{-/-} fish. (C) Loss of *chd5* does not result in an overt developmental phenotype, depicted here at 96 hpf.

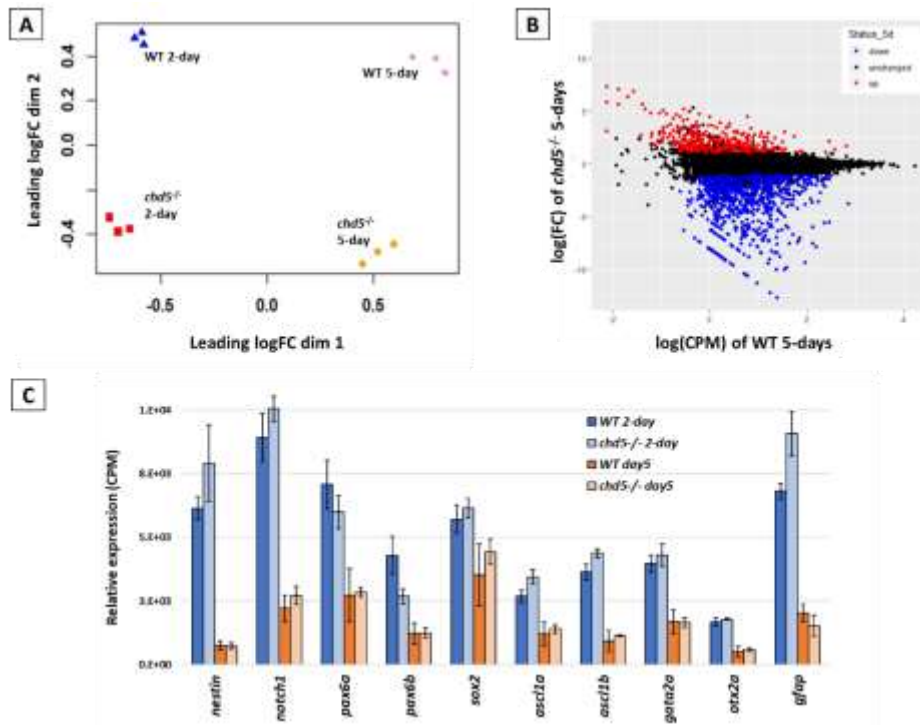


Figure 3.2 Quality assessment of RNA-seq data.

(A) Multidimensional scaling plot generated using the limma package in Bioconductor (Ritchie et al. 2015) that depicts the pairwise $\log_2(\text{fold change})$ distances between the samples. Only genes found to be differentially expressed relative to WT were included in the calculation. (B) Mean difference plot depicting differential expression in *chd5*^{-/-} (y-axis) against average expression in WT (x-axis) in the 2 day-old brain (B) and 5 day-old brains (C). Each data point represents a single gene. Genes that are differentially expressed 2-fold change or higher (FDR < 0.05) in the *chd5*-null tissue are shown in red (significantly increased expression) or blue (significantly decreased expression). (C) Relative expression in counts per million (CPM) of established markers of undifferentiated neural stem cells shows that expression is lower at 5-days in both WT and *chd5*^{-/-}. Bars=s.d.

Three biological replicates were harvested for each sample, sequenced with ~100 million paired-end reads, and the resulting sequences were mapped to the DanRer11 genome build. Quality assessment was performed using the Bioconductor packages DESeq2 and limma. Multidimensional scaling plot depicts the pairwise $\log_2(\text{fold change})$ distances between samples using genes found to be differentially expressed relative to wild-type (WT) (Figure 3.2 A). Differentially expressed genes (DEGs) relative to WT were identified using the edgeR package and Fisher's exact test with a significance threshold of $\alpha < 0.05$ and a fold change threshold of > 2-fold difference relative to WT (Robinson, McCarthy, and Smyth 2010; Fisher 1922). Our analysis identified 17,995 genes are represented in this dataset.

We identified a substantial set of significantly differentially expressed genes (DEGs) in our mutants compared to WT. These genes are both up and down regulated, suggesting *Chd5* is necessary for both activation and repression of genes during brain development in zebrafish, consistent with previous analyses (Pisansky et al. 2017). In total, approximately 1,500 DEGs were identified for each time point (Figure 3.2 B). The large number of DEGs suggested to us that we were able to capture a critical time when the effect of loss of *chd5* is more apparent than previous analyses, that identified far fewer differentially expressed genes using later developmental time points relative to the stage of our zebrafish (Pisansky et al. 2017; Hwang et al. 2018). Although we observe a substantial number of DEGs, we do not observe any overt differences in the overall structure of the brains obtained from our mutant embryos, suggesting that there is not a gross morphological defect at the tissue level. Consistent with this observation, we do not observe significant differences in the expression of markers of neurogenesis from 2- to 5-day in WT and our mutant embryos (Figure 3.2 C).

Analysis of 2-day and 5-day old WT brains provides insight into zebrafish brain development.

We utilized the WT samples harvested in this experiment to determine gene expression changes across this developmental window. We identify 4,065 genes with a significant increase in gene expression at 5-days compared to 2-days, and 2,081 that exhibit a significant decrease of 2-fold change or higher and FDR <0.05. To independently verify our gene expression changes we performed an intersection analysis using our DEGs and those developmentally-regulated genes measured from whole embryo transcriptomes (comparing long-pec to 5-day samples) (White et al. 2017). This analysis showed that approximately 50% of our DEGs were also identified in their analysis (Table 3.1). We hypothesize the differences may be seen because of our tissue specificity and higher sequencing depth, nonetheless these data indicate we are capturing the developmentally-regulated transcriptome in these samples.

To explore the molecular networks that these observed changes in gene expression enrich for we examined gene ontology (GO) terms associated with biological processes and molecular function and Kyoto Encyclopedia of Genes and Genomes (KEGG) pathway enrichment. From GO and KEGG we determined pathway enrichment for genes that increase in expression at 5-days, and for those DEGs which decrease expression at 5-days independently. We see an increase in genes that enrich in pathways that are consistent with the overall maturation and differentiation of

the brain tissue, such as synaptic transmission and signaling pathways (Figure 3.3). We also observe an increase in metabolic genes, consistent with the observation that metabolic activity increase correlates with the differentiation and patterning in embryonic tissues (Roy et al. 2013). Furthermore, we observe a decrease in pathways associated with early development such as Wnt and Notch signaling, as well as a decrease in Cell cycle genes, consistent with the acquisition of terminal-differentiation of cells in the brain (Figure 3.3) (Hardwick et al. 2015).

Table 3.1 Overlap of developmentally identified genes in long-pec compared to 5-day whole embryos (White et al. 2017) overlaps strongly with the genes that are differentially expressed in our WT brain transcriptome analysis.

Sample A	Sample B	Observed	Expected	p-value
WT 5-day DEG up	5-day comparison up	1942	566	0
WT 5-day DEG up	5-day comparison down	31	391	1
WT 5-day DEG down	5-day comparison up	43	283	1
WT 5-day DEG down	5-day comparison down	860	196	0

WT 5-day DEGs refers to our RNA sequencing data, and 5-day comparison data represents the DEGs calculate from the comparison of long-pec to 5-day whole embryos (White et al. 2017). Differentially expressed gene sets were shown to have a high degree of overlap, validating that we are identifying developmentally regulated genes in our tissue-specific transcriptome data set.

We also evaluated the gene expression changes by comparing 2- to 5-day in our *chd5* mutant lines and analyzed the intersection of the DEGs to the WT developmentally-regulated genes. We found that these data sets overlap significantly, consistent with the lack of a detectable phenotype differences in the *chd5*-null brains that appear to largely develop normally (data not shown). However, this overlap does not show the magnitude of changes in the mutant versus wild-type. It is possible that the expression of these genes in our mutant fish are changing across development in a similar expression pattern (increase or decrease), but that they are also differentially expressed at either or both time points compared to age matched WT embryo brains.

Ingenuity pathway analysis (IPA, Qiagen) predicts the causal changes observed in omics data, such as RNAseq. We used IPA to identify key regulators predicted to explain the gene expression patterns observed in both the WT developmental DEGs, and in gene expression changes observed in our *chd5*^{-/-} mutants compared to WT at 2- and 5-days. The upstream regulator analysis uses the Ingenuity® Knowledge Base to predict the effects of transcriptional regulators (i.e. transcription factors, microRNAs, chemicals etc.) and their target genes and the direction of

the observed changes. We used an overlap p-value <0.01 , and report the predicted regulators that exhibit a strong activation z-score (>2 for activating, and <-2 for inhibiting networks). We observed 189 upstream regulators that are significantly activated (Table 3.2), and 70 that are inhibited in WT at 5-days (Table 3.3). These pathways include many neural specific terms, as well as transcription regulates that are known to promote neurogenesis and cell-cycle control.

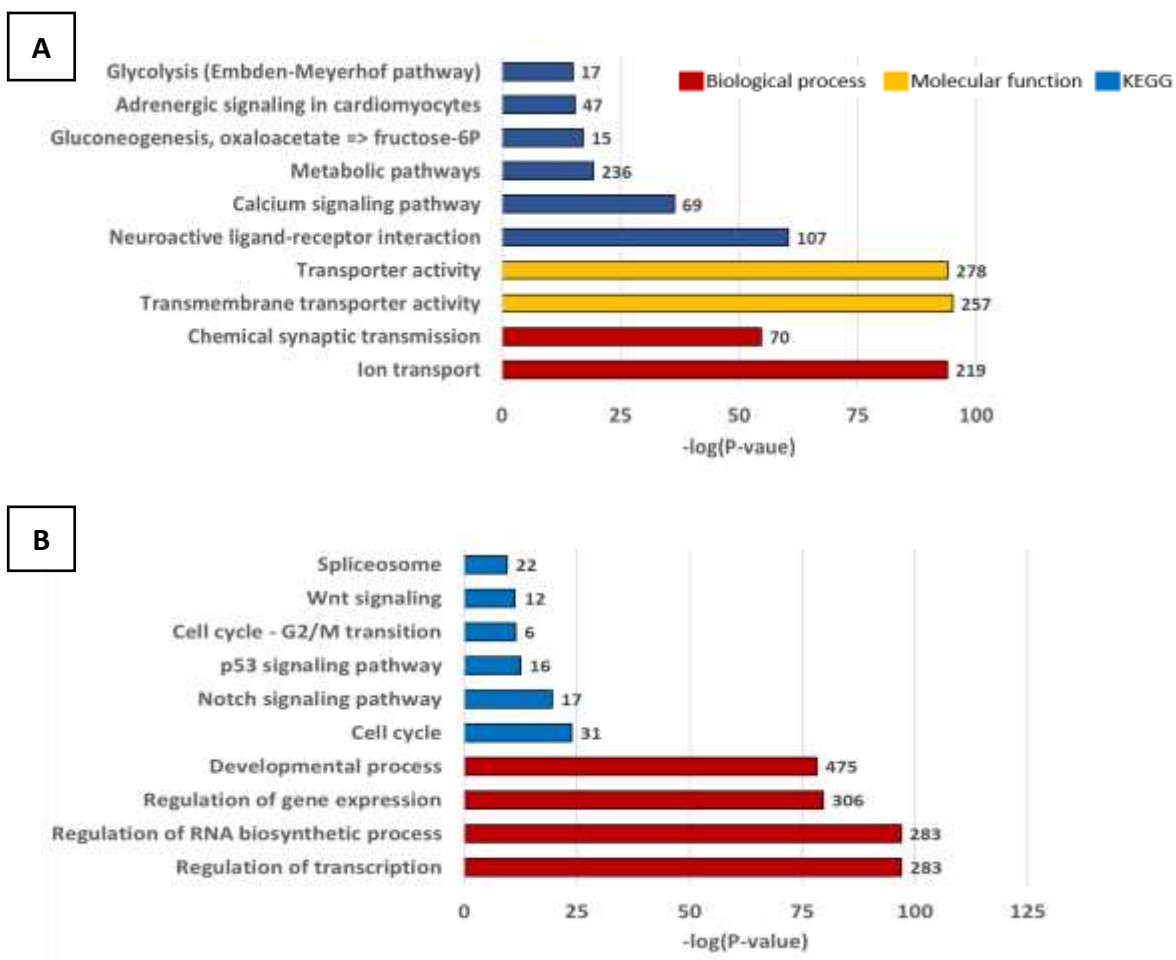


Figure 3.3 Changes in gene expression during development in WT embryos enriches for numerous neurogenic programs.

(A) Increased DEGs and (B) Decreased DEGs, (all DEGs are 2-fold change or higher, FDR <0.05). The colors denote the category the pathway terms were enriched from, and the numbers adjacent to each bar indicates the number of target genes in the category.

Table 3.2 Predicted activated pathways enriched in wild-type DEGs list from 2- to 5-days.

Upstream Regulator	Molecule Type	Activation z-score	p-value of overlap
ITPR2	ion channel	2	0.00487
CAV1	transmembrane receptor	2.01	0.0000244
NFATC4	transcription regulator	2.02	0.00262
OSM	cytokine	2.024	0.000119
KDM5B	transcription regulator	2.026	2.14E-08
P2RY2	G-protein coupled receptor	2.033	0.00624
DICER1	enzyme	2.035	0.00086
EGR1	transcription regulator	2.043	0.00000236
ADRB3	G-protein coupled receptor	2.049	0.00896
KRAS	enzyme	2.052	1.14E-10
AQP1	transporter	2.06	0.000747
CD38	enzyme	2.067	0.00195

Table 3.3 Predicted inhibited pathways enriched in wild-type DEGs list from 2- to 5-days.

Upstream Regulator	Molecule Type	Activation z-score	p-value of overlap
CCND1	transcription regulator	-5.42	8.53E-08
EGLN	group	-4.461	0.00402
RABL6	other	-4.139	6.62E-10
E2f	group	-4.109	0.00000223
PTGER2	G-protein coupled receptor	-4.039	0.0000019
KDM5A	transcription regulator	-4.037	0.000255
REST	transcription regulator	-3.874	1.09E-16
TBX2	transcription regulator	-3.805	0.000000834
NR0B2	ligand-dependent nuclear receptor	-3.692	0.00000392
FOXM1	transcription regulator	-3.613	0.00000076
EP400	other	-3.456	4.19E-08
LIN9	other	-3.4	0.0000058

Chd5 is required to promote proper gene expression during development of the zebrafish brain.

To determine what genes require Chd5 to be properly expressed during development, we determined the up-regulated and down-regulated DEGs at each time point, compared to the WT sample of the same time point (Figure 3.5). We found that at 2-days there are 561 up-regulated DEGs, compared with 473 at 5-days. We found that the number of down-regulated DEGs was

consistently higher at each time point, with 961 at 2-days and 1141 genes at 5-days. We analyzed the intersections between sets of DEGs to determine if *chd5* regulates a conserved set of genes between 2- and 5-days. The intersection of the increased DEGs at 2- and 5- day, as well as the decreased DEGs exhibit significantly larger than expected by chance overlap in gene expression outcomes (Figure 3.5). In contrast, intersections between DEG sets that are differentially expressed in opposite directions (i.e. up at 2-day and down at 5-day) were not significant.

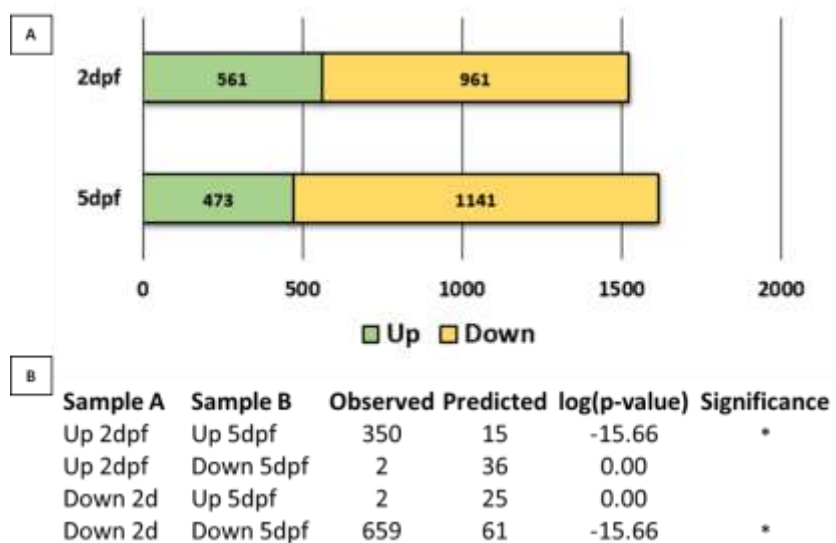


Figure 3.4 Summary of differentially expressed genes.

(A) Total numbers of genes identified as differentially expressed in *chd5*^{-/-} embryo brains at the indicated time point relative to WT. Gene sets corresponding to statistically significant increases in expression are shaded green, and those corresponding to significant decreases in expression are shaded yellow. Differential expression was determined based on mean counts per million using the edgeR package and Fisher's exact test using a significance threshold of $\alpha < 0.05$ and a fold change threshold of ≥ 2 -fold change relative to WT.

(B) Intersection analysis between DEGs determine relative to WT of opposite expression effects in the indicated samples. Observed: number of genes in common between the indicated gene sets. Predicted: number of genes predicted to be in common by chance. Log(*p*-value): exponent of the *p*-value obtained using Fisher's exact test with a null hypothesis of an intersection that is no greater than expected by chance. Significance: ** = $\alpha \leq 10^{-15}$.

To formally examine the interaction of the genes that exhibit expression changes at 2- and 5-day we performed GO and KEGG pathway analyses. These results suggested that the metabolic processes that synthesize neurotransmitters such as catecholamine, serotonin and dopamine are down regulated (*tph1a, sult1st3, dbh, sult1st1, tph1b*) and that at 5-days glycolysis is failing to be upregulated (*pkmb, gpib, aldob, aldoab, gapdh, pgam2*), consistent with defects in neural

differentiation (Figure 3.6). Of note, we do not see an increase in other CHD subfamily II remodelers, suggesting that the CRISPR-generated nonsense allele does not result in activation of compensatory mechanisms related to homologous proteins, as has previously been reported (Rossi et al. 2015).

IPA shows few enriched terms at 2-day that are predicted to be strongly inhibited or activated (3 predicted to be inhibited). At 5-days there are 22 significantly inhibited predicted pathways, and 5 pathways predicted to be activated (Table 3.4). Of the inhibited pathways, many of these regulators (HNF1A, FOXA2, HNF4A, EIF2AK3) have roles in metabolic functions, consistent with the GO and KEGG pathway analysis.

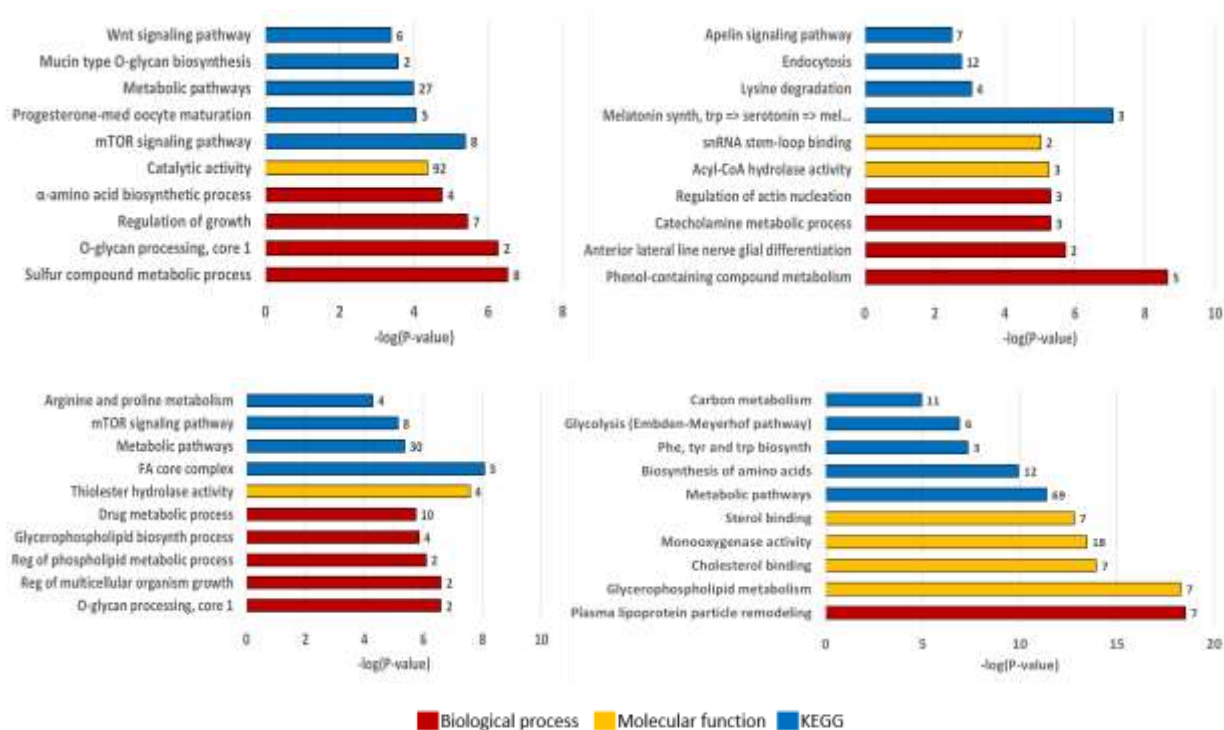


Figure 3.5 Chd5 regulates numerous metabolic activities during brain development by GO/KEGG pathway analysis.

(A) 2-day increased DEGs, (B) 2-day decreased DEGs, (C) 5-day increased DEGs, (D) 5-day decreased DEGs (all DEGs are 2-fold change or higher, FDR <0.05). The colors denote the category the pathway terms were enriched from, and the numbers adjacent to each bar indicates the number of target genes in the category.

Chd5 loss leads to misregulation of neural development pathways.

Upon closer examination of the genes that exhibit expression that is dependent on Chd5, we observed a significant decrease in genes involved in monoaminergic neurotransmitter synthesis. Monoaminergic neurons use specific neurotransmitters derived from amino acid intermediates that includes dopamine, and serotonin. The monoamine neurotransmitter catecholamine is derived from tyrosine and synthesized by enzymes that are specifically expressed in the sympathetic nervous system. The sympathetic neurons are the cellular type that gives rise to neuroblastoma (Pei et al. 2013). We observe a significant decrease in genes involved in the development of these neurons in embryos lacking *chd5*^{-/-}, consistent with a role for Chd5 in differentiation and tumor suppression.

Table 3.4 Upstream regulator analysis predicts transcriptional networks are largely inhibited in the absence of Chd5 at 5-days old.

Upstream Regulator	Molecule Type	Activation z-score	p-value of overlap
HNF1A	transcription regulator	-3.512	3.09E-05
ERBB2	kinase	-3.179	1.28E-01
FOXA2	transcription regulator	-3.13	1.23E-04
HGF	growth factor	-3.077	2.40E-02
MYCN	transcription regulator	-2.98	1.86E-02
BRD4	kinase	-2.954	2.96E-02
HNF4A	transcription regulator	-2.933	6.54E-07
LHX1	transcription regulator	-2.739	8.84E-04
PPARG	ligand-dep. nuclear receptor	-2.696	1.67E-02
PRL	cytokine	-2.568	7.72E-03

In situ analysis confirms the failure of sympathetic ganglion cells to properly differentiation in Chd5^{-/-} embryos.

To characterize the phenotype of decreased expression of these candidate genes we performed whole-mount in situ hybridization (ISH) analysis to determine the spatio-temporal expression of genes that mark these cells) as previously described (Thisse and Thisse 2008). Two genes that we have identified from our data set are the terminal differentiation markers *tyrosine hydroxylase (th)* and *dopamine beta hydroxylase (dbh)* that mark sympathetic ganglion cells. Our data suggests that *chd5* is necessary for proper differentiation of these cells. We engineered probes to *dbh* and *th* and performed ISH on 5 day old embryos (Figure 3.7). We show that in some *chd5*^{-/-}

$^{-/-}$ embryos *dbh* and *th* staining are reduced, consistent with our observation that the RNA levels are decreased in the mutant embryos.

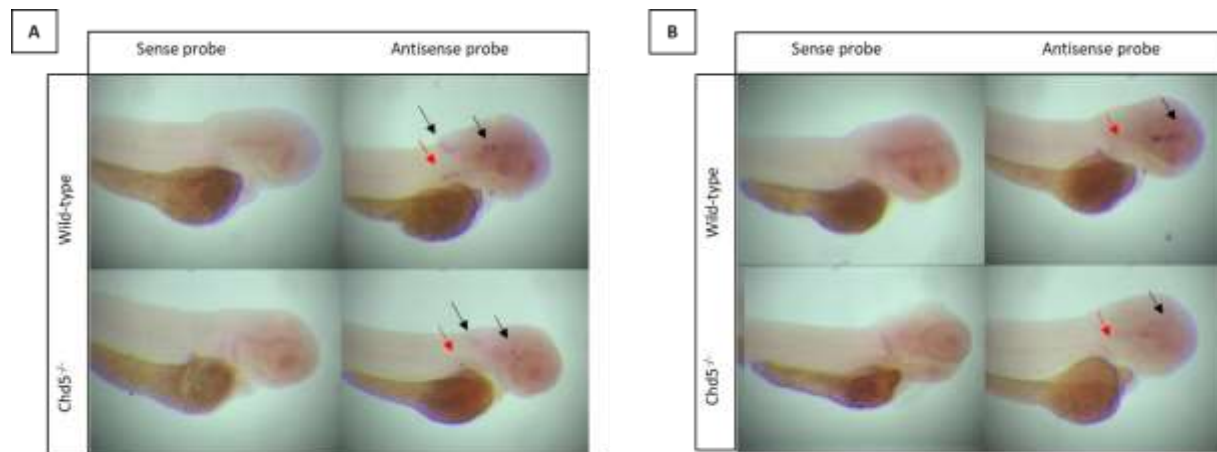


Figure 3.6 In situ analysis of genes that mark sympathetic ganglion cells.

- (A) DBH staining is reduced in some embryos in *chd5* knockouts at 5 dpf compared to wild-type. Red arrow indicates the superior cervical ganglion. Quantification
 (B) TH similarly to (A) shows reduced expression throughout the cranial features of *chd5* knockout embryos.

3.3 Discussion

Vertebrate neurogenesis is characterized by the commitment of neuroepithelia precursors cells to become the mature neurons and glial-cells that comprise the central nervous system. This process of cellular differentiation requires the coordinate action of both extrinsic and intrinsic mechanisms, such as signaling events and transcriptional changes. Gene expression changes and chromatin reorganization are both well documented hallmarks of neurogenesis, however the role of much of these chromatin-based factors contribute to neurogenesis is not well understood. In particular, here we have examined how the neural-specific CHD remodeler, Chd5, promotes proper transcription in the developing zebrafish brain. Zebrafish are ideally suited for this analysis, because CHD5 is a vertebrate-specific chromatin remodeler, and zebrafish embryos are produced in large clutches externally from the mother making harvesting of tissue comparatively easy.

To examine how loss of *chd5* affects the developing zebrafish brain, we used RNA sequencing to examine the transcriptome of the whole brains during a strong wave of secondary neurogenesis

that occurs from 2- to 5-days in zebrafish embryos. We hypothesized that *chd5* is necessary for proper gene expression in these tissues during development for several reasons. First, we have demonstrated that zebrafish *chd5* exhibits the characteristic enzymatic properties of CHD remodelers to mobilize nucleosomes (Bishop et al. 2015), murine Chd5 has been shown to bind to the transcriptional start site of genes and is also associated with the repressive histone mark H3K27me3 (Egan et al. 2013b), and finally because previously RNA sequencing studies have identified some transcripts that require *CHD5* to be properly expressed (Pisansky et al. 2017; Egan et al. 2013b). However, these previous transcriptome analyses have been limited to either stem cell experiments or late-stage mouse brain tissue and we hypothesized that these studies may be missing a substantial number of transcripts because these tissues are not undergoing neurogenesis but instead are primarily differentiated.

Using transcriptomics, we observed that loss of *chd5* leads to 1522 and 1614 differentially expressed genes in 2-day and 5-day old brains compared to wild-type, respectively (Figure 3.4). This number of differentially expressed transcripts is substantially more genes than previously identified, suggesting that we have captured a critical window of development that requires the *chd5* (Pisansky et al. 2017; Egan et al. 2013b). We observe that these genes contribute to a number of biologically important pathways known to contribute to neurogenesis, especially biosynthetic pathways such as glycolysis and biosynthesis of amino acids, which suggested one or more neurotransmitters, which are derived from amino acids may not be being synthesized properly. Of the genes identified, we found several enzymes known to be important for synthesis of neurotransmitters, including *tph1a*, *sult1st3*, *dbh*, *sult1st1*, *tph1b*. The reduction of *dbh* expression was particularly intriguing because this is a late stage marker for a subtype of neurons called sympathetic ganglion cells. SGCs are a type of cell that when transformed can lead to neural tumors called neuroblastoma. A hallmark of tumors such as neuroblastoma is that these malignant changes often occur in genes that control cell survival, cellular proliferation and the mechanisms that direct differentiation programs for these cells. Therefore, because epigenetic mechanisms that direct gene expression can substantially influence these programs, loss of differentiation markers for SGCs is a substantial finding. This is the first reported evidence that *chd5* may play a role in the development of these cells specifically. We demonstrated that the change in *dbh* expression associate with loss of *chd5* results in loss of these cells by ISH, consistent with a role for *chd5* in suppression of tumor formation in neuroblastoma. Importantly, we also see reduced staining in

another marker of SGCs that is not significantly differentially expressed in our mutant embryos. This gene, *th* is a key component of the serotonergic neural systems and the rate limiting enzyme in synthesis of dopamine (DA). Abnormal DA signaling has been implicated in numerous human diseases, including Parkinson's and schizophrenia (Perreault et al. 2014; Narayanan, Rodnitzky, and Uc 2013). This suggest that *CHD5* may play yet unrevealed roles in the pathology of these diseases and could also provide a new therapeutic target for the treatment of such disorders.

In conclusion, we have identified a gene expression signature associated with loss of *chd5* in the developing zebrafish brain. These data further suggest that the function of Chd5 in promoting differentiation of neurons, in particular of the sympathetic system is crucial to vertebrate development. This also suggests that loss of *chd5* may sensitize the cells known to give rise to neuroblastoma to further genomic instability and promote transformation of these cells to a malignant state. Further investigation into the consequence of losing this chromatin remodeler in the pathology of neuroblastoma cells is needed to determine what therapeutic strategies may be affective against tumors that exhibit loss of CHD5. However, with the identification of these transcriptional changes we may be able to predict treatment options for these malignancies and we further demonstrate that zebrafish are a suitable model system to study changes associated with loss of *chd5*.

CHAPTER 4. CHD5 PROMOTES SPLICING DURING BRAIN DEVELOPMENT IN ZEBRAFISH EMBRYOS

4.1 Introduction

During development of the vertebrate neural system, the transcriptome undergoes sophisticated changes to promote maturation of these tissues. Neurogenesis includes the differentiation of neural precursor cells to mature neurons, migration of cells, and formation of synaptic connections between neurons. Extensive work has detailed the transcriptional programs that direct these processes (Pensold and Zimmer 2018; Hamby, Coskun, and Sun 2008; Yao et al. 2016), and alternative splicing (AS) events that produce transcript and protein variants are a widespread hallmark of neurogenesis (Vuong, Black, and Zheng 2016; Hakim et al. 2017; Su, D, and Tarn 2018). Transcript diversity is increased by the alternate inclusion of introns and exons through AS, which is catalyzed by the action of the spliceosome. For example, AS can alter the localization of protein products, the enzymatic function of the protein, and the interaction of these proteins with complexes and ligands in the cell (Kelemen et al. 2013).

Nearly all multi-exon genes undergo AS, often in a tissue-specific manner (Wang et al. 2008; Mollet et al. 2010; Pan et al. 2008). Misregulation of AS in neuronal processes is linked to numerous human diseases, including autism (Hamada et al. 2016; Lee et al. 2016), amyotrophic lateral sclerosis (Da Cruz and Cleveland 2011) and neurodegeneration (Jia, Mu, and Ackerman 2012). Further, aberrant splicing changes have been recognized as important factors in cancer biology (Martinez-Montiel et al. 2018), including in neuroblastoma (Li et al. 2008). The ubiquity of AS and its consequences for neural development and disease underscore the importance of identifying epigenetic mechanisms that promote proper tissue-specific splicing.

Chromatin architecture plays an important role in directing splicing outcomes. Splicing largely occurs cotranscriptionally and is affected by the rate of RNA Polymerase II elongation. The nascent transcript remains associated with chromatin and RNA Pol II during splicing, and this tight connection has been shown to induce chromatin remodeling (Bhatt et al. 2012; Tilgner et al. 2012; Alexander et al. 2010). Histone modifications have been correlated with splicing events, for example overexpression of SET2 in hMSC cells causes an increase in H3K36me3 and aberrant retention of polypyrimidine tract-binding protein (PTB)-dependent exons (Luco et al. 2010). Similarly, increased H3K4me3 led to an increase in exons normally repressed by PTB (Luco et al.

2010). Less understood, is how chromatin remodeling proteins may influence splice site choice. Chromatin remodelers can space nucleosomes along the DNA template, and nucleosome occupancy direct splice site selection. Therefore, studies that illuminate how remodelers may inform splicing is important to elucidate the mechanisms of alternative splicing.

Evolutionarily, the diversification of epigenetic factors in neural cells has provided additional regulatory complexity to these highly specialized these cells. One such factor is *CHD5*, a neural- and vertebrate-specific member of the CHD family of chromatin remodelers. Loss of *CHD5* has been implicated in both tumor formation and autism (Kolla et al. 2014; Pisansky et al. 2017). We have shown that *chd5*, the zebrafish homologue of *CHD5* is required for proper gene expression in developing fish brains. Surprisingly, when we analyzed this data for differential isoform use, we found extensive changes to the transcriptome. The analysis of this data is ongoing, but the progress made to date will be discussed below. Together, the results of this chapter highlight a previously unknown role of Chd5 in neural development.

4.2 Experimental Results

To examine the effect of loss of *chd5* on splicing, we used the JunctionSeq toolset (move ref to here) to analyze 558,461 features across the 30,229 genes in our zebrafish RNA sequencing samples described above (Hartley and Mullikin 2016). In short, we isolated brain tissue from 2-day and 5-day old wild-type and *chd5*^{-/-} fish and obtained >100,000 reads for each biological replicate (n=3). We performed 3 comparisons: first we identified differential splicing events (DSEs) that occur during development of the WT brains between two days and five days of age (comparison of 2-day to 5-day WT tissue; herein referred to as “WT5v2-day”). Second, we examined the effects of loss of *chd5* at the two-day developmental time point by comparing 2-day *chd5*^{-/-} versus 2-day WT (“2-daySE”). Finally, we performed a similar comparison at the 5-day time point (“5-daySE”).

JunctionSeq identifies differential usage of exons and splice junctions (both characterized and novel) relative to the expression level of the gene (Table 4.1). Differential splice junction usage indicates intron retention because increased levels of retained introns will alter splice junction counts without changing the counts for flanking exons (Hartley and Mullikin 2016). Using significance thresholds of $\alpha < 0.01$ and fold change > 2 , we identified more than 5,000 differentially used features (across 2,177 genes) in the WT5v2-day comparison. These results are

consistent with previous reports that a large percent of genes undergo changes in isoform use during neurogenesis (Liu et al. 2018). In the 2-daySE comparison we observe 1,936 features that are increased and 2,307 features that are decreased in *chd5*^{-/-} compared to WT. Similarly, the 5-daySE comparison revealed 1,545 and 2,070 features that are increased and decreased, respectively.

We did not observe a bias in the number of differential splicing events (DSE) in more highly expressed genes, as is evident from the distribution of features shown in the MA plot, (Figure 4.1). Many features that are differentially used in *chd5*^{-/-} vs. WT brains at two days of development are also differentially used at five days (Figure 4.2). This strong overlap suggests that the events that require *chd5* to occur properly are misregulated at both time points, or that changes that occur at 2-days are propagated through to 5-days.

Table 4.1 Summary of differentially spliced features and by direction of change (increase or decrease) calculated using JunctionSeq.

	Total	Exon		Splice Junction		Novel Splice Site	
		Increase	Decrease	Increase	Decrease	Increase	Decrease
WT5v2-day	5034	1087	1107	877	994	589	380
day2-SE	4243	651	882	407	507	878	918
day5-SE	3615	448	763	331	430	766	877

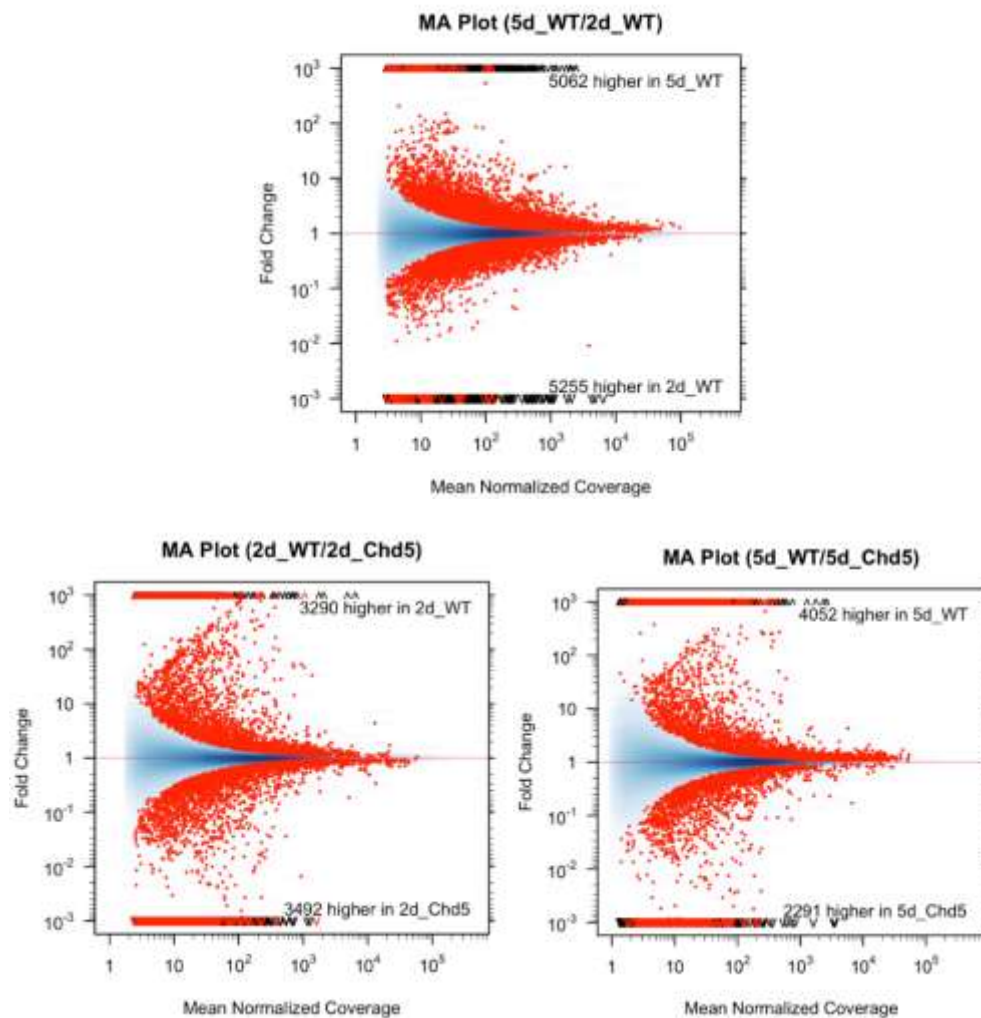


Figure 4.1 MA Plots for each comparison (WT5v2-day, 2-daySE and 5-daySE) showing the differential exon, junction or novel feature usage plotted as the fold change as a function of the gene expression level (mean normalized coverage).

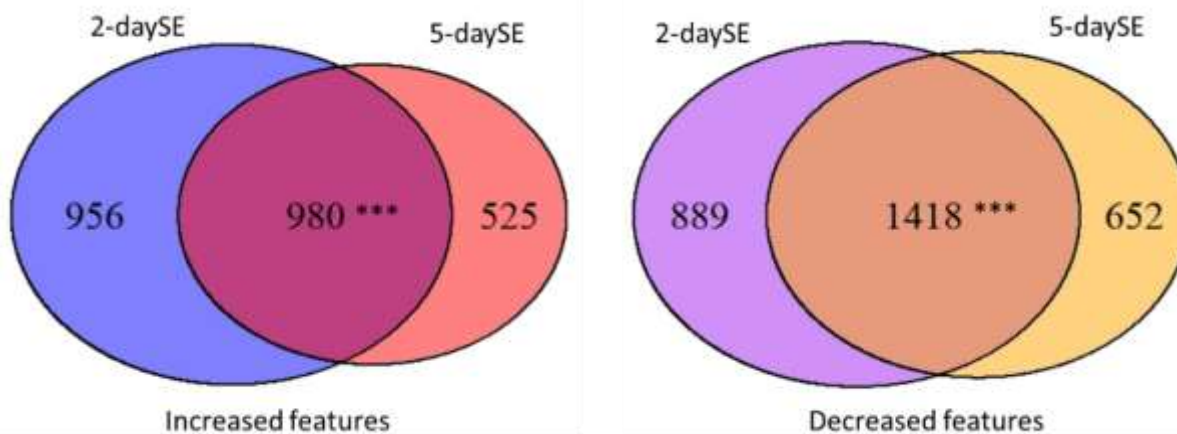


Figure 4.2 The differential splicing events identified in brains that are missing *chd5* show a striking overlap comparing the 2-day to 5-day splice changes.

Intersection analysis between DSEs that increased or decreased in usage at five days vs. at two days of development. DSEs were identified in *chd5*^{-/-} relative to WT brains of the indicated ages. Observed number of genes in common between the indicated gene sets is represented in the overlapped circles. *P*-values were obtained using Fisher's exact test with a null hypothesis of an intersection that is no greater than expected by chance. Significance: *** = $\alpha \leq 10^{-15}$.

A possible explanation for the changes in splice junction and exon usage in *chd5*^{-/-} brains is that Chd5 is necessary to promote expression or promote silencing of splicing factors. However, we examined expression of known splicing factors in our RNA sequencing data set and found few splicing factors that are misexpressed in *chd5*^{-/-} fish, suggesting there are likely additional mechanisms causing the differential splicing signature observed in our mutant fish brains (Table 4.2). As a chromatin remodeler, it is possible that the remodeling action of Chd5 creates changes in the chromatin structure that inform splice site selection and exon usage. Additional experiments are needed to determine if chromatin structure plays a role in the splicing signature that we have identified in our mutant embryos.

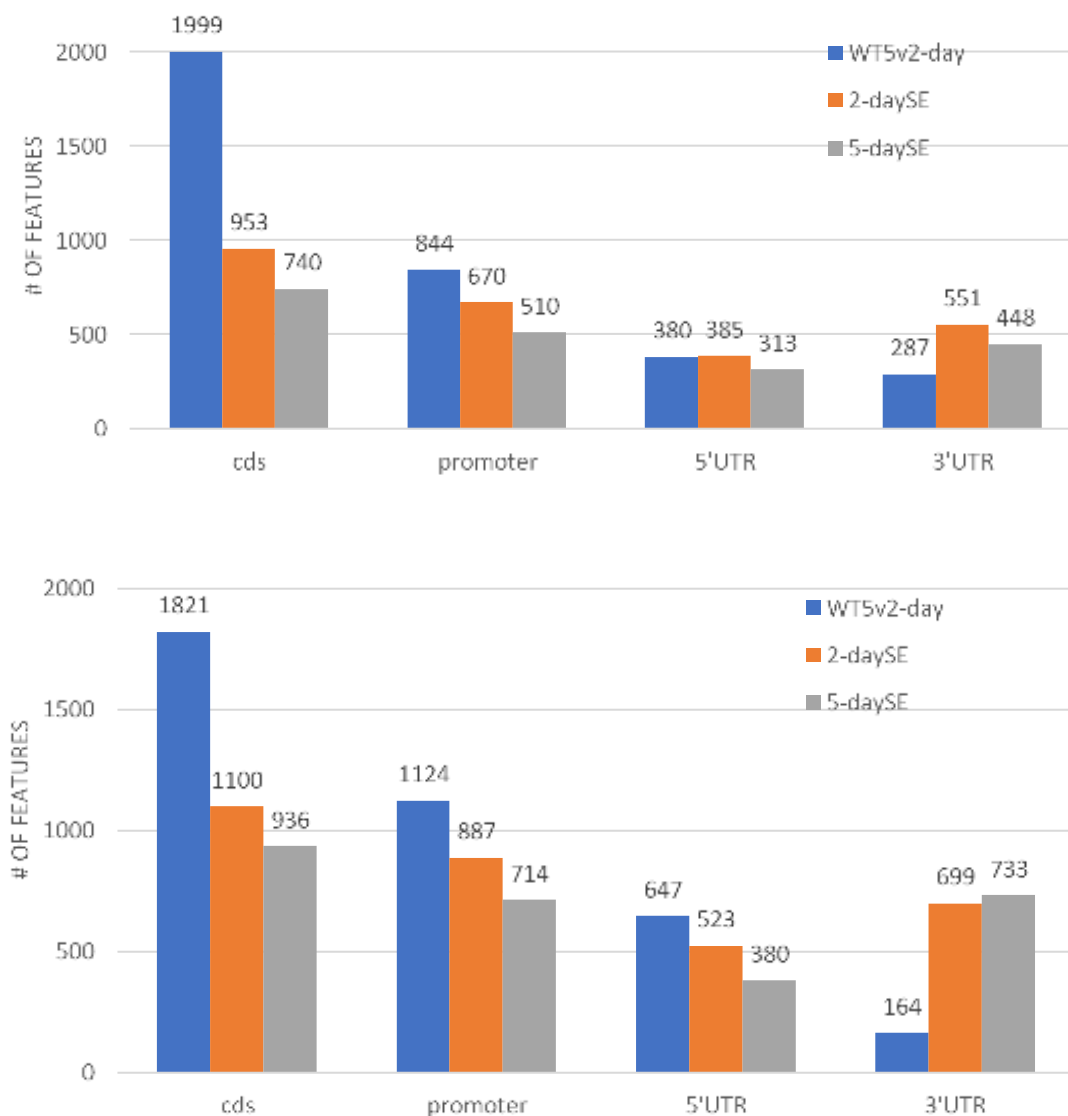
Table 4.2 Known splicing factors exhibit differential expression in *chd5*^{-/-} brains at 2-day and 5-day compared to WT embryos.

Gene name	logFC			Description
	2-day	5-day	WT (2- to 5-day)	
smu1b	0.18	-1.66	5.15	SMU1, DNA replication regulator and spliceosomal factor b
rbm11	-5.04	-2.64	3.64	RNA binding motif protein 11
prmt7	0.37	-3.68	3.19	protein arginine methyltransferase 7
dazap1	-0.74	-1.18	3.14	DAZ associated protein 1
srek1	-4.85	-6.60	0.74	splicing regulatory glutamine/lysine-rich protein 1
mdm2	-1.18	-2.32	0.66	MDM2 oncogene, E3 ubiquitin protein ligas
phf5a	3.23	2.07	0.35	PHD finger protein 5A
znf326	-1.46	-2.73	-0.06	zinc finger protein 326
snu13a	1.14	1.10	-0.22	SNU13 homolog, small nuclear ribonucleoprotein a (U4/U6.U5)
prpf38a	2.44	2.72	-0.82	pre-mRNA processing factor 38A
rbpms2a	-1.01	-0.26	-1.52	RNA binding protein, mRNA processing factor 2a
rbpms2b	-1.15	0.08	-2.25	RNA binding protein, mRNA processing factor 2b

Differential expression was calculated using edgeR between pairwise samples as follows: 2-day *chd5*^{-/-} versus 2-day WT (2-day), 5-day *chd5*^{-/-} versus 5-day WT (5-day), and WT 5-day versus WT 2-day (WT (2- to 5-day)). Orange shading indicates significant decreased expression in the mutant embryos relative to WT (fold change >2 and *p*-value <0.05), and green shading indicates significantly increased expression (fold change >2, and *p*-value <0.05). Red text indicates values that are not significant (*p*-value >0.05). Black text without shading indicates that the expression of the gene did not change significantly (fold change >2) in the comparison.

To further investigate these features, we sought to identify what regions of the gene these DSEs map to (coding sequence, 5'UTR, 3'UTR or promoters). We broke the DSEs into features with increased expression and decreased expression. We find that the majority of DSE in WT5v2-day map to coding regions of the gene, consistent with the majority of the changes occurring in exons (43.6%) (Figure 4.3). We noticed that the 3' UTR contains more DSEs identified in either 2-daySE or 5-daySE compared to WT5v2-day. Intriguingly, DSEs that map to novel features are also much higher in our mutant lines compared to WT5v2-day. In WT5v2-day we observe only 969 novel splice sites (19.2% of DSE), but in 2-daySE and 5-daySE we observe 1,796 (42.3%) and 1,643 (45.4%), respectively.

Figure 4.3 Bar graph showing the proportion of splicing events (exons, splice site and novel splice sites) that map to the indicated regions of the gene for increased (upper graph) or decreased (lower graph) usage.



Genomic ranges was used to call annotated gene features using GRCz11 genome build. The DSEs that exhibit at least a fold change of 2 or greater (FDR <0.01) were used to generate the graph. Numbers above each bar represent the total number of features that fall into each category for the indicated sample comparison.

To understand the splicing changes we sought to identify what regions of the gene these DSEs map to (coding sequence, 5'UTR, 3'UTR or promoters), which will allow us to generate new hypotheses about the causes of the observed changes. We separated the DSEs into two groups based on whether the features exhibited higher usage (Figure 4.3A) or lower usage (Figure 4.3B). We found that the majority of DSE in WT5v2-day are located in the coding regions of the gene, consistent with the highest percent of the changes occurring in exons (43.6%). Compared to WT5v2-day, a higher percentage of DSEs identified with loss of *Chd5* were found in the 3' UTR. This effect is more pronounced in features with decreased usage (Figure 4.3B). Intriguingly, DSEs representing novel features are represented much more highly in the *chd5*^{-/-} comparisons vs. during normal development (WT5v2-day). In WT5v2-day we observed 969 novel splice sites (19.2% of DSE), but in 2-daySE and 5-daySE we observed 1,796 (42.3%) and 1,643 (45.4%), respectively, suggesting that *Chd5* is necessary to promote proper processing of transcripts.

To examine the novel DSEs found in the *chd5*^{-/-} samples, we calculated their DNA-base content (AT%) to determine if these features are more similar to exons or noncoding regions of the genome such as introns and junctions in DNA base composition. We found that novel splicing features have an average AT% of 62.55%, which is comparable to the known DSE that map to splice junctions (64.03% AT content) than the exons (55.92% AT content) (Figure 4.4). These data suggest that the novel features largely comprise noncoding regions of the genome. Because these novel features appear to be noncoding we wondered specifically what part of the genome these features map to. We mapped these novel splice junctions to the gene features across the *Danio* genome and found that the majority of these features map to the 3'UTR (Figure 4.5). Altered 3' end use suggests that our *chd5*^{-/-} zebrafish may have altered polyadenylation, in addition to the altered splicing we observe. Surprisingly, when we examine the expression level of known genes that promote polyadenylation, we do not observe any statistically significant changes at the transcript level, suggesting there are other processes that promote polyA site selection that are misregulated when *chd5* is absent (Table 4.3).

We hypothesized that the genes that are differentially spliced would likely fall into networks are involved in neuronal processes, as *chd5* is most highly expressed in neurons. We used gene ontology (GO) analysis to identify biological processes that are overrepresented among the genes containing at least one DSE. For this analysis, we separated the 2-daySE or 5-daySE lists based on DSE type (exon, splice site, novel splice site) and whether the feature was increased

or decreased in *chd5*^{-/-} (giving us 6 categories in total for each time point). Strikingly, we observed an enrichment of neural-development associated genes only in the novel feature types that exhibit decreased usage. This was observed at both two and five days but was particularly enriched in the 5-day sample (Tables 4.4 and 4.5).

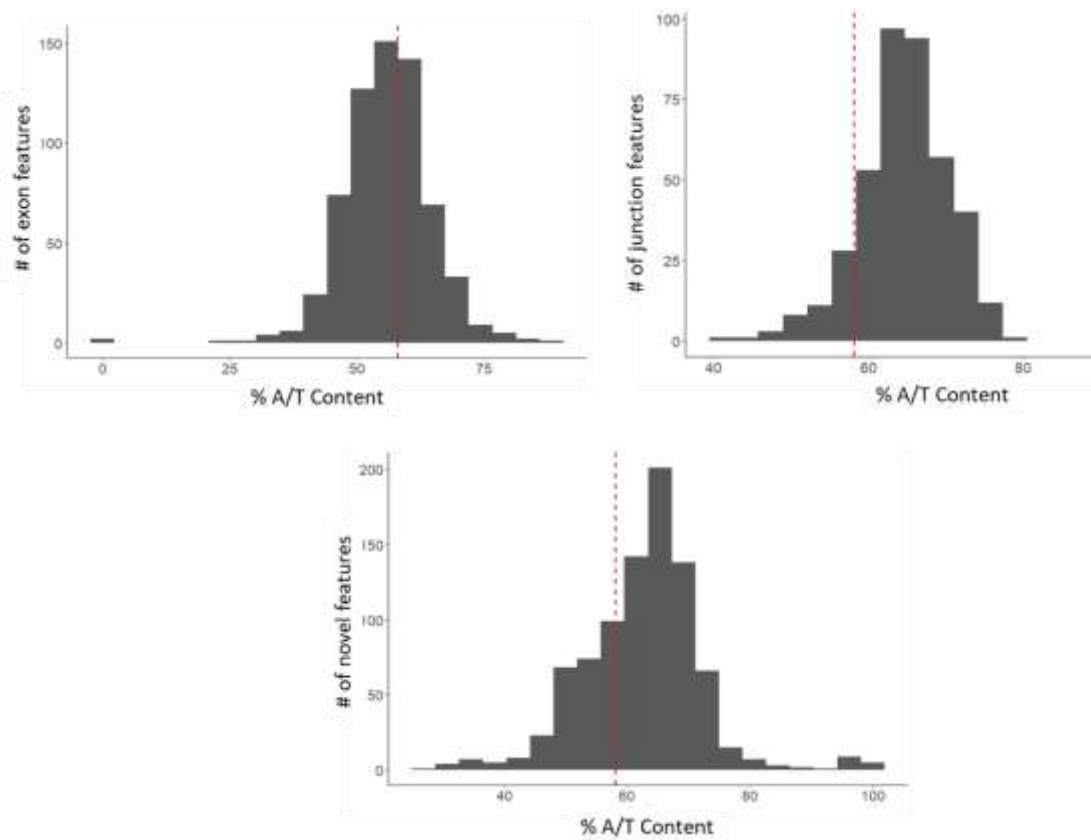


Figure 4.4 DNA content analysis shows that the enrichment of A/T nucleotides is highest in junctions and novel features, compared to exons, indicated novel features are most likely noncoding features of the genome.

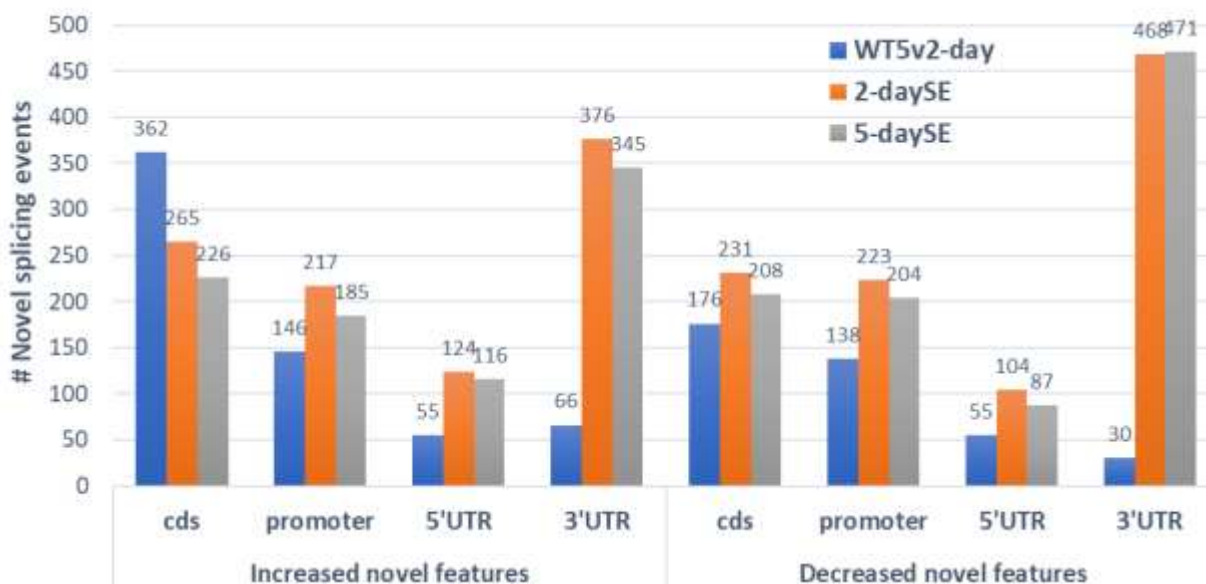


Figure 4.5 Novel splicing features are enriched in the 3' UTR of genes at both 2-day and 5-day in the *chd5* mutant embryos.

Table 4.3 Known polyadenylation genes are not differentially expressed in the absence of *chd5* in developing zebrafish brains, as determined at 2- or 5-days compared to WT.

Gene	logFC			Description
	2-day	5-day	WT 5v2-day	
<i>cpsf2</i>	-0.01	0.03	-1.11	cleavage and polyadenylation specific factor 2
<i>ybx1</i>	0.07	0.14	-1.10	Y box binding protein 1
<i>exosc2</i>	-0.04	0.12	-1.03	exosome component 2
<i>cpeb1a</i>	-1.07	-1.15	-0.58	cytoplasmic polyadenylation element binding protein 1a
<i>cpeb3</i>	0.02	0.12	1.05	cytoplasmic polyadenylation element binding protein 3
<i>cpeb4a</i>	0.79	1.48	1.19	cytoplasmic polyadenylation element binding protein 4a

Differential expression was calculated using edgeR between pairwise samples as follows: 2-day *chd5*^{-/-} versus 2-day WT (2-day), 5-day *chd5*^{-/-} versus 5-day WT (5-day), and WT 5-day versus WT 2-day (WT (2- to 5-day)). Red boxes indicate significant decreased expression in the mutant embryos (fold change >2 and p-value <0.05), and green boxes indicate significantly increased expression (Fold change >2, and p-value <0.05). Red texts indicates values that are not significant (p-value >0.05).

Table 4.4 GO biological processes that are associate with decreased novel features in the 2-daySE comparison.

TermID	Term	logP	Gene Symbols
GO:0048679	regulation of axon regeneration	-9.03	tnc,sfpq,rgma,il6st
GO:0098813	nuclear chromosome segregation	-8.85	cdc14ab,ercc4,spdl1,rad21a,ran,ewsr1a,znf207b,znf207a,zgc:85936
GO:0007059	chromosome segregation	-8.34	ercc4,spdl1,cdc14ab,ewsr1a,rad21a,ran,znf207a,zgc:85936,znf207b,ddx3b
GO:0021954	central nervous system neuron development	-8.29	dcc,ntn1b,emx3,nr4a2a,ewsr1a,sfpq
GO:0018107	peptidyl-threonine phosphorylation	-6.85	dclk2a,bsk146,dclk1b,camk2b1,phkg2
GO:0007019	microtubule depolymerization	-6.76	stmn4l,stmn2b,stmn2a
GO:0031577	spindle checkpoint	-6.76	spdl1,znf207b,znf207a
GO:0071840	cellular component organization or biogenesis	-6.73	atg4a,pbrm1l,tcirg1b,tardbp,rps6,aspm,ttc39c,ran,eif4bb,cxcl12a,ercc4,kctd7,rpl35a,znf207a,ift20,znf207b,ctnnb1,kif3b,arpc5a,tdrd3,stmn4l,nop2,dpysl4,prmt8b,asna1,dclk2a,atg16l1,zgc:85936,dpysl5a,dnm1a,emsy,tnc,arnt2,tbl1xr1b,nusap1,sfpq,mbd3b,stmn2a,emx3,wdr55,ndrg4,akap12b,svila,noa1,snap29,elmo2,cdc14ab,nefmb,napbb,dcc,ewsr1a,luc7l3,atg9b,ptk2ab,cnr1,h2afx1,wdr45b,fcho2,kdm6bb,prnprs3,pfn2,ntn1b,zgc:158803,si:ch211-173p18.3,prpf39,ndufaf3,dclk1b,spdl1,isca1,dpysl3,noc2l,wrbb,kat2b,stmn2b,supt16h,pak7,eif3eb,tmsb,nop10,rad21a,ube2a,nphp3
GO:0006376	mRNA splice site selection	-6.37	zgc:158803,prpf39,luc7l3

Table 4.5 GO biological processes that are associate with decreased novel features in the 5-daySE comparison.

TermID	Term	logP	Gene Symbols
GO:0010975	regulation of neuron projection development	-6.78	sfpq,dcc,ntn1b,dpysl3,cxcl12a,rgma,il6st,lrrk2
GO:0021955	central nervous system neuron axonogenesis	-6.64	sfpq,dcc,ntn1b,emx3
GO:0021954	central nervous system neuron development	-6.62	emx3,ewsr1a,ntn1b,dcc,sfpq
GO:0120035	regulation of plasma membrane bounded cell projection organization	-6.58	vdac3,rgma,il6st,sfpq,dcc,ntn1b,dpysl3,cxcl12a,lrrk2
GO:0031344	regulation of cell projection organization	-6.58	ntn1b,dpysl3,cxcl12a,sfpq,dcc,rgma,il6st,vdac3,lrrk2
GO:0070570	regulation of neuron projection regeneration	-6.29	il6st,rgma,sfpq
GO:0071678	olfactory bulb axon guidance	-6.21	dcc,ntn1b
GO:0021537	telencephalon development	-6.07	emx3,zdhhc16a,ntn1b,dcc
GO:0060322	head development	-5.64	cxcl12a,arnt2,pycr1b,dcc,mir9-7,mpp5a,emx3,prmt8b,wls,ddx3b,acvr2aa,pax6b,ntn1b,prnprs3,her15.1,sfpq,dixdc1a,ndrg4,zdhhc16a,crabp2b,ywhag1
GO:0060560	developmental growth involved in morphogenesis	-5.61	zeb2b,pigp,akap12b,tardbp,dcc,ptk7a,eaf2
GO:0003401	axis elongation	-5.60	pigp,akap12b,zeb2b,ptk7a,eaf2
GO:0007417	central nervous system development	-5.46	dixdc1a,sulf1,ndrg4,appa,zdhhc16a,ewsr1a,crabp2b,ywhag1,pax6b,sar1b,ntn1b,prnprs3,her15.1,sfpq,wls,ddx3b,acvr2aa,bcan,cxcl12a,arnt2,pycr1b,dcc,mpp5a,emx3,prmt8b
GO:0007420	brain development	-5.43	dixdc1a,crabp2b,ywhag1,zdhhc16a,ndrg4,sfpq,her15.1,prnprs3,ntn1b,pax6b,ddx3b,wls,acvr2aa,dcc,pycr1b,cxcl12a,arnt2,prmt8b,emx3,mpp5a
GO:0030900	forebrain development	-5.36	wls,dixdc1a,zdhhc16a,ntn1b,cxcl12a,arnt2,pax6b,dcc,emx3
GO:0018210	peptidyl-threonine modification	-5.16	dclk2a,dclk1b,camk2b1,phkg2
GO:0021952	central nervous system projection neuron axonogenesis	-5.05	ntn1b,dcc,emx3

Next we wanted to know if only novel features are changing at the 3' UTR or if additional changes are occurring in our mutant embryos compared to the changes which occur normally across development. We mapped all features (exons, splice junctions and novel splice junctions) against the GRCz11 (*Danio rerio* genome build) annotated 3' UTRs (summarized in Table 4.6). We observe a large proportion of changes occurring in the 3' UTR in our mutant embryos compared to WT, further supporting that we likely have a termination defect in our mutant embryos, in addition to the alternative splicing identified in differentially used exons and splice sites. We also determined that the changes that are observed in our 2day-SE samples overlap significantly

with the changes observed at 5day-SE (Table 4.7). The strong overlap suggests several possibilities about the timing of these observed change. One explanation that remains to be determined is that these changes are occurring at an earlier time point (prior to 2-days) where Chd5 is necessary to promote proper transcript processing. These data do strongly suggest that Chd5 is required for proper splicing and polyadenylation in the developing zebrafish brain.

Table 4.6 We observe a large number of changes occurring in the 3' UTR using the observed changes in all differentially utilized features in *chd5* mutants compared to WT.

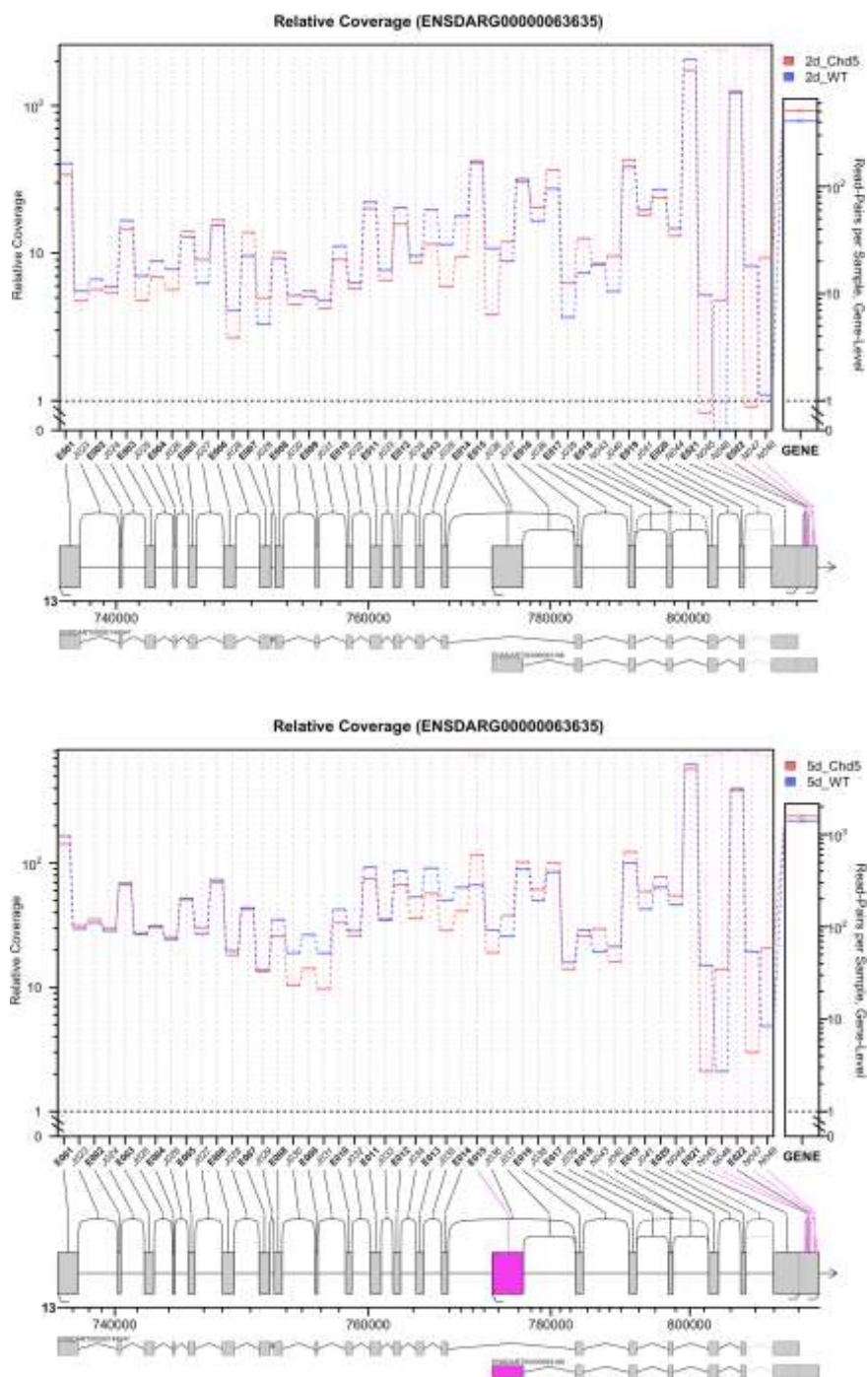
	Increase WT5v2	Decrease WT5v2	Increase 2-day	Decrease 2-day	Increase 5-day	Decrease 5-day
Exons	168	83	145	184	76	222
Junctions	51	48	23	39	22	35
Novel	62	27	371	464	338	467
Total:	281	158	539	687	436	724

Table 4.7 Features that specifically change in the 3' UTR of genes in our mutant embryos exhibits significant overlap at 2-day and 5-day.

Sample A	Sample B	Observed	Predicted	<i>p</i> -value
day2-SE increase	day5-SE increase	326	5.64	0
day2-SE increase	day5-SE decrease	0	9.37	1
day2-SE decrease	day5-SE increase	0	7.19	1
day2-SE decrease	day5-SE decrease	534	11.95	0

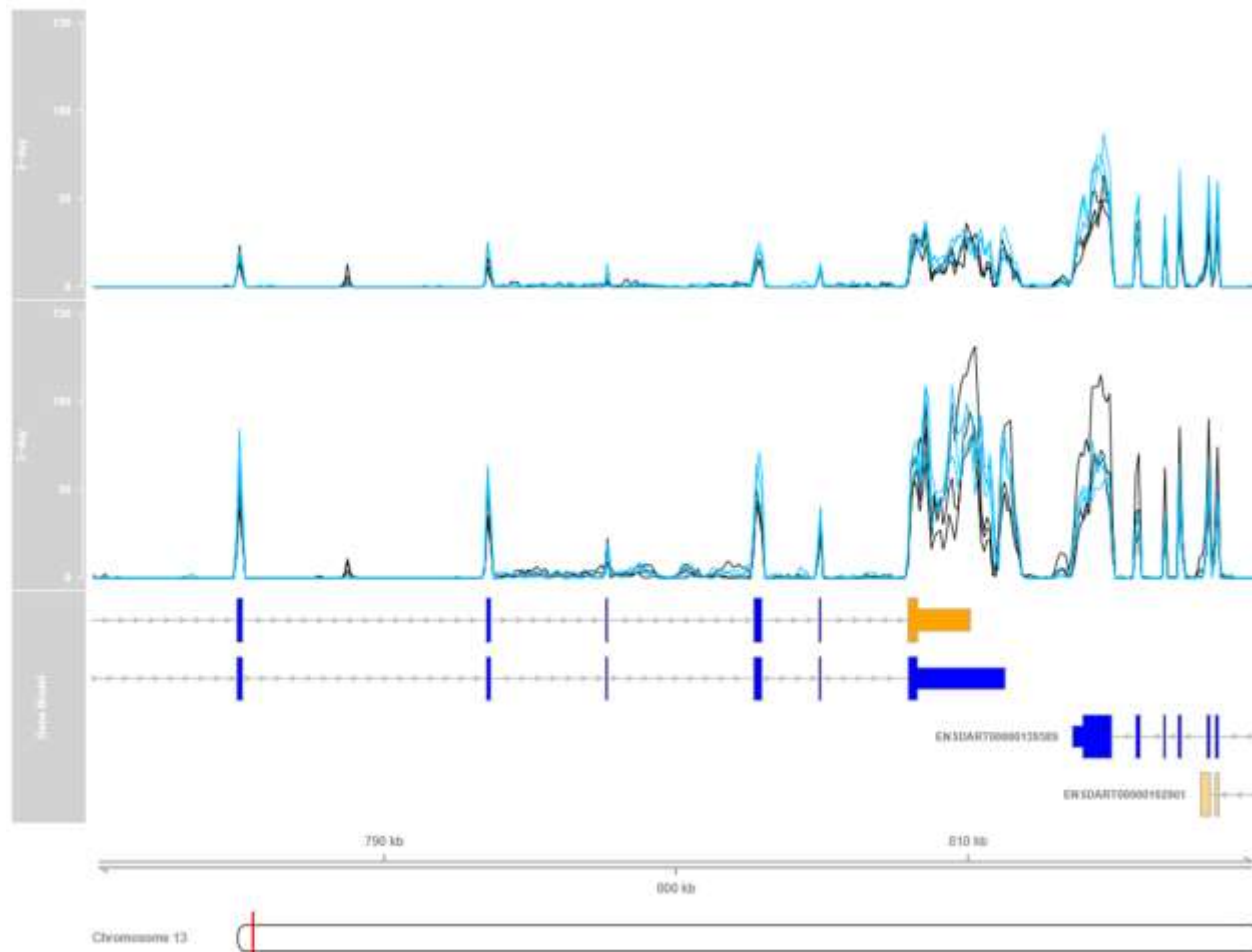
We also sought to visualize these changes using wiggle plots and the Gviz package. This tool allows us to show how the read coverage reflects the indicated changes calculated using the JunctionSeq package. This method of visualization also gives us the ability to compare the expression and usage of gene features at both 2-day and 5-day, in our mutant and WT embryos. We picked several example genes based on either their change in feature use, or on their predicted role in biological processes we hypothesize reflect the phenotypes previously ascribed to loss of *chd5* in mice, namely altered dendritic arborization and neural differentiation.

Figure 4.6 Gene profile plot for Neurexin1b shows significantly differentially used features calculated by JunctionSeq at 2-day and 5-day.



Blue (WT) and red (*chd5*^{-/-}) lines corresponds to the expression level for each feature (exon or splice junction) as normalized read-pair counts (main panel/graph of figure). Differentially used features are labeled in pink. The bottom panel shows a line drawing of the neurexin1b gene. The box on the far right shows the relative overall expression level of the gene between the samples.

Figure 4.7 Representative Gviz plot to examine splicing/termination defects observed in our *chd5* knockout embryos compared to WT, at both 2- and 5-days.



The 3'UTR of Neurexin3b is shown (a gene involved in neural development). Black lines represent each biological replicate of WT, and blue shows each replicated of the *chd5*^{-/-} brains at the indicated time (2-day, top and 5-day, lower panel). The gene model shows two transcriptional variants of Neurexin1b.

4.3 Discussion

The molecular mechanisms that drive AS are of increasing interest for their role in development and human disease (Liang et al. 2019; Illig et al. 2019; Li and Yu 2018; Martinez-Montiel et al. 2018; Larsen et al. 2017; Annalora, Marcus, and Iversen 2017; Lee et al. 2016). AS is a critical platform to generate complexity in the proteome from the limited number of genes present. Here we show that the chromatin remodeler Chd5 is necessary for proper regulation of splicing events during brain development in *Danio rerio*. In addition to the transcriptional changes that are observed in *chd5*^{-/-} zebrafish (detailed in Chapter 3), the observation that several thousand

genes are differentially spliced, and possibly alternatively polyadenylated, opens up new views on the critical role Chd5 plays in neurogenesis. However, it is necessary to define if these changes do result in alternative polyadenylation, and we propose to use 3' rapid amplification of cDNA ends (RACE) experiments in both WT and *chd5*^{-/-} as previously described to determine this (Ma and Hunt 2015), and also northern blots to examine the length of the transcripts.

One hypothesis we explored is that in the absence of Chd5, core splicing components may be misexpressed. However, when we examine the transcriptome for overall expression of splicing factors, we find only a few examples of differentially expressed genes, and these genes are generally failing to be activated (Table 4.2). Further investigation into the characterization of these misexpressed splicing factors is needed, but several of these candidates provide compelling explanations for the CHD5-dependent phenotypes. For example, the RNA-binding protein (RBP) *rbps2a/b* (Hermes) is required in zebrafish to promote retinal axon arborization (a dominant-negative version of Hermes lead to a reduction in branches of these neurons) (Hornberg et al. 2013). Another misexpressed splicing factor is the *p53*-negative regulator *mdm2*, which mediates stress responses of cells including neurons, and has significant impacts on tumorigenesis and cell cycle regulation (Hu, Feng, and Levine 2012). Another possible explanation for the transcriptome phenotype associated with loss of Chd5 is that the splicing changes may be causative of the gene expression changes observed in developing brains that lack *chd5*. Analyses to determine changes to core transcription factors and other key players in gene expression is ongoing.

Of interest in understanding the mechanism behind these transcript processing defects is determining what chromatin features, or RNA-guided mechanisms may be misregulated when Chd5 is absent. This data does not provide a mechanistic model for how Chd5 is directing splicing, be it in direct interactions with the transcripts or indirectly through gene expression changes for example. Recently, nucleosome distribution preferentially across exons has suggested that histone density correlates with inclusion levels of exons (Schwartz, Meshorer, and Ast 2009; Kim, Park, et al. 2018). Furthermore, exon-intron boundaries are defined by histone marks that may facilitate splice site selection, though the mechanisms require continued investigation (Schwartz, Meshorer, and Ast 2009). We have demonstrated that zebrafish Chd5 remodels nucleosomes, and therefore it remains possible that altered nucleosome positioning in our mutants may influence the differential splicing features we observe (Bishop et al. 2015).

Another feature of substantial interest given the role of CHD5 in the NuRD complex, is how DNA methylation and hydroxymethylation may also play a role in the differential splicing observed in *chd5*^{-/-} brain tissue. DNA methylation has been shown in humans, Arabidopsis and honey bees to correlate with exon-intron boundaries, suggesting this is another feature that is evolutionarily conserved to mark these boundaries for AS (Chodavarapu et al. 2010; Hodges et al. 2009; Lyko et al. 2010). Analysis of 5-hmC has been hindered by the difficulty in discerning this mark from 5-mC, but 5-hmC is known to be more highly abundant in the brain than in other tissues. Recently, using restriction-enzyme digestion and microarray analysis it was shown that 5-hmC is enriched at the exon-intron boundary in the brain (Khare et al. 2012). Remarkably, 100% of constitutive exons contain higher levels of 5-hmC than alternative spliced exons, suggesting that this mark may play a role in determining AS (Khare et al. 2012). These are areas that require further exploration in the absence of Chd5.

Finally, transcript cleavage and pA are required steps to generate the functional mRNA for translation. Most eukaryotic genes (an estimated 70%) contain multiple pA sites, resulting in diverse transcript outcomes through alternative pA (Neve et al. 2017). Numerous 3' end processing defects have been reported that contribute to human disease, such as tumorigenesis, hematological disorders, endocrine disease and neurological diseases such as Alzheimer's and Parkinson's (Curinha et al. 2014). Tissue differences in pA profiles has recently been described in several studies, and one of the most striking findings is that the brain and testes (Miura et al. 2013; Wang et al. 2008; Liu et al. 2007; Wang et al. 1993; MacDonald 2019). However, pA sites are poorly conserved across species (Ara et al. 2006; Derti et al. 2012), so it remains to be determined if CHD5 plays similar roles in both splicing and pA selection in higher-order eukaryotes.

CHAPTER 5. ESTABLISHMENT OF MOUSE EMBRYONIC STEM CELL KNOCKOUT LINES TO MODEL THE CONSEQUENCE OF LOSS OF CHD5 ON NEURAL DIFFERENTIATION

5.1 Introduction

The current understanding of CHD5 suggest that it is necessary to promote neurogenesis, however the phenotypes associated with CHD5 are relatively mild considering the strong data linking CHD5 to human pathologies (Fatemi et al. 2014; Zhao, Wang, et al. 2014; Zhao, Meng, et al. 2014; Wang, He, et al. 2013; Koyama et al. 2012; Li et al. 2012; Wu, Zhu, Li, Fu, Su, Fu, Zhang, Luo, Sun, Fu, et al. 2012; Zhao et al. 2012; Wong et al. 2011b). Regarding the role of CHD5's contribution to neurogenesis and tumor suppression, biochemical and genome wide analyses are needed to determine how CHD5 plays these roles. Characterization of the domains of CHD5 shows that the CDs bind to the repressive epigenetic modification H3K27me3 (trimethylation of histone H3 at lysine 27), and this action is necessary for proper expression of genes enriched for this mark during differentiation of neural tissue (Egan et al. 2013b). CHD5 is also recruited to chromatin through its tandem N-terminal PHD domains, which simultaneously bind to two H3 tails, preferring the unmodified substrate in this in vitro assay (Oliver et al. 2012). Furthermore, the PHD domains have been shown to be essential for CHD5-mediated tumor suppression (Paul et al. 2013a).

In addition to these studies of CHD5, it has been shown that CHD3-related proteins are subunits in Mi-2/NuRD complexes and the NuRD complex has been suggested to play a major role in gene repression through the deacetylation of histones in vertebrates (Wolffe, Urnov, and Guschin 2000; Quan et al. 2014; Potts et al. 2011; Allen, Wade, and Kutateladze 2013). The NuRD complex has recently been implicated in fine-tuning gene expression at active sites of transcription and can result in both an increase or decrease in transcription (Bornelov et al. 2018). Consistently, chromatin immunoprecipitation (ChIP) data shows that CHD5 binds to the transcriptional start site of actively transcribed genes (Egan et al. 2013b). These data raise the prospect that CHD5 also promotes activation of a cohort of genes, particularly of those that are directly involved in neural development (Egan et al. 2013b). However, much remains to be learned regarding the specific biochemical mechanisms by which CHD5 contributes to gene expression and tumor suppression.

Transcriptomics studies from our lab indicate that zebrafish *chd5* promotes proper gene expression and splicing during a critical window in early brain development when significant differentiation is occurring. However, as these sequencing studies were undertaken in intact tissue samples, we are examining the average transcriptional effects across the hundreds of cellular subtypes found in the brain, such as multiple neural subtypes and glial cells. Furthermore, the ability to critically investigate the contribution of chromatin features or perform comparative analyses of our observed changes in zebrafish is highly limited, primarily because of the complexity of the tissue and the lack of publicly available datasets. Similarly, it will be of great interest to determine if these novel splicing changes that we identified in our zebrafish brains are conserved in higher vertebrates.

To that end, we have begun work to engineer CRISPR/Cas9 knockouts of *CHD5* in cell culture models. Cell culture has many molecular tools available to complement, and expand our insights gained from zebrafish. Originally, we designed guide RNAs that target human *CHD5* and cloned them into a Cas9-expressing vector (Sanjana, Shalem, and Zhang 2014) and transfected SH-SY5Y cells with these constructs. Although clonal selection of these transfected identified mutations in *CHD5*, loss of *CHD5* resulted in an extreme growth defect in these cells (data not shown). Due to the growth defects observed in SH-SY5Y neuroblastoma cells, we turned to mouse embryonic stem cells (ESCs) to continue our work. Using mESCs, we will have numerous molecular tools available to us to study the consequence of losing Chd5 in a mammalian system, including characterized antibodies, established ChIP protocols and numerous studies available from the GEO repository. The mESCs have been widely used to characterize events that occur as a consequence of in vitro differentiation of these cells into neurons through application of retinoic acid (RA) (Gholamitabar Tabari et al. 2018; Wu et al. 2017; Yang et al. 2017; Sharova et al. 2016). Additionally, we have secured funding from the Purdue Center for Cancer Research to implement an RNA-seq study of mouse embryonic stem cells undergoing neural differentiation to determine if the changes we have observed in developing zebrafish brains are conserved.

5.2 Experimental Results

We have generated CRISPR/Cas9 constructs that contain gRNA that target the murine Chd5 upstream of the annotated domains (Table 5.1). In short, we cloned a sgRNA downstream of the U6 promoter of the lentiCRISPR-v2 vector, which contains the *Streptococcus pyogenes* Cas9

nuclease (Sanjana, Shalem, and Zhang 2014). After confirming gRNA sequences by low-throughput sequencing, we packed lentivirus particles and subsequently transduced mESCs with each of the three *Chd5* targeting gRNAs that we had designed. Each of these gRNAs target *Chd5* N-terminal to the annotated CD and PHD domains. Next, we used puromycin selection to create a pool of cells that had been successfully transduced and undertook clonal selection to identify loss-of-function alleles of murine *CHD5*.

Table 5.1 Guide RNA sequences targeting murine *Chd5*.

Target Exon	gRNA sequence (5' to 3')	Strand
4	GTCCTCGGGACAACACTCATGG	Forward
10	GCTGAACCTTTGCCCTTCAGC	Reverse
11	GAGCCGTAATCAAAGGGTGG	Reverse

Using western blot analysis, we screened through clonal cells for reduced CHD5 protein levels, consistent with deleterious mutations obtained at the genomic locus corresponding to *CHD5*. We identified several clones from our western blot that demonstrate reduced levels of the band corresponding to the predicted molecular weight of CHD5 (Figure 5.1). This antibody targets the middle region of the protein, so it will not identify any truncated *CHD5* generated by these gRNAs (GeneTex, anti-CHD5). Sequencing analysis to find knockout cells suggests that we have obtained two knockout alleles of *CHD5* from these lines (Figure 5.2). Consistent with the loss of *CHD5* from these cells, quantitative PCR (q-PCR) shows that the transcript levels of *CHD5* are reduced in the ESCs compared to cells treated with a control gRNA (Figure 5.3).

Using these knockout cells we now have a system to further study the consequence of loss of *CHD5* on the transcriptome during neural differentiation. To do this we need to identify appropriate conditions to differentiate the cells into neurons using retinoic acid. First to test the ability of these cells to undergo differentiation we used WT, gRNA control lines and the knockout cells to generate embryoid bodies. Normally, mESCs will aggregate into a ball of pluripotent stem cells, called embryoid bodies (Martin 1981). We do not expect loss of *CHD5* to result in failure to form embryoid bodies, which would be consistent with the observation that knockout animals are grossly phenotypically indistinguishable from WT. Indeed, we observed a consistent ability of the cells to cluster into EBs of approximately the same diameter by empirical observation.

Next, we tested the ability of these cells to differentiate into neurons using retinoic acid induction. shRNA-mediated knockdown of *CHD5* has been used previously to explore the contribution of *CHD5* to retinoic acid-induced differentiation in SH-SY5Y cells, in which that observed that knockdown of *CHD5* leads to a failure of these cells to acquire markers of differentiated neurons (Egan et al. 2013a). We will characterize the differentiation phenotype of retinoic acid-treated CHD5-KO cells in a similar fashion, using immunohistochemistry and qPCR to test for the relative expression of known differentiation markers. Specifically, we will examine the differentiation phenotype of cells with and without *CHD5* using phase-contrast microscopy and antibody staining for the neural markers *tyrosine hydroxylase* and *synaptophysin* and by examining expression of previously identified *CHD5*-dependent genes (Egan et al. 2013a).

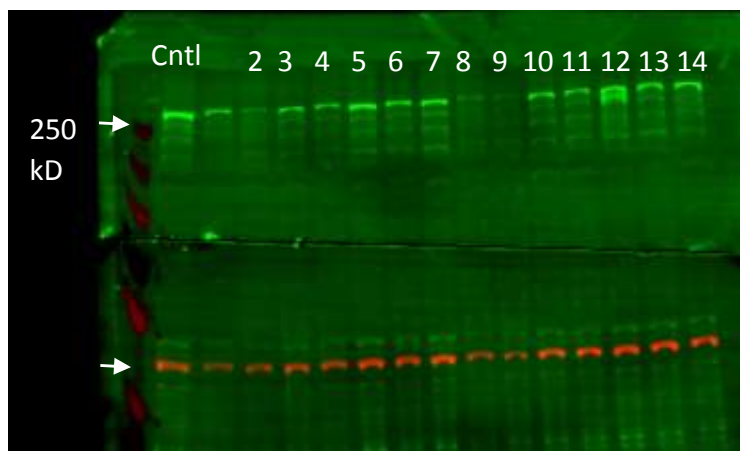


Figure 5.1 Western blot analysis of clonal cell populations to identify possible knockout lines. Total cellular extract was run on a gradient SDS-page gel and probed with CHD5 antibody (250 kd band) or beta-actin as a loading control (red band in lower gel). Clones such as lane 2, 8 and 9 were further characterized to find knockout alleles. (Antibody: GeneTex anti-CHD5).

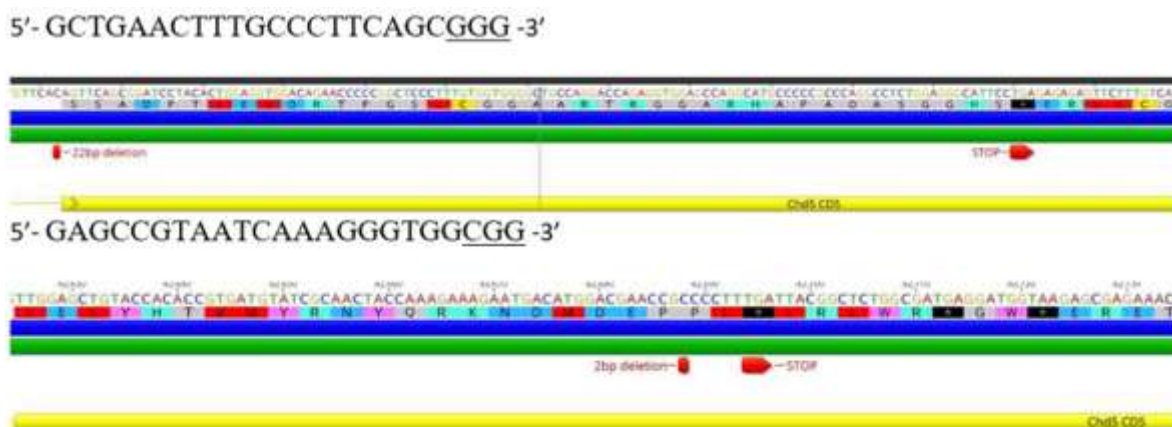


Figure 5.2 CRISPR/Cas9 induced mutations in *CHD5* result in formation of premature stop codons in the coding sequence to create gene knockouts. The gRNA sequence used to target the region is shown above the identified null allele, and the PAM sequences are underlined. The mutations identified by sequencing are shown in red boxes, and the in-frame stop codon is shown.

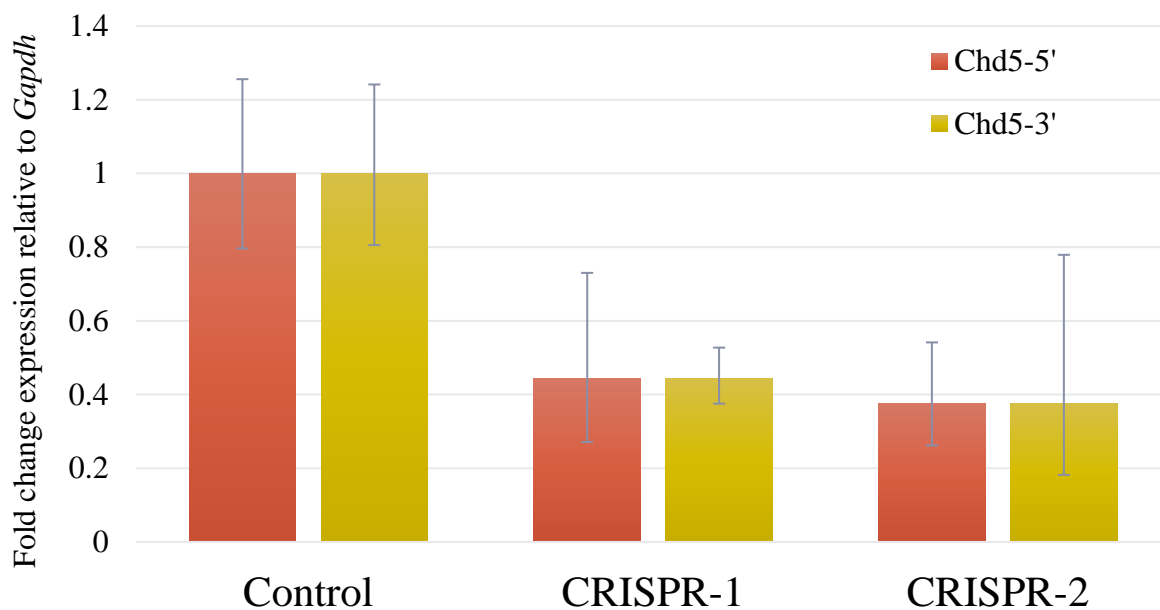


Figure 5.3 Quantitative PCR shows a reduction of *CHD5* transcript in mouse ESCs, consistent with nonsense mediated decay caused by deleterious mutations to the gene. Fold change of *Chd5* is shown relative to *Gapdh*. Cells were harvested at day 0 (D0). Error bars are standard deviation of two technical replicates.

To test if *CHD5* knockout mESCs are responsive to RA, we first generated EBs and then added 10 micromolar RA to the cells and observed them for presence of characteristic neural structures such as arborization. We harvest the cells after 5-days of RA treatment, and performed qPCR analysis of known neural markers to identify if these cells had acquired neural gene expression patterns similarly to WT cells. However, these experiments reflect only one biological replicate and will need to be repeated with additional replicates to determine if the observed trends are consistent. We hypothesized that loss of *CHD5* would result in a failure of these cells to acquire the gene expression pattern of terminally differentiated neurons. We observed that the WT cells robustly express the neural precursor marker *Nestin* and the terminal neural differentiation marker *Tubb3*. Similarly, *CHD5*^{-/-} cells respond to RA treatment and acquire expression of *Nestin*, but fail to express *Tubb3* to the same extent as observe in WT. These results are consistent with *CHD5*^{-/-} mESCs beginning to differentiate toward neural lineages but failing to activate into terminally differentiated cells (Figure 5.4). This protocol will need further optimization to determine the necessary time to robustly test if loss of *CHD5* is causing these cells to fail to differentiate over longer time periods. Additionally, we will test this differentiation by immunohistochemistry, as mentioned above.

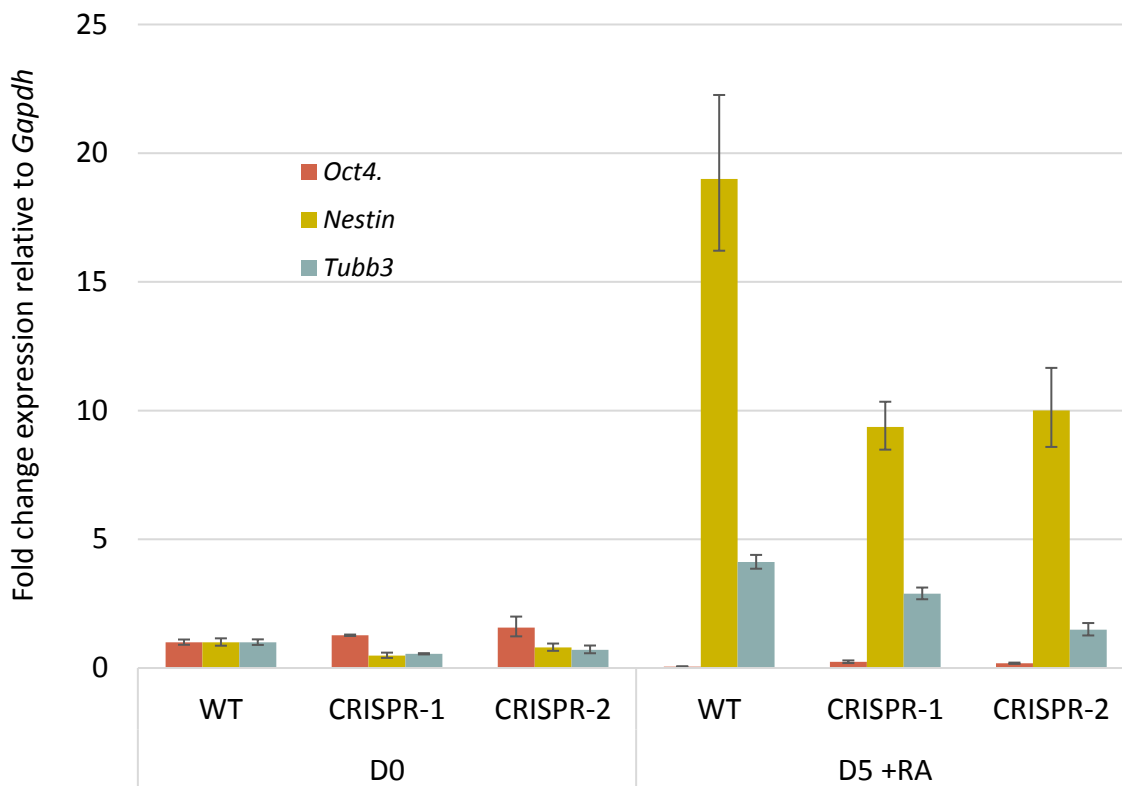


Figure 5.4 *CHD5*-KO cells fail to express markers of neural differentiation compared to WT. Fold change of the pluripotency marker *Oct4*, the neural precursor cell marker *Nestin* and the differentiated neuronal marker *Tubb3* are shown relative to the housekeeping gene *Gapdh*. Cells were harvested at day 0 (D0), or 5-days after retinoic acid addition (D5+RA). Error bars are standard deviation of 2 technical replicates.

5.3 Discussion

These early results demonstrate that we have successfully engineered knockout alleles of *CHD5* using CRISPR/Cas9 in mESCs. Furthermore, we have begun characterization of these cells as they undergo neural differentiation using retinoic acid, a well established method that has been previously used to examine knockdown of *CHD5* in SH-SY5Y cells (Egan et al. 2013b). We will use cells that carry a knockout allele of *CHD5* and compare the undifferentiated and retinoic acid-differentiated cells to wild-type controls to examine both differential gene expression and splicing alterations, allowing us to determine what changes are conserved from zebrafish to a mammalian system (Chapters 3 and 4). We have purchased 40,000 reads for 3 biological replicates of both undifferentiated and RA differentiated cells, in both WT and *CHD5*^{-/-}. The results of this

transcriptomics study will substantially increase our understanding of how *CHD5* is promoting neural differentiation.

An advantage of cell culture models is the availability of public repositories of many RNA-seq, ChIP-seq, ATAC-seq and methylation mapping studies performed under similar conditions, which we can use to overlap with our data, allowing us to make informed hypotheses about how *CHD5* is contributing to differentiation processes. Development of this model also gives us the opportunity to undertake our own analysis of H3K27me3 enriched loci by ChIP, as well as other chromatin marks as these protocols and antibodies are widely available. Of particular interest is the connection of the NuRD complex with DNA methylation and hydroxymethylation through the *MBD3* subunit, as well as the possible connection of *CHD5* to conserved functions of the plant subfamily II remodeler PICKLE which has been shown to promote incorporation of the histone variant H2A.Z into the chromatin template. Hypotheses will we further test in this system are described below, please see future directions.

CHAPTER 6. ONGOING PROJECTS

6.1 Introduction

A confounding aspect of previous functional analysis of *CHD5* remodelers is that knock-down phenotypes give the appearance of being stronger than knock-out phenotypes. Initial reports describing ablation of *CHD5* in mice describe spermatogenesis defects leading to decreased male fertility, but no detectable neurological or tumor phenotypes (Zhuang et al. 2014; Li et al. 2014), despite extensive previous data indicating that *CHD5* promotes neurogenesis and acts as a potent tumor suppressor (Kolla et al. 2014; Egan et al. 2013b). Although a subsequent report revealed that mice conditionally ablated for *CHD5* in neural tissue exhibit symptoms consistent with an autism spectrum disorder (Pisansky et al. 2017), the corresponding neural phenotypes appear much less severe than reported for knock-down of *CHD5* in mouse embryonic brains (Nitarska et al. 2016; Egan et al. 2013b).

Similarly, our characterization of *chd5*^{-/-} fish to date has not revealed a strong tumor or neurological phenotype in the absence of an additional perturbation. We have previously used morpholino knockdown of *chd5* to examine phenotypic changes associated with this loss during development, and we observed a microcephaly phenotype. This phenotype demonstrates that *chd5* is necessary for promoting head and eye development, consistent with the expression pattern of *Chd5* as demonstrated by Western blot using our homemade polyclonal antibody (Figure 6.1). However, when we inject the morpholino into *chd5* knockout embryos, we observe microcephaly phenotypes, indicating that *chd5* is not required for this phenotype and is therefore likely an off target effect, a known problem with morpholino knockdowns (Schulte-Merker and Stainier 2014) (Figure 6.2).

Cancer is a complex disease, that likely arises as the consequence of genetic interaction between numerous pathways that direct cell growth, division and differentiation. Therefore, we have designed two strategies to investigate the contribution of *Chd5* in the context of fish that are predisposed to tumor formation. We have preliminary evidence that in combination with mutation of the tumor suppressor *tp53*, loss of *chd5* leads to an increase in the rate of development of malignant peripheral nerve sheath tumors (MPNSTs), and a decrease in time to tumor formation. We also have begun steps to develop a model predisposed to neuroblastoma using overexpression

of the human oncogene, *MYCN*. A thorough mechanistic understanding of how chromatin-based processes contribute to tumor development is a promising avenue to develop targeted cancer therapies. Establishment of a role for *chd5* in tumor suppression in zebrafish will provide a unique biological context to characterize the role of *CHD5* in tumor suppression, as well as to undertake high throughput screens to identify compounds that ameliorate the phenotypic consequence resulting from loss of this tumor suppressor.

Based on our initial success in using combinatorial mutations to reveal a role for *chd5* in tumorigenesis, we have further leveraged the power of zebrafish to examine the effect of a small number of compounds on the phenotype of *chd5*^{-/-} embryos using a directed approach. Small molecules are easily applied to large batches of zebrafish embryos, making it an ideal model system to examine chemical-genetics. We have chosen to use a panel of epigenetic inhibitor compounds available from Cayman Chemicals, and known oncological therapies to test for epigenetic and developmental pathways that are perturbed by loss of *chd5*. We have identified several compounds that give severe phenotypes in *chd5*^{-/-} fish compared to WT. The targets of these compounds are known, and thus phenotypes arising from these treatments will provide testable hypotheses concerning specific pathways in which *chd5* acts. Importantly, these observed phenotypes in *chd5*-deficient fish are likely lead candidate therapeutics for *CHD5*-deficient tumors.

The observations of discrepancies between knockdown and knockout phenotypes raise the prospect that genetic redundancy is masking the true consequence of loss of *CHD5* and thus the extent of its contribution to neurogenesis and tumor suppression in vertebrates. The highly similar remodelers *CHD3* and *CHD4* represent likely candidates for such redundant factors. Although knock-down of *CHD3*, *CHD4*, and *CHD5* have different effects on neural development in mouse embryos (Nitarska et al. 2016), there is extensive evidence for functional redundancy that is specifically revealed by genetic ablation. For example, the role of the related remodeler *CHD1* in +1 nucleosome turnover during transcription in the context of the closely related remodeler *Chd2* is revealed by use of a dominant negative version of *CHD1* but not by ablation of *CHD1* (Skene et al. 2014). Based on these precedents, we propose using a novel gene replacement strategy to generate an endogenous dominant negative allele of the zebrafish *chd5* gene and thereby generate a novel robust context for examining the role of *CHD5* remodelers in neural development and tumorigenesis. This approach uses CRISPR/Cas9 technologies and homology directed repair to create a two-step gene replacement method that we are optimizing in the zebrafish.

In addition to these ongoing projects, I will conclude the future directions chapter by discussing the results obtained through our RNA sequencing project and additional analyses that are ongoing and would likely provide useful continuations of these projects. The transcriptomics analysis of the brains of our *chd5* loss-of-function mutants revealed numerous pathways that have known roles in promoting neural development (Chapter 3). An important consideration for these results is how they may inform how CHD5 acts as a tumor suppressor gene. It also remains to be determined what the direct target genes are of *chd5*. Critically, another result obtained through these sequencing studies is the potential role of Chd5 in promoting splicing. However, whether Chd5 has a direct role in promoting these changes cannot be determined from these analyses, so additional experiments are needed. The continuing research on these projects will be discussed below.

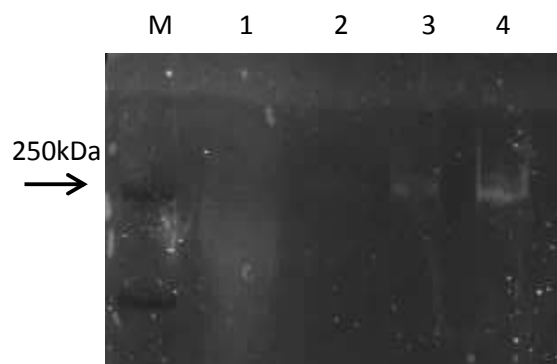


Figure 6.1 Chd5 is preferentially expressed in the neural tissues of adult zebrafish

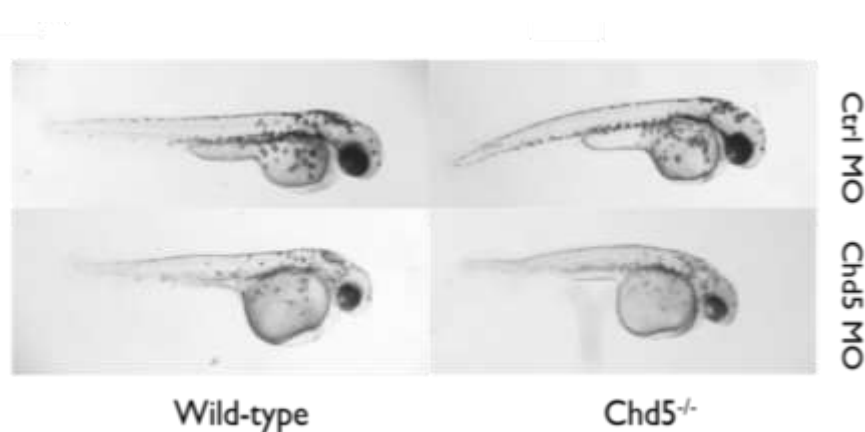


Figure 6.2 Chd5 is not required to observe morpholino phenotypes, indicating likely off-target effects of this knockdown approach to study *chd5*.

6.2 Genetic interaction models to reveal a role for *chd5* in promoting tumorigenesis

A thorough mechanistic understanding of how chromatin-based processes contribute to tumor development is a promising avenue to develop targeted cancer therapies. Establishment of a role for *chd5* in tumor suppression in zebrafish will provide a unique biological context to characterize the role of *CHD5* in tumor suppression, as well as to undertake high throughput screens to identify compounds that ameliorate the phenotypic consequence resulting from loss of this tumor suppressor. To characterize the tumor suppressive role of *chd5*, the zebrafish ortholog of human *CHD5*, we have used CRISPR/Cas9 to generate protein null alleles of *chd5* (*chd5*^{-/-}) as determined by both DNA sequence analysis and by western analysis using polyclonal antibodies that we generated to Chd5 protein. Similar to characterization in the mouse model system, loss of *chd5* in zebrafish results in no overt developmental phenotype (Li et al. 2014; Zhuang et al. 2014).

To study the contribution of *chd5* to tumor suppression pathways in zebrafish, we have combined our *chd5* knockout with other genetic alterations linked to tumor development. Functional analysis of the well-known tumor suppressor *tp53* provides a robust precedent for the utility of this type of approach. Mutation of *tp53* alone in zebrafish results in development of malignant peripheral nerve sheath tumors (MPSTs) in 28% of fish by 16.5 months (Berghmans et al. 2005). By combining the *tp53* mutation with other genetic perturbations, including both overexpression and genetic ablation, it is possible to engineer additional tumor models including melanoma (Patton et al. 2005; Dovey, White, and Zon 2009), Ewing's sarcoma (Leacock et al. 2012; Lu et al. 2013), and hepatoma (Lu et al. 2013).

Based on previous development of a robust melanoma model in zebrafish (Patton et al. 2005), and the observed loss of *CHD5* in human melanomas (Cerami et al. 2012), we generated *chd5*^{-/-}*tp53*^{M214K} (N=22), and *chd5*^{-/-}*Tg(mitfa-BRAF*^{V600E}*)* (N=176) fish to test the hypothesis that loss of *chd5* coupled with the aforementioned genetic perturbations will result in melanoma. It was previously observed that *Tg(mitfa-BRAF*^{V600E}*)tp53*^{M214K} fish develop melanoma whereas fish carrying either mutation alone do not (Patton et al. 2005). Although we do not observe melanomas in either of our double mutants, we do observe MPNSTs in 60% of *chd5*^{-/-}*tp53*^{M214K} fish, a rate which is dramatically higher than the previously reported rate observed in *tp53*^{M214K} mutant zebrafish (Figure 6.3) (Berghmans et al. 2005). It is important to note, however, that our results were obtained using a small population size of double mutant fish (N=22). To robustly establish that loss of *chd5* accelerates the time to tumor formation and penetrance of MPNSTs in fish with

mutant *tp53*, we have expanded our populations of double mutant and control (*tp53*^{M214K} only) fish to N=160 each, enabling us to detect an increase tumor rate as small as 5%.

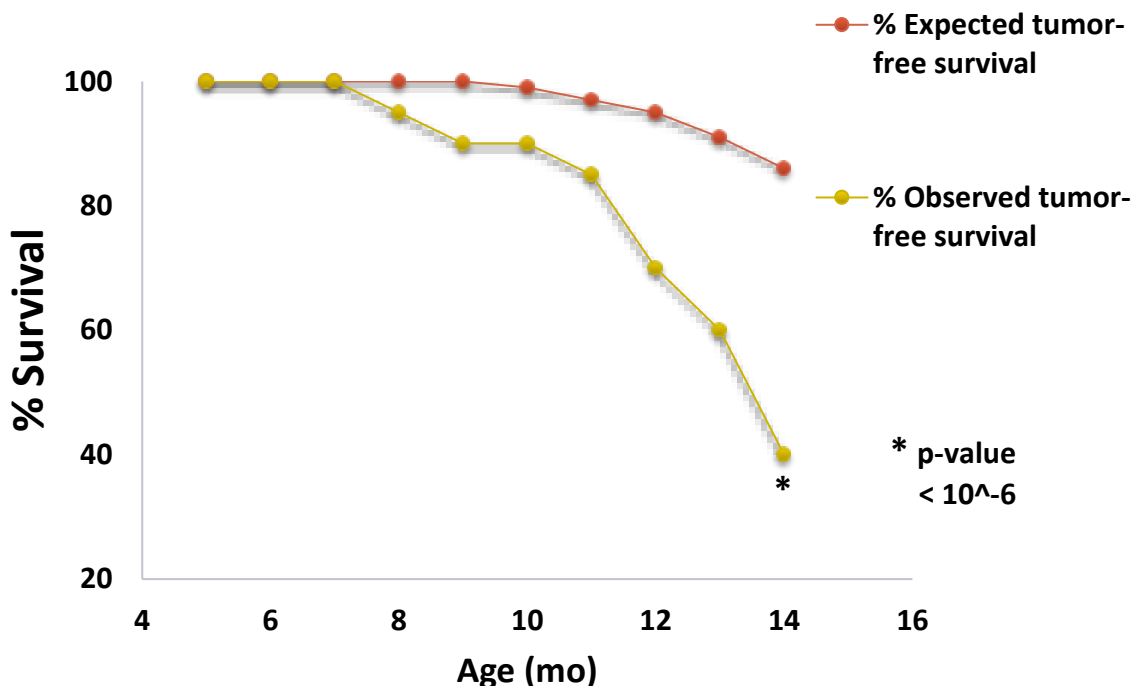


Figure 6.3 Tumor-free survival is decreased in zebrafish containing both *p53* and *chd5* alterations compared to *p53* mutation alone.

We will also use these lines to examine the role of *chd5* in the apoptotic response. Apoptosis plays a critical role in determination of cancer progression, and is frequently interrupted during carcinogenesis (Lowe and Lin 2000). Based on previous characterization of mice deficient in *Chd5* (Bagchi *et al.* 2007), we hypothesize that transcriptional pathways that promote the apoptotic response will be compromised. We will treat single and double mutant fish with gamma irradiation and then use TUNEL assay to examine apoptosis in whole embryos, and single embryo qRT-PCR to assay gene expression levels of key genes that are upregulated during apoptosis, including *mdm2*, *bax* and *p21*. If *chd5*^{-/-} embryos exhibit reduced TUNEL staining and altered gene expression in responses to irradiation, consistent with a failure to induce apoptosis, then we propose to use these embryos to perform RNAseq analysis to determine transcripts that are dependent on *chd5*. The results from this analysis will allow us to determine what pathways *chd5*

may work in to promote apoptosis, which is likely to contribute to its tumor suppressive function on cells.

In addition to our *tp53* mutant lines, we are also generating a neuroblastoma model that was recently characterized and has a drastically reduced time to tumor formation compared to the MPNST model. In brief, overexpression of the human *MYCN* oncogene in sympathetic neurons in zebrafish results in neuroblastoma at 11 weeks in 17.3% of transgenic fish (Zhu et al. 2012). When *MYCN* overexpression was coupled with expression of an oncogenic mutation in ALK, a receptor tyrosine kinase, the time to tumor formation was decreased to only 5 weeks, with a penetrance of 55.6%, demonstrating that this *MYCN*-dependent line is responsive to manipulation of other tumorigenic pathways. Similarly, loss of the tumor suppressor *nfla* and heterozygosity for the duplication *nflb* in *MYCN* overexpressing fish leads to 82.6% tumor penetrance at just 4 weeks of age. Given that loss of *CHD5* has previously been strongly linked to neuroblastoma (Naraparaju et al. 2016), we will determine if inactivation of *chd5* is sufficient to enhance development of neuroblastoma in zebrafish lines that overexpress *MYCN* (Zhu et al. 2012).

CHD5 is commonly lost or silenced in neuroblastomas (Fujita et al. 2008; Garcia et al. 2010; Higashi et al. 2015; Koyama et al. 2012). Additionally, *CHD5* has been shown to be necessary for neural differentiation in mice (Egan et al. 2013b). We will test the hypothesis that loss of *chd5* results in increased rates or accelerates neuroblastoma in fish that overexpress *MYCN*. I have cloned the human *MYCN* gene into a vector under control of the *dbh* promoter, and also engineered vectors that will express *dbh*-GFP or RFP. By using coinjection we can screen for concatemerization of the *MYCN* and fluorescent gene in the sympathetic ganglion cells (marked by expression of the DBH promoter). If we find the tumor rate is increased, we will use molecular analyses to examine the pathogenic pathways that are activated or silenced in these tumors. We hypothesize that loss of *chd5* will alter the differentiation status of the *MYCN* overexpressing neuroblasts, and that these cancer cells will exhibit embryonic gene expression characteristics. To test this hypothesis we will use histological analysis and immunostaining to determine expression patterns of the known neural differentiation markers Hu and TH and by targeted qPCR of tumor samples.

6.3 Chemical-genetic screen of zebrafish lacking the chromatin remodeler *chd5*

To characterize the role of *chd5*, the zebrafish ortholog of human *CHD5*, we have used the CRISPR-Cas9 system to generate knock out lines that lack full-length *CHD5* protein, as described above. These lines do not exhibit an overt developmental phenotype, which is consistent with the absence of an obvious brain defect in mice lacking *Chd5* (Zhuang et al. 2014; Bergs et al. 2014). In contrast, *Chd5* knock-down in mice results in defective neuronal differentiation and neural migration (Egan et al. 2013b; Nitarska et al. 2016). Similarly, we observed a phenotype of microcephaly using morpholinos, consistent with neurological defects in the context of *chd5* knockdown. However, subsequent characterization of the morpholino shows that when we inject the morpholino into fish that are missing *chd5* we still observe these microcephaly phenotypes, suggesting that these phenotypes are caused by off-target effects of the morpholino.

Additional work is critically needed to clarify the discrepancies of these results. We hypothesize that loss of *chd5* in zebrafish embryos results in a modest epigenetic defect that will be revealed by impairing additional epigenetic pathways. To understand the role of *chd5* during development as well as its potential interaction with other epigenetic pathways, we have begun a chemical-genetic screen. Small molecules are easily applied to large batches of zebrafish embryos, making it an ideal model system for chemical genetics. Importantly, if we observe that *chd5*-deficient fish are specifically susceptible to one or more epigenetic inhibitors, this will allow us to identify lead candidate therapeutics for *CHD5*-deficient tumors. In particular, we focused on inhibitors of histone deacetylases (based on the supposition that *chd5*^{-/-} embryos might be more sensitive to these compounds due to the predicted decrease in the histone deacetylase-containing Mi-2/NuRD complex (Kolla et al. 2015; Potts et al. 2011)) and on the cyclin-dependent kinase inhibitor roscovitine (Bach et al. 2005) due to the demonstration that toxicity of this compound is reduced upon differentiation of SH-SY5Y cells (Ribas and Boix 2004), suggesting that *chd5*^{-/-} embryos might exhibit increased sensitivity to this compound as a result of impaired differentiation.

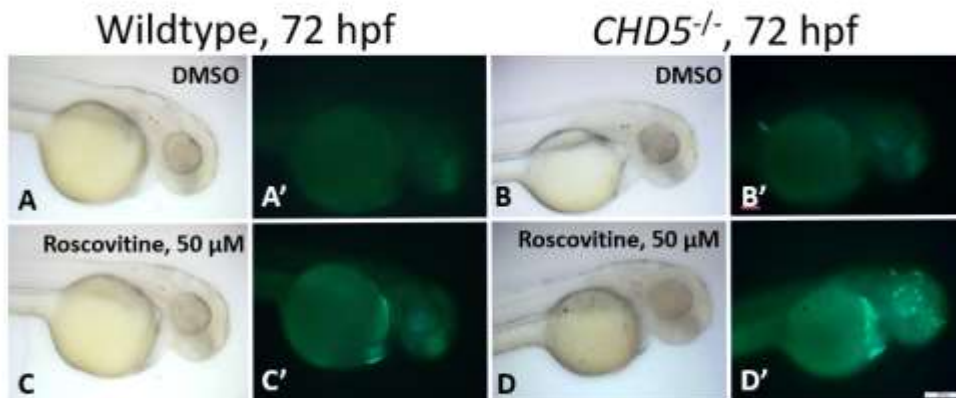


Figure 6.4 Loss of *chd5* results in increased cell death in zebrafish embryos treated with roscovitine.

Embryos were treated with the indicated dose of roscovitine from 56-72 hours post fertilization, then stained with acridine orange to mark apoptotic cells. Wild-type (A,C) and *chd5*^{-/-} fish (B,C) were treated with DMSO (A,B) or 50 μ M roscovitine (B,D). Cell death results in uptake of acridine orange which is indicated by increased fluorescence.

We found that zebrafish lacking *chd5* exhibit increased cell death in the head and retina in response to the cyclin-dependent kinase inhibitor roscovitine (Figure 6.1), which currently is being investigated as an anti-cancer drug (Kalra et al. 2017; Cicenas et al. 2015). Roscovitine has previously been shown to promote apoptosis of SH-SY5Y neuroblastoma cells (Ribas and Boix 2004), but this sensitivity is lost upon differentiation of these cells (Davidoff et al. 1992). As *CHD5* has been shown to promote neural differentiation in mammals (Egan et al. 2013a; Nitarska et al. 2016), increased roscovitine sensitivity in *chd5*^{-/-} fish is consistent with a potential defect in neural differentiation in these fish. Using this data, we have proposed studies using in vitro differentiation cell models (described above) to build on these findings and determine whether *CHD5* similarly contributes to neural differentiation and roscovitine sensitivity in mouse embryonic stem cells and thereby establish that we can use our *chd5*^{-/-} fish to gain new insights into Chd5 function that are directly relevant to anti-tumor therapies in humans.

In addition to these target compounds we have chosen to use a panel of epigenetic inhibitor compounds available from Cayman Chemicals to test for epigenetic and developmental pathways that perturbed by loss of *chd5*. The targets of these compounds are known, and thus phenotypes arising from these treatments will provide testable hypotheses concerning specific pathways in which *chd5* acts. We have now identified several additional compounds that result in severe developmental abnormalities in *chd5*^{-/-} but not wild-type embryos. One set of compounds that we

have prioritized characterization of the histone deacetylase (HDAC) inhibitors. CHD5 is a member of the nucleosome remodeling and deacetylase (NuRD) complex, which couples the histone deacetylase activity of HDAC1/2 with the chromatin remodeling activity of the subfamily II CHD proteins. We have used several HDAC inhibitors including SAHA, TSA and valproate and characterized the corresponding developmental phenotypes (Table 6.1). Excitingly, in each case we have observed a spinal curvature defect in the *chd5*^{-/-} but not wild-type embryos. We also observe enhancement of some non-specific phenotypes such as edema (swelling of the pericardial sac), failed inflation of the swim bladder, and swelling of the yolk sac.

Table 6.1 Zebrafish embryos lacking *chd5* exhibit increased sensitivity to epigenetic inhibitors compared to wild-type embryos treated continuously from 1-3 days.

Drug	TSA	Valproate	JQ1
Conc.	0.3 μ M	50 μ M	1 μ M
wild-type	0%	20%	1%
<i>chd5</i> ^{-/-}	11%	72%	50%

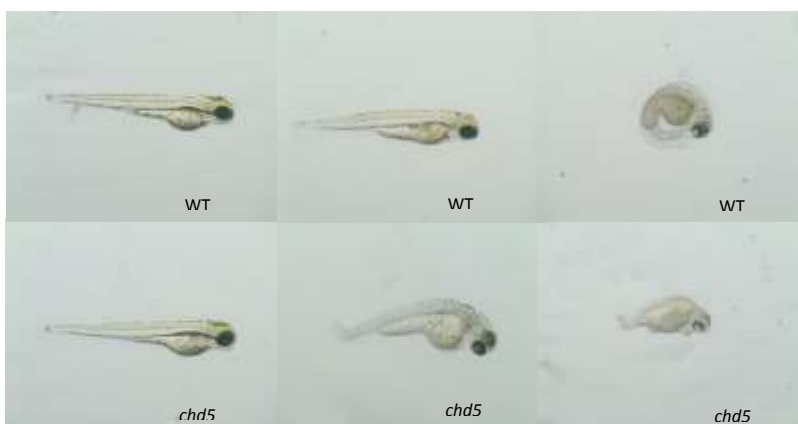


Figure 6.5 Representative images of (+)-JQ1 treated embryos.

Embryos were collected and staged from wild-type or *chd5*^{-/-} breeding pairs, 6 embryos were placed into each well of a 48-well plate and treated with the indicated amount of drug starting at 6hpf. Drugs and media were replaced every 24h. Phenotypes were scored daily until 5dpf. Representative images of 3dpf wild-type and *chd5*^{-/-} embryos treated with the BET bromodomain inhibitor (+)-JQ1 (Magnification= 10x).

Another epigenetic inhibitor we tested is the bromodomain inhibitor (+)-JQ1 which also shows a preferential effect of creating developmental abnormalities in our *chd5* knockout embryos (Figure 6.2) (Filippakopoulos et al. 2010). In the presence of 500nM JQ1 wild-type fish are normal (Table 6.2) but 14% of *chd5*^{-/-} fish exhibit a syndrome of deformed spines, small heads, and altered eye development. These data represent the first time that ablation of a CHD5 remodeler has been shown to give rise to a somatic phenotype in vertebrates and further indicate that loss of *CHD5* results in increased sensitivity to epigenetic perturbation.

Table 6.2 Chd5 knockout fish exhibit a dose-dependent response to JQ1 treatment at 3-days.

	DMSO	100nM	500nM	1uM	5uM
WT	0/15	0/16	0/22	1/25 (5%)	No survival (n=22)
<i>chd5</i> ^{ctrl}	0/18	0/19	5/37 (13.5%)	8/38 (21%)	No survival (n=20)

To further investigate these phenotypes we will also use *in situ* hybridization to examine other developmental features that may be altered in our treated embryos. To demonstrate that phenotypes of interest are dependent on the loss of *chd5*, we will determine if the phenotypes can be rescued by mRNA injection of full length *chd5*. We continue to screen through the other compounds in our library of epigenetic inhibitors to identify compounds that preferentially affect the development of *chd5*^{-/-} fish. As with the HDAC inhibitors, we anticipate that the HuC-GFP lines will assist in detailed characterization of the neural phenotype. In the future, we will combine the results of our chemical genetic screen with our efforts to identify a tumor phenotype for *chd5*^{-/-} fish. In brief, we will test the hypothesis tumors resulting from loss of *chd5* will exhibit heightened sensitivity to compounds that perturb the development of *chd5*^{-/-} embryos. Thus, we anticipate that our combined efforts will contribute to development of novel therapies for cancer patients who have tumors with a molecular phenotype of reduced expression of *CHD5*.

6.4 Homologous recombination strategy to engineer a dominant-negative allele of *Chd5* in zebrafish

Perturbations of epigenetic regulatory networks contribute to numerous human developmental abnormalities and diseases. Elucidation of the specific contribution of an epigenetic factor to a process of interest with the goal of designing therapeutic strategies is often complicated by the mutual interdependence and redundancy of epigenetic regulators. Such regulatory network complexity is a confounding characteristic of many processes underlying human disease. To be able to address these questions robustly, we have been working to establish new strategies that expand, accelerate, and decrease the cost of genetic manipulation in zebrafish. This research has the potential to dramatically expand the utility of new experimental strategies that enhance the power of forward and reverse genetics in zebrafish.

We have begun work to establish a CRISPR-based homologous recombination system for gene disruption and subsequent allele replacement, using *chd5* as a model to test our methods and to establish a new context to understand how *chd5* contributes to neurogenesis and tumor suppression. Our lab is using zebrafish as a model to investigate the contribution of *chd5* to these processes. However, despite the widespread use of CRISPR-Cas9 technology in zebrafish, few reports have been published that demonstrate success in using homologous recombination (HR) in zebrafish, and these processes often leave behind exogenous DNA sequence that can limit the use of these methods to engineer changes in coding regions of genes (Albadri, Del Bene, and Revenu 2017; Hoshijima, Juryneec, and Grunwald 2016). To address this shortcoming and to develop our desired genetic alterations in *chd5*, we are adapting a gene replacement strategy that was first developed in *Drosophila* for use in zebrafish.

We hypothesize that genetic redundancy from closely related remodelers *CHD3* and *CHD4* is masking the true consequence of loss of *CHD5* and thus the extent of its contribution to neurogenesis and tumor suppression in vertebrates. Previously, it has been shown that a dominant-negative (DN) allele of *CHD1*, a closely related remodeler, exhibits phenotypes otherwise not revealed in the knockout of *CHD1* (Skene et al. 2014). We propose that generation of a DN allele of *CHD5* will abrogate this genetic redundancy and reveal the role of *CHD5* in neural development and tumor suppression.

Generation of a dominant negative allele of *chd5* will provide the opportunity to engineer a new and unique model to better address the role of *CHD5* in neural development and tumor

suppression. Zebrafish provide us with a strong model system in which to study both of these processes. Our lab has demonstrated that several neurogenic differentiation pathways are misregulated in knockout zebrafish, and that loss of *chd5* in a poised system does promote an increase in tumor penetrance, indicating that it contributes to tumor suppression. Implementation of the proposed gene replacement strategies will significantly expand our zebrafish toolkit, and widely benefit the research community that utilize zebrafish as a model system.

To overcome the proposed redundancy of *CHD3/4/5*, we have engineered a strategy to generate a K to R substitution in the ATPase domain of *chd5*, an approach which has consistently generated a dominant negative version of closely related ATP-dependent remodelers (Skene et al. 2014). To generate the *chd5*^{K737R} allele, we have developed a vector-based HR strategy compatible with the piggyBac (PBac) transposase previously used in mice, *Drosophila*, and human cells to generate scarless genomic modifications (Termglinchan et al. 2017; Woodard and Wilson 2015; Yusa 2015; Uetake, Oka, and Niki 2011; Bonin and Mann 2004). In short, this vector contains homologous arms with the K737R substitution, flanking a constitutively expressed GFP marker. The target genome locus is cut by CRISPR-Cas9 to induce DNA repair using this vector to promote HR. When incorporated into the genome by HR, the *chd5* acts as a knock-out in this gene because of the GFP insertion (Figure 6.4). Fish are selected for GFP expression indicating that they have incorporated the modification. This GFP is engineered to be removable because it is flanked by PBac transposase sites that enables subsequent excision of GFP by PBac transposase to create the in-frame mutation.

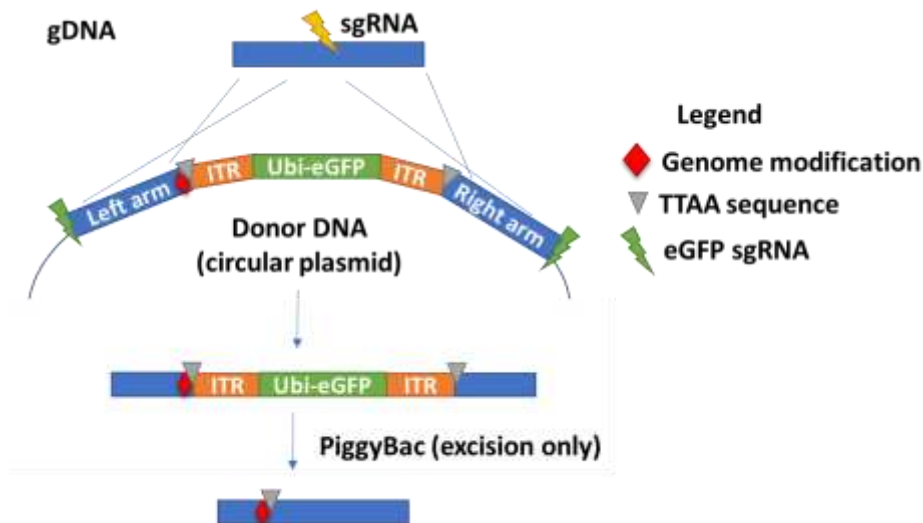


Figure 6.6 Schematic of CRISPR-based homologous recombination strategy to promote gene replacement using a two-step method.

CRISPR is used both to cut the target locus and release the donor fragment. Desired gene replacement events are detected by eGFP fluorescence and confirmed by PCR amplification using primers that flank the integration event. This reporter construct is seamlessly excised in a subsequent step by piggyBac transposase.

We have robust preliminary data that this novel knock-in strategy will work in zebrafish. We use Golden Gate (Engler, Kandzia, and Marillonnet 2008) to assemble our donor vectors, thus allowing assembly of any donor construct using two synthesized donor arms and conserved piggyBac and vector pieces. Embryos are injected with a donor vector, gRNAs that target the locus of interest and eGFP sites in the vector, and Cas9 and fish in which there is integration of the eGFP reporter are easily identified (Figure 6.5). We have successfully promoted homologous recombination at two genes, *tyr* and *chd5* with high efficiency (Table 6.3). Furthermore, we have shown that these events represent HR as scored by PCR-based detection of predicted junctions (Figure 6.6).

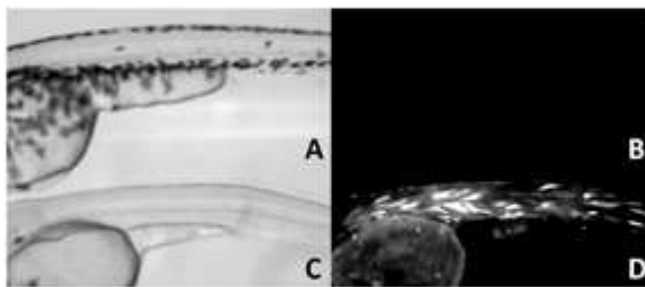


Figure 6.7 Putative homologous recombination events are easily scored by GFP fluorescence. Uninjected (A, B) or injected (C, D) embryos, imaged under white light (A, C) or fluorescence (B, D) at 72 hpf at 6.3x magnification.

To improve upon our previous work to establish these lines, we are currently working to incorporate two primary modifications to our HR design based on unpublished observations shared at the 13th International Zebrafish Conference. First, to generate the desired genomic modification, we will use Cas9 mRNA instead of protein, as it has been suggested this increases the frequency of HR. It has been speculated that Cas9 protein induces a double-strand break before template DNA is paired with its homologous sequence and therefore the DNA is repaired by non-homologous end joining before HR can occur. Second, we previously used long (>3 kb) HR arms, however it has been suggested that the size of the vector may decrease the efficiency of translocation into the nucleus, so we are engineering new donor templates that contain 500-1000 base pairs of homologous sequence.

Our goal is to perform microinjection with these templates and CRISPR reagents (N=150 fish) and then screen these fish for GFP fluorescence and by PCR to establish that these fish are modified at the *chd5* locus. Subsequently, we will grow up these fish and then cross these fish to wild-type mates and examine the progeny for germline transmission of the desired HR modification. The germline transmission will be easily observable because of the presence of GFP in the offspring.

Table 6.3 High efficiency of homologous recombination strategy employing piggyBac to target zebrafish genes.

Locus	HR Arm Length (bp)	Modification	sgRNA efficiency	KI Screening	%GFP	%HR in F0
<i>tyr</i>	190/200	Small insertion	>90%	GFP, PCR	95% (130/137)	80% (11/14)
<i>chd5</i>	250/250	SNP	40-60%	GFP, PCR	65% (36/56)	100% (16/16)

In addition to creating fish that contain our HR vector, a critical step in engineering the DN is engineering a strategy to express PBac in zebrafish. The homologous sequence flanks a constitutively expressed GFP marker, allowing us to select fish carrying the desired replacement event through use of a fluorescent marker that will be subsequently seamlessly removed by PBac to remove any exogenous sequences. We have engineered zebrafish that contain a constitutively

expressed PBac that when crossed with HR modified fish will result in a constitutively expressed *chd5*^{K737R} that is expressed under the control of endogenous regulatory sequences (Figure 6.6). However, it remains possible that this DN allele will severely disrupt development or could be lethal. To examine the possibility that conditional expression of *chd5*^{K737R} exhibits a distinct (and perhaps more easily characterized) phenotype in neural tissue, we are developing an alternate approach to control the expression of the DN allele.

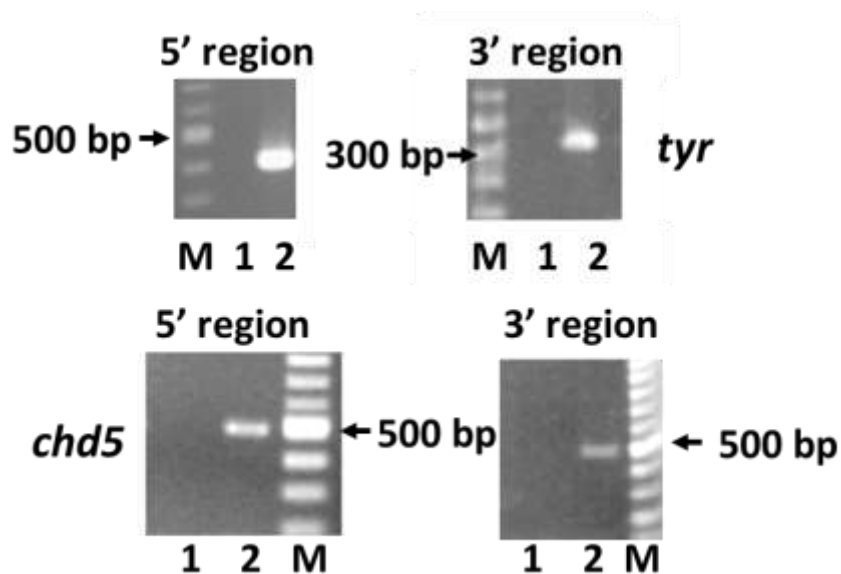


Figure 6.8 PCR verification of homologous recombination at *tyrosinase* and *chd5*. Lane 1 = WT genomic DNA, lane 2 = F0 transgenic fish genomic DNA. Expected sizes: *tyr*= 433 bp for 5' and 365 bp for 3'; *chd5*= 503 bp for 5' and 504 bp for 3'.

We have developed transgenic zebrafish that express the PBac transposase constitutively and in an inducible/neural specific fashion. We have used the tetracycline inducible Gal4/UAS system (Pang et al. 2015). In short, we have cloned zebrafish neural promoters, *neurog1* promoter (for undifferentiated neurons), *dbh* promoter (for differentiated neurons) and *ath5* promoter (for eye-specific expression) that we will use to express the transcription factor Gal4 fused to an estrogen receptor (Gal4-ERT). Using this system, Gal4 can only become nuclear localized when the fish are treated with tamoxifen. These fish will also be modified to incorporate a construct that contains the 4xUAS promoter, which is activated by Gal4, driving expression of PBac. This system allows us to control the spatio-temporal expression of PBac, and thereby control when and where the DN *chd5* allele is expressed.

As an alternative, we are also using recombineering to clone a bacterial artificial chromosome (BAC) that contains the full *chd5* gene, including the promoter and 3' UTR, that carries the dominant negative mutation. This method has been previously used in zebrafish to generate transgenic alleles that successfully recapitulate the expression patterns and levels of the endogenous gene (Suster et al. 2011). We will analyze the resulting *chd5*^{K737R} fish for neural and tumor phenotypes as described in the background. Importantly, use of a conditional promoter for PBac transposase as described will enable us to control expression of the *chd5*^{K737R} if we have severe developmental phenotypes. We anticipate that these studies will substantially clarify the role of the *CHD5* remodeler in both neural differentiation and tumorigenesis, and that these fish will provide the necessary context for many additional experiments.

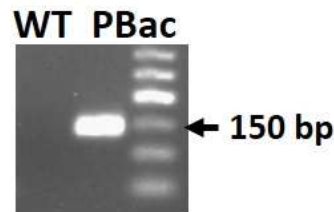


Figure 6.9 Constitutive expression of PiggyBac is observed in zebrafish carrying the transgene. The expression of PBac was tested by PCR using reverse transcribed cDNA extracted from whole 3-day old embryos from either WT or CMV-PiggyBac transgenic fish (n=5).

CHAPTER 7. FUTURE DIRECTIONS

7.1 Characterization of transcriptome phenotypes associated with loss of *chd5*

We have defined a large transcriptional change associated with loss of *chd5* in developing zebrafish brains (Chapter 3, 4). This large data set provides a number of compelling experiments to examine the phenotypes associated with loss of *chd5*.

First, we have identified an *in-situ* phenotype that is consistent with a failure of sympathetic ganglion cells (SGCs) to differentiate properly (Chapter 3, Figure 3.6). We have only examined expression of terminal differentiation markers though, so it remains possible that this phenotype is an indirect readout of an earlier defect in the lineage that derives these cells. There are known markers of early SGCs that are not differentially expressed in our transcriptomics analysis, but it remains possible that these cells exhibit other defects that prevents their proper commitment and differentiation to SGCs. Therefore, we are currently generating additional *in-situ* probes to examine the expression and localization of precursor cells that will develop into SGCs. This data will allow us to establish how early the defect in these cells is occurring and enable us to develop hypotheses about when Chd5 is acting in this lineage to direct differentiation.

Second, this data has raised the prospect that many genes involved in synthesis of neurotransmitters are not expressed properly. Neurotransmitters are critical chemicals that help signal between cells to create synaptic connections, and to respond to environmental stimuli. We have begun work to use HPLC analysis to examine the level of neurotransmitters in the brains of *chd5*^{-/-} embryos during critical stages of development, similarly to previous analyses (Figure 7.1), (Sallinen et al. 2009; Tran, Chatterjee, and Gerlai 2015). If we find that there are differing levels of neurotransmitters in our mutant fish it may reveal a simple therapeutic strategy to improve phenotypes associated with loss of *CHD5* (Kandimalla and Reddy 2017; Trujillo et al. 2009).

If we observe changes to the levels of these neurotransmitters it will suggest to us a way forward with examining phenotypes informed by the molecular biology of the mutant embryos. For example, administering drugs that inhibit dopamine signaling leads to locomotion effects in zebrafish larvae (Ek et al. 2016). We can use our HPLC analysis to determine what behavior deficits occur in the absence of *chd5*.

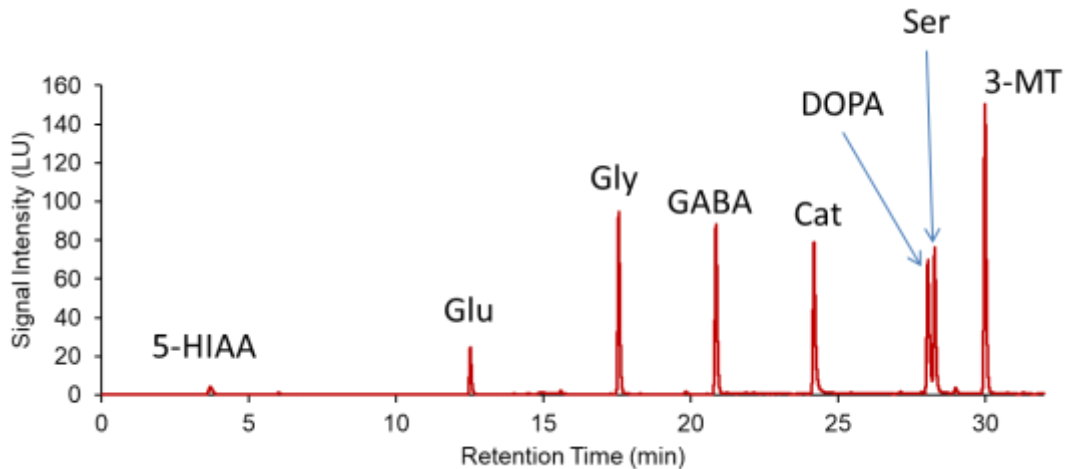


Figure 7.1 HPLC sample chromatogram showing identification of neurotransmitter standards.

HPLC measurements were taken by derivatization of neurotransmitters using OPA to enable fluorescent detection. Peaks are annotated as follows: 5-HIAA (5-hydroxyindole-3-acetic acid); Glu (glutamate); Gly (glycine); GABA (gamma amino butyric acid); Cat (catecholamine); DOPA (dopamine); Ser (Serotonin); 3-MT (3-methoxytyramine).

Third, our data suggest that *chd5*^{-/-} fish may exhibit additional neural phenotypes such as branching defects, a phenotype that has been observed in mice with conditional ablation of *Chd5* (Pisansky *et al.* 2017). Our transcript signature and our AS misregulation occur in genes that linked to neural development and growth (GO terms, Chapter 3 and 4), but it remains to be demonstrated that our fish neurons also fail to generate dendrites to the extent seen in WT. To test this, I am generating several fluorescently tagged neural lines with and without *chd5* and establishing primary neural culture techniques that will allow us to easily visualize neural branching. We are taking two approaches, one in which we use fluorescent tagging of specific cells, and also lines that have more general tags. I have generated *chd5*^{-/-} fish that carry GFAP-GFP (differentiating, early neural precursor cells) and HuC-GFP tagged (differentiated) neurons, and we have engineered constructs to create DBH-GFP, the promoter which marks SGC neurons. We have begun work to establish primary neural cultures using these cells, as previously described (Chen

et al. 2013). We can use these established techniques to image and measure our cells *in vitro* to determine if *chd5* knockout neurons exhibit decreased arborization.

If we identify a branching defect this model provides a compelling tool to look for genetic or chemical ways to rescue the phenotype. For example, we could use morpholino knockdown, or mRNA injection to overexpress genes that are misexpressed in our *chd5* knockout fish and compare the cultured neurons for rescued arborization. Similarly, we will be able to apply chemicals to either the embryos or the neurons in culture to examine changes to the phenotype. If successful, this model will provide us with a unique and powerful tool set to define the molecular and cellular signatures associated with loss of *chd5*.

7.2 Characterization of neural differentiation of mESCs that lack *Chd5*

In Chapter 5, I detailed our efforts to establish a cell culture model to study how loss of *CHD5* affects neural differentiation. The expansion of our tool sets to study *CHD5* is greatly enhanced by use of cell culture, where we will have access to a wide array of established protocols and data sets to probe the changes associated with loss of *Chd5* in this context. We are specifically using mESCs, which appear to grow robustly without *Chd5*, unlike the neuroblastoma cell line we began these experiments with.

First, we must establish proper differentiation conditions to create neural cells in WT and our knockout. Next, we will harvest these cells for total RNA and use NGS to map both differential gene expression and alternative splicing. Importantly, with the data we have obtained from developing zebrafish brains we will be able to determine if changes we determine in mESC differentiation are conserved. Following establishment of these molecular phenotypes, there will be ample genome wide studies to characterize the functional role of *Chd5* in neurogenesis.

One of the strongest motivations for functional characterization of *Chd5* remodelers is provided by biochemical data linking these remodelers to two other critical epigenetic regulatory pathways. Like the related remodelers *Chd3* and *Chd4*, *Chd5* is a component of the histone deacetylase-containing Mi-2/NuRD complex (Kolla et al. 2015; Potts et al. 2011). Mi-2/NuRD plays a significant role in transcriptional repression and can be recruited by DNA methylation and by protein-protein interactions with co-repressors and other transcription factors (Wolffe, Urnov, and Guschin 2000; Denslow and Wade 2007) as well as by 5-hydroxymethylcytosine if the

complex contains MBD3 (Yildirim et al. 2011). In addition, however, Chd5 directly interacts with H3K27me3 via its chromodomains and knock-down of *CHD5* in shRNA results in both decreased levels of H3K27me3 at H3K27me3-enriched loci in SH-SY5Y cells that are induced to differentiate as well as altered expression of H3K27me3-enriched loci (Egan et al. 2013a). ChIP-seq of differentiated SH-SY5Y cells, however, reveal that H3K27me3 is neither necessary nor sufficient for targeting of H3K27me3 (many genes are enriched for Chd5 at the transcription start site with no detectable H3K27me3 and many H3K27me3-enriched genes have no detectable Chd5). Instead, a low level of enrichment of Chd5 is found at a subset of genes that are modestly enriched for H3K4me3 and H3K27me3 at the promoter.

Although the studies described above have provided substantial insight into the role of Chd5, there is much that remains to be done. It remains unknown if loss of Chd5 affects the epigenetic status of genes that are dependent on DNA methylation, as predicted by the presence of Chd5 in the Mi-2/NuRD complex. Similarly, it remains unexplored if Chd5 plays a role at enhancers as predicted by characterization of Mi-2/NuRD complexes containing Chd3 or Chd4 (Bornelov et al. 2018). In addition, the effect of loss of *CHD5* on correlated changes in epigenetic status and gene expression in neural cells in vivo remains undetermined. Further, previous studies have emphasized the role of Chd5 remodelers in differentiating cells, yet Chd5 is abundantly expressed in differentiated neurons (Vestin and Mills 2013). The presumptive role of Chd5 in maintenance of neuronal identity and/or transcriptional regulation in differentiated cells has also yet to be investigated. With our tools we will be able to test if H3K27 methylation status is altered in our knockouts, if DNA methylation is changed and then be able to correlate this to our RNA-sequencing data.

Another active area of our research using this model is based on our results from the zebrafish chemical genetic screen. Importantly, neuroblastoma is primarily a childhood cancer, that occurs during the development of the neural tissues. In vitro models of neural differentiation therefore provide a useful tool in examining how oncogenic mutations affect neurogenesis and subsequent tumor formation. We can use our mESC model to test for tumor suppressive roles of *Chd5* in differentiation mESCs. One of our goals using these cells is to investigate whether ablation of *Chd5* alters sensitivity to roscovitine, as has been demonstrated in similar systems undergoing neural differentiation (Ribas, Boix, and Meijer 2006). Demonstration that mESC undergoing RA-driven differentiation lacking *CHD5* exhibited increased sensitivity to roscovitine would provide

a dramatic demonstration of how loss of *CHD5* can alter sensitivity to anti-tumor agents. Cell viability will be assessed using an MTS reduction assay and comparing the cells to an untreated control to measure percent survival (Ribas and Boix 2004).

Another study we propose to further examine the role of *Chd5* in tumor suppression is based on previous studies that have suggested *CHD5* promotes expression of *Tp53* (Bagchi et al. 2007). However, *CHD5* promotes differentiation of neural cells (Egan et al. 2013a) which results in reduced expression of TP53 (Davidoff et al. 1992). Our chemical phenotype demonstrates that zebrafish embryos treated with roscovitine exhibit increased cell death in *chd5*^{-/-} compared to WT. This observation is not consistent with a model in which *chd5* is promoting expression of *p53*, as we would expect loss of *chd5* to lead to reduced p53 and therefore decreased cell death. To test this, we will use qRT-PCR to examine expression of p53 in mESCs with and without *Chd5* in the absence and presence of retinoic acid. These studies will resolve whether *Chd5* can contribute to negative regulation of *Tp53* and generate a testable model by which *CHD5* contributes to roscovitine sensitivity. Further, demonstration that *CHD5* promotes repression of *Tp53* by promoting differentiation of mESCs would provide compelling evidence that *CHD5* remodelers contribute to both positive and negative regulation of the critical TP53 tumor suppression pathway.

REFERENCES

- Aguilera, C., K. Nakagawa, R. Sancho, A. Chakraborty, B. Hendrich, and A. Behrens. 2011. 'c-Jun N-terminal phosphorylation antagonises recruitment of the Mbd3/NuRD repressor complex', *Nature*, 469: 231-5.
- Aichinger, E., C. B. Villar, S. Farrona, J. C. Reyes, L. Hennig, and C. Kohler. 2009. 'CHD3 proteins and polycomb group proteins antagonistically determine cell identity in *Arabidopsis*', *PLoS Genet*, 5: e1000605.
- Albadri, S., F. Del Bene, and C. Revenu. 2017. 'Genome editing using CRISPR/Cas9-based knock-in approaches in zebrafish', *Methods*, 121-122: 77-85.
- Alexander, R. D., S. A. Innocente, J. D. Barrass, and J. D. Beggs. 2010. 'Splicing-dependent RNA polymerase pausing in yeast', *Mol Cell*, 40: 582-93.
- Allen, H. F., P. A. Wade, and T. G. Kutateladze. 2013. 'The NuRD architecture', *Cell Mol Life Sci*, 70: 3513-24.
- Alunni, A., and L. Bally-Cuif. 2016. 'A comparative view of regenerative neurogenesis in vertebrates', *Development*, 143: 741-53.
- Anderson, J. D., and J. Widom. 2000. 'Sequence and position-dependence of the equilibrium accessibility of nucleosomal DNA target sites', *J Mol Biol*, 296: 979-87.
- Annalora, A. J., C. B. Marcus, and P. L. Iversen. 2017. 'Alternative Splicing in the Cytochrome P450 Superfamily Expands Protein Diversity to Augment Gene Function and Redirect Human Drug Metabolism', *Drug Metab Dispos*, 45: 375-89.
- Ara, T., F. Lopez, W. Ritchie, P. Benech, and D. Gautheret. 2006. 'Conservation of alternative polyadenylation patterns in mammalian genes', *BMC Genomics*, 7: 189.
- Ata, H., K. J. Clark, and S. C. Ekker. 2016. 'The zebrafish genome editing toolkit', *Methods Cell Biol*, 135: 149-70.
- Bach, S., M. Knockaert, J. Reinhardt, O. Lozach, S. Schmitt, B. Baratte, M. Koken, S. P. Coburn, L. Tang, T. Jiang, D. C. Liang, H. Galons, J. F. Dierick, L. A. Pinna, F. Meggio, F. Totzke, C. Schachtele, A. S. Lerman, A. Carnero, Y. Wan, N. Gray, and L. Meijer. 2005. 'Roscovitine targets, protein kinases and pyridoxal kinase', *J Biol Chem*, 280: 31208-19.

- Bagchi, A., C. Papazoglu, Y. Wu, D. Capurso, M. Brodt, D. Francis, M. Bredel, H. Vogel, and A. A. Mills. 2007. 'CHD5 is a tumor suppressor at human 1p36', *Cell*, 128: 459-75.
- Bajpai, R., D. A. Chen, A. Rada-Iglesias, J. Zhang, Y. Xiong, J. Helms, C. P. Chang, Y. Zhao, T. Swigut, and J. Wysocka. 2010. 'CHD7 cooperates with PBAF to control multipotent neural crest formation', *Nature*.
- Bartholomew, B. 2014. 'Regulating the chromatin landscape: structural and mechanistic perspectives', *Annu Rev Biochem*, 83: 671-96.
- Bee, L., S. Fabris, R. Cherubini, M. Mognato, and L. Celotti. 2013. 'The efficiency of homologous recombination and non-homologous end joining systems in repairing double-strand breaks during cell cycle progression', *PLoS One*, 8: e69061.
- Bell, C. C., G. W. Magor, K. R. Gillinder, and A. C. Perkins. 2014. 'A high-throughput screening strategy for detecting CRISPR-Cas9 induced mutations using next-generation sequencing', *BMC Genomics*, 15: 1002.
- Berghmans, S., R. D. Murphey, E. Wienholds, D. Neuberg, J. L. Kutok, C. D. Fletcher, J. P. Morris, T. X. Liu, S. Schulte-Merker, J. P. Kanki, R. Plasterk, L. I. Zon, and A. T. Look. 2005. 'tp53 mutant zebrafish develop malignant peripheral nerve sheath tumors', *Proc Natl Acad Sci U S A*, 102: 407-12.
- Bergs, J. W., N. Neuendorff, G. van der Heijden, E. Wassenaar, P. Rexin, H. P. Elsasser, R. Moll, W. M. Baarends, and A. Brehm. 2014. 'Differential expression and sex chromosome association of CHD3/4 and CHD5 during spermatogenesis', *PLoS ONE*, 9: e98203.
- Betermier, M., P. Bertrand, and B. S. Lopez. 2014. 'Is non-homologous end-joining really an inherently error-prone process?', *PLoS Genet*, 10: e1004086.
- Bhatt, D. M., A. Pandya-Jones, A. J. Tong, I. Barozzi, M. M. Lissner, G. Natoli, D. L. Black, and S. T. Smale. 2012. 'Transcript dynamics of proinflammatory genes revealed by sequence analysis of subcellular RNA fractions', *Cell*, 150: 279-90.
- Bhattacharyya, S., F. Mattioli, and K. Luger. 2018. 'Archaeal DNA on the histone merry-go-round', *FEBS J*.
- Bienz, M. 2006. 'The PHD finger, a nuclear protein-interaction domain', *Trends Biochem Sci*, 31: 35-40.

- Bishop, B., K. K. Ho, K. Tyler, A. Smith, S. Bonilla, Y. F. Leung, and J. Ogas. 2015. 'The chromatin remodeler chd5 is necessary for proper head development during embryogenesis of *Danio rerio*', *Biochim Biophys Acta*, 1849: 1040-50.
- Biswas, D., R. Dutta-Biswas, and D. J. Stillman. 2007. 'Chd1 and yFACT act in opposition in regulating transcription', *Mol Cell Biol*, 27: 6279-87.
- Bode, D., L. Yu, P. Tate, M. Pardo, and J. Choudhary. 2016. 'Characterization of Two Distinct Nucleosome Remodeling and Deacetylase (NuRD) Complex Assemblies in Embryonic Stem Cells', *Mol Cell Proteomics*, 15: 878-91.
- Bonin, C. P., and R. S. Mann. 2004. 'A piggyBac transposon gene trap for the analysis of gene expression and function in *Drosophila*', *Genetics*, 167: 1801-11.
- Bornelov, S., N. Reynolds, M. Xenophontos, S. Gharbi, E. Johnstone, R. Floyd, M. Ralser, J. Signolet, R. Loos, S. Dietmann, P. Bertone, and B. Hendrich. 2018. 'The Nucleosome Remodeling and Deacetylation Complex Modulates Chromatin Structure at Sites of Active Transcription to Fine-Tune Gene Expression', *Mol Cell*, 71: 56-72 e4.
- Burger, A., H. Lindsay, A. Felker, C. Hess, C. Anders, E. Chiavacci, J. Zaugg, L. M. Weber, R. Catena, M. Jinek, M. D. Robinson, and C. Mosimann. 2016. 'Maximizing mutagenesis with solubilized CRISPR-Cas9 ribonucleoprotein complexes', *Development*, 143: 2025-37.
- Carter, B., B. Bishop, K. K. Ho, R. Huang, W. Jia, H. Zhang, P. E. Pascuzzi, R. B. Deal, and J. Ogas. 2018. 'The Chromatin Remodelers PKL and PIE1 Act in an Epigenetic Pathway That Determines H3K27me3 Homeostasis in *Arabidopsis*', *Plant Cell*, 30: 1337-52.
- Cavalier-Smith, T. 2005. 'Economy, speed and size matter: evolutionary forces driving nuclear genome miniaturization and expansion', *Ann Bot*, 95: 147-75.
- Cerami, E., J. Gao, U. Dogrusoz, B. E. Gross, S. O. Sumer, B. A. Aksoy, A. Jacobsen, C. J. Byrne, M. L. Heuer, E. Larsson, Y. Antipin, B. Reva, A. P. Goldberg, C. Sander, and N. Schultz. 2012. 'The cBio cancer genomics portal: an open platform for exploring multidimensional cancer genomics data', *Cancer Discov*, 2: 401-4.
- Chang, H. H. Y., N. R. Pannunzio, N. Adachi, and M. R. Lieber. 2017. 'Non-homologous DNA end joining and alternative pathways to double-strand break repair', *Nat Rev Mol Cell Biol*.

- Chapman, J. R., M. R. Taylor, and S. J. Boulton. 2012. 'Playing the end game: DNA double-strand break repair pathway choice', *Mol Cell*, 47: 497-510.
- Chen, Z., H. Lee, S. J. Henle, T. R. Cheever, S. C. Ekker, and J. R. Henley. 2013. 'Primary neuron culture for nerve growth and axon guidance studies in zebrafish (*Danio rerio*)', *PLoS ONE*, 8: e57539.
- Chen, Z., S. Li, S. Subramaniam, J. Y. Shyy, and S. Chien. 2017. 'Epigenetic Regulation: A New Frontier for Biomedical Engineers', *Annu Rev Biomed Eng*, 19: 195-219.
- Chernyavskaya, Y., B. Kent, and K. C. Sadler. 2016. 'Zebrafish Discoveries in Cancer Epigenetics', *Adv Exp Med Biol*, 916: 169-97.
- Cho, S. W., S. Kim, Y. Kim, J. Kweon, H. S. Kim, S. Bae, and J. S. Kim. 2014. 'Analysis of off-target effects of CRISPR/Cas-derived RNA-guided endonucleases and nickases', *Genome Res*, 24: 132-41.
- Chodavarapu, R. K., S. Feng, Y. V. Bernatavichute, P. Y. Chen, H. Stroud, Y. Yu, J. A. Hetzel, F. Kuo, J. Kim, S. J. Cokus, D. Casero, M. Bernal, P. Huijser, A. T. Clark, U. Kramer, S. S. Merchant, X. Zhang, S. E. Jacobsen, and M. Pellegrini. 2010. 'Relationship between nucleosome positioning and DNA methylation', *Nature*, 466: 388-92.
- Choi, E. S., A. Stralfors, A. G. Castillo, M. Durand-Dubief, K. Ekwall, and R. C. Allshire. 2011. 'Identification of noncoding transcripts from within CENP-A chromatin at fission yeast centromeres', *The Journal of biological chemistry*, 286: 23600-7.
- Cicenas, J., K. Kalyan, A. Sorokinas, E. Stankunas, J. Levy, I. Meskinyte, V. Stankevicius, A. Kaupinis, and M. Valius. 2015. 'Roscovitine in cancer and other diseases', *Ann Transl Med*, 3: 135.
- Clapier, C. R., and B. R. Cairns. 2009. 'The biology of chromatin remodeling complexes', *Annu Rev Biochem*, 78: 273-304.
- Cong, L., F. A. Ran, D. Cox, S. Lin, R. Barretto, N. Habib, P. D. Hsu, X. Wu, W. Jiang, L. A. Marraffini, and F. Zhang. 2013. 'Multiplex genome engineering using CRISPR/Cas systems', *Science*, 339: 819-23.
- Corallo, D., S. Candiani, M. Ori, S. Aveic, and G. P. Tonini. 2016. 'The zebrafish as a model for studying neuroblastoma', *Cancer Cell Int*, 16: 82.
- Corley, M., and K. L. Kroll. 2015. 'The roles and regulation of Polycomb complexes in neural development', *Cell Tissue Res*, 359: 65-85.

- Curinha, A., S. Oliveira Braz, I. Pereira-Castro, A. Cruz, and A. Moreira. 2014. 'Implications of polyadenylation in health and disease', *Nucleus*, 5: 508-19.
- Da Cruz, S., and D. W. Cleveland. 2011. 'Understanding the role of TDP-43 and FUS/TLS in ALS and beyond', *Curr Opin Neurobiol*, 21: 904-19.
- Dahlem, T. J., K. Hoshijima, M. J. Jurynek, D. Gunther, C. G. Starker, A. S. Locke, A. M. Weis, D. F. Voytas, and D. J. Grunwald. 2012. 'Simple methods for generating and detecting locus-specific mutations induced with TALENs in the zebrafish genome', *PLoS Genet*, 8: e1002861.
- Davidoff, A. M., J. C. Pence, N. A. Shorter, J. D. Iglehart, and J. R. Marks. 1992. 'Expression of p53 in human neuroblastoma- and neuroepithelioma-derived cell lines', *Oncogene*, 7: 127-33.
- Davis, A. J., and D. J. Chen. 2013. 'DNA double strand break repair via non-homologous end-joining', *Transl Cancer Res*, 2: 130-43.
- Deal, R. B., J. G. Henikoff, and S. Henikoff. 2010. 'Genome-wide kinetics of nucleosome turnover determined by metabolic labeling of histones', *Science*, 328: 1161-4.
- Deindl, S., W. L. Hwang, S. K. Hota, T. R. Blosser, P. Prasad, B. Bartholomew, and X. Zhuang. 2013. 'ISWI remodelers slide nucleosomes with coordinated multi-base-pair entry steps and single-base-pair exit steps', *Cell*, 152: 442-52.
- Denslow, S. A., and P. A. Wade. 2007. 'The human Mi-2/NuRD complex and gene regulation', *Oncogene*, 26: 5433-8.
- Derti, A., P. Garrett-Engele, K. D. Macisaac, R. C. Stevens, S. Sriram, R. Chen, C. A. Rohl, J. M. Johnson, and T. Babak. 2012. 'A quantitative atlas of polyadenylation in five mammals', *Genome Res*, 22: 1173-83.
- Dovey, M., R. M. White, and L. I. Zon. 2009. 'Oncogenic NRAS cooperates with p53 loss to generate melanoma in zebrafish', *Zebrafish*, 6: 397-404.
- Drabsch, Y., B. E. Snaar-Jagalska, and P. Ten Dijke. 2017. 'Fish tales: The use of zebrafish xenograft human cancer cell models', *Histol Histopathol*, 32: 673-86.

- Du, X., T. Wu, J. Lu, L. Zang, N. Song, T. Yang, H. Zhao, and S. Wang. 2012. 'Decreased expression of chromodomain helicase DNA-binding protein 5 is an unfavorable prognostic marker in patients with primary gallbladder carcinoma', *Clinical & translational oncology : official publication of the Federation of Spanish Oncology Societies and of the National Cancer Institute of Mexico*.
- Egan, C. M., U. Nyman, J. Skotte, G. Streubel, S. Turner, D. J. O'Connell, V. Rraklli, M. J. Dolan, N. Chadderton, K. Hansen, G. J. Farrar, K. Helin, J. Holmberg, and A. P. Bracken. 2013a. 'CHD5 Is Required for Neurogenesis and Has a Dual Role in Facilitating Gene Expression and Polycomb Gene Repression', *Developmental cell*, 26: 223-36.
- . 2013b. 'CHD5 is required for neurogenesis and has a dual role in facilitating gene expression and polycomb gene repression', *Dev Cell*, 26: 223-36.
- Eichler, J., and M. W. Adams. 2005. 'Posttranslational protein modification in Archaea', *Microbiol Mol Biol Rev*, 69: 393-425.
- Ek, F., M. Malo, M. Aberg Andersson, C. Wedding, J. Kronborg, P. Svensson, S. Waters, P. Petersson, and R. Olsson. 2016. 'Behavioral Analysis of Dopaminergic Activation in Zebrafish and Rats Reveals Similar Phenotypes', *ACS Chem Neurosci*, 7: 633-46.
- Engler, C., R. Kandzia, and S. Marillonnet. 2008. 'A one pot, one step, precision cloning method with high throughput capability', *PLoS ONE*, 3: e3647.
- Enriquez, P. 2016. 'CRISPR-Mediated Epigenome Editing', *Yale J Biol Med*, 89: 471-86.
- Ernsberger, U., and H. Rohrer. 2018. 'Sympathetic tales: subdivisions of the autonomic nervous system and the impact of developmental studies', *Neural Dev*, 13: 20.
- Ernst, J., P. Kheradpour, T. S. Mikkelsen, N. Shores, L. D. Ward, C. B. Epstein, X. Zhang, L. Wang, R. Issner, M. Coyne, M. Ku, T. Durham, M. Kellis, and B. E. Bernstein. 2011. 'Mapping and analysis of chromatin state dynamics in nine human cell types', *Nature*, 473: 43-9.
- Farnung, L., S. M. Vos, C. Wigge, and P. Cramer. 2017. 'Nucleosome-Chd1 structure and implications for chromatin remodelling', *Nature*, 550: 539-42.
- Fatemi, M., T. A. Paul, G. M. Brodeur, B. Shokrani, H. Brim, and H. Ashktorab. 2014. 'Epigenetic silencing of CHD5, a novel tumor-suppressor gene, occurs in early colorectal cancer stages', *Cancer*, 120: 172-80.

- Fei, J., S. E. Torigoe, C. R. Brown, M. T. Khuong, G. A. Kassavetis, H. Boeger, and J. T. Kadonaga. 2015. 'The prenucleosome, a stable conformational isomer of the nucleosome', *Genes Dev*, 29: 2563-75.
- Feng, W., M. A. Khan, P. Bellvis, Z. Zhu, O. Bernhardt, C. Herold-Mende, and H. K. Liu. 2013. 'The chromatin remodeler CHD7 regulates adult neurogenesis via activation of SoxC transcription factors', *Cell Stem Cell*, 13: 62-72.
- Filippakopoulos, P., J. Qi, S. Picaud, Y. Shen, W. B. Smith, O. Fedorov, E. M. Morse, T. Keates, T. T. Hickman, I. Felletar, M. Philpott, S. Munro, M. R. McKeown, Y. Wang, A. L. Christie, N. West, M. J. Cameron, B. Schwartz, T. D. Heightman, N. La Thangue, C. A. French, O. Wiest, A. L. Kung, S. Knapp, and J. E. Bradner. 2010. 'Selective inhibition of BET bromodomains', *Nature*, 468: 1067-73.
- Fisher, R. A. 1922. 'On the interpretation of χ^2 from contingency tables, and the calculation of P', *Journal of the Royal Statistical Society*, 85: 87-94.
- Flanagan, J. F., B. J. Blus, D. Kim, K. L. Clines, F. Rastinejad, and S. Khorasanizadeh. 2007. 'Molecular implications of evolutionary differences in CHD double chromodomains', *J Mol Biol*, 369: 334-42.
- Flanagan, J. F., L. Z. Mi, M. Chruszcz, M. Cymborowski, K. L. Clines, Y. Kim, W. Minor, F. Rastinejad, and S. Khorasanizadeh. 2005. 'Double chromodomains cooperate to recognize the methylated histone H3 tail', *Nature*, 438: 1181-5.
- Flaus, A., D. M. Martin, G. J. Barton, and T. Owen-Hughes. 2006. 'Identification of multiple distinct Snf2 subfamilies with conserved structural motifs', *Nucleic Acids Res*, 34: 2887-905.
- Fu, Y., D. Reyon, and J. K. Joung. 2014. 'Targeted genome editing in human cells using CRISPR/Cas nucleases and truncated guide RNAs', *Methods Enzymol*, 546: 21-45.
- Fujita, T., J. Igarashi, E. R. Okawa, T. Gotoh, J. Manne, V. Kolla, J. Kim, H. Zhao, B. R. Pawel, W. B. London, J. M. Maris, P. S. White, and G. M. Brodeur. 2008. 'CHD5, a tumor suppressor gene deleted from 1p36.31 in neuroblastomas', *J Natl Cancer Inst*, 100: 940-9.
- Gagnon, J. A., E. Valen, S. B. Thyme, P. Huang, L. Ahkmetova, A. Pauli, T. G. Montague, S. Zimmerman, C. Richter, and A. F. Schier. 2014. 'Efficient mutagenesis by Cas9 protein-mediated oligonucleotide insertion and large-scale assessment of single-guide RNAs', *PLoS One*, 9: e98186.

- Garcia, I., G. Mayol, E. Rodriguez, M. Sunol, T. R. Gershon, J. Rios, N. K. Cheung, M. W. Kieran, R. E. George, A. R. Perez-Atayde, C. Casala, P. Galvan, C. de Torres, J. Mora, and C. Lavarino. 2010. 'Expression of the neuron-specific protein CHD5 is an independent marker of outcome in neuroblastoma', *Mol Cancer*, 9: 277.
- Garneau, J. E., M. E. Dupuis, M. Villion, D. A. Romero, R. Barrangou, P. Boyaval, C. Fremaux, P. Horvath, A. H. Magadan, and S. Moineau. 2010. 'The CRISPR/Cas bacterial immune system cleaves bacteriophage and plasmid DNA', *Nature*, 468: 67-71.
- Gasiunas, G., R. Barrangou, P. Horvath, and V. Siksnys. 2012. 'Cas9-crRNA ribonucleoprotein complex mediates specific DNA cleavage for adaptive immunity in bacteria', *Proc Natl Acad Sci U S A*, 109: E2579-86.
- Gaspar-Maia, A., A. Alajem, F. Polesso, R. Sridharan, M. J. Mason, A. Heidersbach, J. Ramalho-Santos, M. T. McManus, K. Plath, E. Meshorer, and M. Ramalho-Santos. 2009. 'Chd1 regulates open chromatin and pluripotency of embryonic stem cells', *Nature*, 460: 863-8.
- Gholamitabar Tabari, M., S. G. A. Jorsaraei, M. Ghasemzadeh-Hasankolaei, A. A. Ahmadi, and M. Amirikia. 2018. 'Evaluation of Novel Mouse-Specific Germ Cell Gene Expression in Embryonic Stem Cell-Derived Germ Cell-Like Cells In Vitro with Retinoic Acid Treatment', *Cell Reprogram*, 20: 245-55.
- Gkikopoulos, T., P. Schofield, V. Singh, M. Pinskaya, J. Mellor, M. Smolle, J. L. Workman, G. J. Barton, and T. Owen-Hughes. 2011. 'A role for Snf2-related nucleosome-spacing enzymes in genome-wide nucleosome organization', *Science*, 333: 1758-60.
- Gonzales, A. P., and J. R. Yeh. 2014. 'Cas9-based genome editing in zebrafish', *Methods Enzymol*, 546: 377-413.
- Gunther, K., M. Rust, J. Leers, T. Boettger, M. Scharfe, M. Jarek, M. Bartkuhn, and R. Renkawitz. 2013. 'Differential roles for MBD2 and MBD3 at methylated CpG islands, active promoters and binding to exon sequences', *Nucleic Acids Res Suppl*, 41: 3010-21.
- Haeussler, M., K. Schonig, H. Eckert, A. Eschstruth, J. Mianne, J. B. Renaud, S. Schneider-Maunoury, A. Shkumatava, L. Teboul, J. Kent, J. S. Joly, and J. P. Concordet. 2016. 'Evaluation of off-target and on-target scoring algorithms and integration into the guide RNA selection tool CRISPOR', *Genome Biol*, 17: 148.

- Hakim, N. H., B. Y. Majlis, H. Suzuki, and T. Tsukahara. 2017. 'Neuron-specific splicing', *Biosci Trends*, 11: 16-22.
- Hall, J. A., and P. T. Georgel. 2007. 'CHD proteins: a diverse family with strong ties', *Biochem Cell Biol*, 85: 463-76.
- Hamada, N., H. Ito, T. Nishijo, I. Iwamoto, R. Morishita, H. Tabata, T. Momiyama, and K. Nagata. 2016. 'Essential role of the nuclear isoform of RBFOX1, a candidate gene for autism spectrum disorders, in the brain development', *Sci Rep*, 6: 30805.
- Hamby, M. E., V. Coskun, and Y. E. Sun. 2008. 'Transcriptional regulation of neuronal differentiation: the epigenetic layer of complexity', *Biochim Biophys Acta*, 1779: 432-7.
- Harada, A., S. Okada, D. Konno, J. Odawara, T. Yoshimi, S. Yoshimura, H. Kumamaru, H. Saiwai, T. Tsubota, H. Kurumizaka, K. Akashi, T. Tachibana, A. N. Imbalzano, and Y. Ohkawa. 2012. 'Chd2 interacts with H3.3 to determine myogenic cell fate', *EMBO J*, 31: 2994-3007.
- Harada, B. T., W. L. Hwang, S. Deindl, N. Chatterjee, B. Bartholomew, and X. Zhuang. 2016. 'Stepwise nucleosome translocation by RSC remodeling complexes', *Elife*, 5.
- Hardwick, L. J., F. R. Ali, R. Azzarelli, and A. Philpott. 2015. 'Cell cycle regulation of proliferation versus differentiation in the central nervous system', *Cell Tissue Res*, 359: 187-200.
- Hargreaves, D. C., and G. R. Crabtree. 2011. 'ATP-dependent chromatin remodeling: genetics, genomics and mechanisms', *Cell Res*, 21: 396-420.
- Hartley, S. W., and J. C. Mullikin. 2016. 'Detection and visualization of differential splicing in RNA-Seq data with JunctionSeq', *Nucleic Acids Res*, 44: e127.
- Hauk, G., and G. D. Bowman. 2011. 'Structural insights into regulation and action of SWI2/SNF2 ATPases', *Curr Opin Struct Biol*, 21: 719-27.
- Hauk, G., J. N. McKnight, I. M. Nodelman, and G. D. Bowman. 2010. 'The chromodomains of the Chd1 chromatin remodeler regulate DNA access to the ATPase motor', *Mol Cell*, 39: 711-23.
- Hayes, M. N., and D. M. Langenau. 2017. 'Discovering novel oncogenic pathways and new therapies using zebrafish models of sarcoma', *Methods Cell Biol*, 138: 525-61.
- He, S., C. B. Jing, and A. T. Look. 2017. 'Zebrafish models of leukemia', *Methods Cell Biol*, 138: 563-92.

- Henikoff, S., and M. M. Smith. 2015. 'Histone variants and epigenetics', *Cold Spring Harb Perspect Biol*, 7: a019364.
- Hennig, B. P., K. Bendrin, Y. Zhou, and T. Fischer. 2012. 'Chd1 chromatin remodelers maintain nucleosome organization and repress cryptic transcription', *EMBO reports*, 13: 997-1003.
- Higashi, M., V. Kolla, R. Iyer, K. Naraparaju, T. Zhuang, S. Kolla, and G. M. Brodeur. 2015. 'Retinoic acid-induced CHD5 upregulation and neuronal differentiation of neuroblastoma', *Mol Cancer*, 14: 150.
- Hill, J. T., B. L. Demarest, B. W. Bisgrove, Y. C. Su, M. Smith, and H. J. Yost. 2014. 'Poly peak parser: Method and software for identification of unknown indels using sanger sequencing of polymerase chain reaction products', *Dev Dyn*, 243: 1632-6.
- Hisano, Y., S. Ota, and A. Kawahara. 2014. 'Genome editing using artificial site-specific nucleases in zebrafish', *Dev Growth Differ*, 56: 26-33.
- Ho, K. K., H. Zhang, B. L. Golden, and J. Ogas. 2013a. 'PICKLE is a CHD subfamily II ATP-dependent chromatin remodeling factor', *BBA - Gene Regul Mech*, 1829: 199-210.
- . 2013b. 'PICKLE is a CHD subfamily II ATP-dependent chromatin remodeling factor', *Biochim Biophys Acta*, 1829: 199-210.
- Hodges, E., A. D. Smith, J. Kendall, Z. Xuan, K. Ravi, M. Rooks, M. Q. Zhang, K. Ye, A. Bhattacharjee, L. Brizuela, W. R. McCombie, M. Wigler, G. J. Hannon, and J. B. Hicks. 2009. 'High definition profiling of mammalian DNA methylation by array capture and single molecule bisulfite sequencing', *Genome Res*, 19: 1593-605.
- Hoffmeister, H., A. Fuchs, F. Erdel, S. Pinz, R. Grobner-Ferreira, A. Bruckmann, R. Deutzmann, U. Schwartz, R. Maldonado, C. Huber, A. S. Dendorfer, K. Rippe, and G. Langst. 2017. 'CHD3 and CHD4 form distinct NuRD complexes with different yet overlapping functionality', *Nucleic Acids Res*.
- Hornberg, H., F. Wollerton-van Horck, D. Maurus, M. Zwart, H. Svoboda, W. A. Harris, and C. E. Holt. 2013. 'RNA-binding protein Hermes/RBPMS inversely affects synapse density and axon arbor formation in retinal ganglion cells in vivo', *J Neurosci*, 33: 10384-95.
- Hoshijima, K., M. J. Jurynek, and D. J. Grunwald. 2016. 'Precise genome editing by homologous recombination', *Methods Cell Biol*, 135: 121-47.

- Howe, K., M. D. Clark, C. F. Torroja, J. Torrance, C. Berthelot, M. Muffato, J. E. Collins, S. Humphray, K. McLaren, L. Matthews, S. McLaren, I. Sealy, M. Caccamo, C. Churcher, C. Scott, J. C. Barrett, R. Koch, G. J. Rauch, S. White, W. Chow, B. Kilian, L. T. Quintais, J. A. Guerra-Assuncao, Y. Zhou, Y. Gu, J. Yen, J. H. Vogel, T. Eyre, S. Redmond, R. Banerjee, J. Chi, B. Fu, E. Langley, S. F. Maguire, G. K. Laird, D. Lloyd, E. Kenyon, S. Donaldson, H. Sehra, J. Almeida-King, J. Loveland, S. Trevanion, M. Jones, M. Quail, D. Willey, A. Hunt, J. Burton, S. Sims, K. McLay, B. Plumb, J. Davis, C. Clee, K. Oliver, R. Clark, C. Riddle, D. Elliot, G. Threadgold, G. Harden, D. Ware, S. Begum, B. Mortimore, G. Kerry, P. Heath, B. Phillimore, A. Tracey, N. Corby, M. Dunn, C. Johnson, J. Wood, S. Clark, S. Pelan, G. Griffiths, M. Smith, R. Glithero, P. Howden, N. Barker, C. Lloyd, C. Stevens, J. Harley, K. Holt, G. Panagiotidis, J. Lovell, H. Beasley, C. Henderson, D. Gordon, K. Auger, D. Wright, J. Collins, C. Raisen, L. Dyer, K. Leung, L. Robertson, K. Ambridge, D. Leongamornlert, S. McGuire, R. Gilderthorp, C. Griffiths, D. Manthravadi, S. Nichol, G. Barker, S. Whitehead, M. Kay, J. Brown, C. Murnane, E. Gray, M. Humphries, N. Sycamore, D. Barker, D. Saunders, J. Wallis, A. Babbage, S. Hammond, M. Mashreghi-Mohammadi, L. Barr, S. Martin, P. Wray, A. Ellington, N. Matthews, M. Ellwood, R. Woodmansey, G. Clark, J. Cooper, A. Tromans, D. Grafham, C. Skuce, R. Pandian, R. Andrews, E. Harrison, A. Kimberley, J. Garnett, N. Fosker, R. Hall, P. Garner, D. Kelly, C. Bird, S. Palmer, I. Gehring, A. Berger, C. M. Dooley, Z. Ersan-Urun, C. Eser, H. Geiger, M. Geisler, L. Karotki, A. Kirn, J. Konantz, M. Konantz, M. Oberlander, S. Rudolph-Geiger, M. Teucke, C. Lanz, G. Raddatz, K. Osoegawa, B. Zhu, A. Rapp, S. Widaa, C. Langford, F. Yang, S. C. Schuster, N. P. Carter, J. Harrow, Z. Ning, J. Herrero, S. M. Searle, A. Enright, R. Geisler, R. H. Plasterk, C. Lee, M. Westerfield, P. J. de Jong, L. I. Zon, J. H. Postlethwait, C. Nusslein-Volhard, T. J. Hubbard, H. Roest Crolius, J. Rogers, and D. L. Stemple. 2013. 'The zebrafish reference genome sequence and its relationship to the human genome', *Nature*, 496: 498-503.
- Hruscha, A., P. Krawitz, A. Rechenberg, V. Heinrich, J. Hecht, C. Haass, and B. Schmid. 2013. 'Efficient CRISPR/Cas9 genome editing with low off-target effects in zebrafish', *Development*, 140: 4982-7.

- Hsieh, J., and X. Zhao. 2016. 'Genetics and Epigenetics in Adult Neurogenesis', *Cold Spring Harb Perspect Biol*, 8.
- Hsu, P. D., and F. Zhang. 2012. 'Dissecting neural function using targeted genome engineering technologies', *ACS Chem Neurosci*, 3: 603-10.
- Hsu, P., A. Ma, M. Wilson, G. Williams, J. Curotta, C. F. Munns, and S. Mehr. 2014. 'CHARGE syndrome: a review', *J Paediatr Child Health*, 50: 504-11.
- Hu, W., Z. Feng, and A. J. Levine. 2012. 'The Regulation of Multiple p53 Stress Responses is Mediated through MDM2', *Genes Cancer*, 3: 199-208.
- Hwang, D. W., A. Jaganathan, P. Shrestha, Y. Jin, N. El-Amine, S. H. Wang, M. Hammell, and A. A. Mills. 2018. 'Chromatin-mediated translational control is essential for neural cell fate specification', *Life Sci Alliance*, 1: e201700016.
- Hwang, K. L., and W. Goessling. 2016. 'Baiting for Cancer: Using the Zebrafish as a Model in Liver and Pancreatic Cancer', *Adv Exp Med Biol*, 916: 391-410.
- Hwang, W. Y., Y. Fu, D. Reyon, A. P. Gonzales, J. K. Joung, and J. R. Yeh. 2015. 'Targeted Mutagenesis in Zebrafish Using CRISPR RNA-Guided Nucleases', *Methods Mol Biol*, 1311: 317-34.
- Illig, D., M. Navratil, J. Kelecic, R. Conca, I. Hojsak, O. Jadresin, M. Coric, J. Vukovic, M. Rohlf, S. Hollizeck, J. Bohne, C. Klein, and D. Kotlarz. 2019. 'Alternative Splicing Rescues Loss of Common Gamma Chain Function and Results in IL-21R-like Deficiency', *J Clin Immunol*.
- Ishihara, K., M. Oshimura, and M. Nakao. 2006. 'CTCF-dependent chromatin insulator is linked to epigenetic remodeling', *Mol Cell*, 23: 733-42.
- Iyer, V., B. Shen, W. Zhang, A. Hodgkins, T. Keane, X. Huang, and W. C. Skarnes. 2015. 'Off-target mutations are rare in Cas9-modified mice', *Nat Methods*, 12: 479.
- Jao, L. E., S. R. Wentz, and W. Chen. 2013. 'Efficient multiplex biallelic zebrafish genome editing using a CRISPR nuclease system', *Proc Natl Acad Sci U S A*, 110: 13904-9.
- Jia, Y., J. C. Mu, and S. L. Ackerman. 2012. 'Mutation of a U2 snRNA gene causes global disruption of alternative splicing and neurodegeneration', *Cell*, 148: 296-308.
- Jiang, M., J. Stanke, and J. M. Lahti. 2011. 'The connections between neural crest development and neuroblastoma', *Current topics in developmental biology*, 94: 77-127.

- Jinek, M., K. Chylinski, I. Fonfara, M. Hauer, J. A. Doudna, and E. Charpentier. 2012. 'A programmable dual-RNA-guided DNA endonuclease in adaptive bacterial immunity', *Science*, 337: 816-21.
- Jing, Y., and R. Lin. 2013. 'PICKLE is a repressor in seedling de-etiolation pathway', *Plant signaling & behavior*, 8.
- Jing, Y., D. Zhang, X. Wang, W. Tang, W. Wang, J. Huai, G. Xu, D. Chen, Y. Li, and R. Lin. 2013. 'Arabidopsis chromatin remodeling factor PICKLE interacts with transcription factor HY5 to regulate hypocotyl cell elongation', *Plant Cell*, 25: 242-56.
- Jung, C., J. A. Hawkins, S. K. Jones, Jr., Y. Xiao, J. R. Rybarski, K. E. Dillard, J. Hussmann, F. A. Saifuddin, C. A. Savran, A. D. Ellington, A. Ke, W. H. Press, and I. J. Finkelstein. 2017. 'Massively Parallel Biophysical Analysis of CRISPR-Cas Complexes on Next Generation Sequencing Chips', *Cell*, 170: 35-47 e13.
- Kalra, S., G. Joshi, A. Munshi, and R. Kumar. 2017. 'Structural insights of cyclin dependent kinases: Implications in design of selective inhibitors', *Eur J Med Chem*, 142: 424-58.
- Kalueff, A. V., A. M. Stewart, and R. Gerlai. 2014. 'Zebrafish as an emerging model for studying complex brain disorders', *Trends Pharmacol Sci*, 35: 63-75.
- Kandimalla, R., and P. H. Reddy. 2017. 'Therapeutics of Neurotransmitters in Alzheimer's Disease', *J Alzheimers Dis*, 57: 1049-69.
- Kelemen, O., P. Convertini, Z. Zhang, Y. Wen, M. Shen, M. Falaleeva, and S. Stamm. 2013. 'Function of alternative splicing', *Gene*, 514: 1-30.
- Khare, T., S. Pai, K. Koncevicus, M. Pal, E. Kriukiene, Z. Liutkeviciute, M. Irimia, P. Jia, C. Ptak, M. Xia, R. Tice, M. Tochigi, S. Morera, A. Nazarians, D. Belsham, A. H. Wong, B. J. Blencowe, S. C. Wang, P. Kapranov, R. Kustra, V. Labrie, S. Klimasauskas, and A. Petronis. 2012. '5-hmC in the brain is abundant in synaptic genes and shows differences at the exon-intron boundary', *Nat Struct Mol Biol*, 19: 1037-43.
- Kim, H., H. Jo, H. D. Seo, H. S. Park, and D. Lee. 2018. 'Chd1p recognizes H3K36Ac to maintain nucleosome positioning near the transcription start site', *Biochem Biophys Res Commun*, 503: 1200-06.
- Kim, Y. E., C. Park, K. E. Kim, and K. K. Kim. 2018. 'Histone and RNA-binding protein interaction creates crosstalk network for regulation of alternative splicing', *Biochem Biophys Res Commun*, 499: 30-36.

- Kimmel, C. B., W. W. Ballard, S. R. Kimmel, B. Ullmann, and T. F. Schilling. 1995. 'Stages of embryonic development of the zebrafish', *Dev Dyn*, 203: 253-310.
- Kolla, V., K. Naraparaju, T. Zhuang, M. Higashi, S. Kolla, G. A. Blobel, and G. M. Brodeur. 2015. 'The tumour suppressor CHD5 forms a NuRD-type chromatin remodelling complex', *Biochem J*, 468: 345-52.
- Kolla, V., T. Zhuang, M. Higashi, K. Naraparaju, and G. M. Brodeur. 2014. 'Role of CHD5 in Human Cancers: 10 Years Later', *Cancer Res*, 74: 652-8.
- Konev, A. Y., M. Tribus, S. Y. Park, V. Podhraski, C. Y. Lim, A. V. Emelyanov, E. Vershilova, V. Pirrotta, J. T. Kadonaga, A. Lusser, and D. V. Fyodorov. 2007. 'CHD1 motor protein is required for deposition of histone variant H3.3 into chromatin in vivo', *Science*, 317: 1087-90.
- Kotani, H., K. Taimatsu, R. Ohga, S. Ota, and A. Kawahara. 2015. 'Efficient Multiple Genome Modifications Induced by the crRNAs, tracrRNA and Cas9 Protein Complex in Zebrafish', *PLoS One*, 10: e0128319.
- Koyama, H., T. Zhuang, J. E. Light, V. Kolla, M. Higashi, P. W. McGrady, W. B. London, and G. M. Brodeur. 2012. 'Mechanisms of CHD5 Inactivation in neuroblastomas', *Clin Cancer Res*, 18: 1588-97.
- Kozol, R. A. 2018. 'Prenatal Neuropathologies in Autism Spectrum Disorder and Intellectual Disability: The Gestation of a Comprehensive Zebrafish Model', *J Dev Biol*, 6.
- Kriaucionis, S., and N. Heintz. 2009. 'The nuclear DNA base 5-hydroxymethylcytosine is present in Purkinje neurons and the brain', *Science*, 324: 929-30.
- Lande-Diner, L., and H. Cedar. 2005. 'Silence of the genes--mechanisms of long-term repression', *Nat Rev Genet*, 6: 648-54.
- Larsen, P. A., M. W. Lutz, K. E. Hunnicutt, M. Mihovilovic, A. M. Saunders, A. D. Yoder, and A. D. Roses. 2017. 'The Alu neurodegeneration hypothesis: A primate-specific mechanism for neuronal transcription noise, mitochondrial dysfunction, and manifestation of neurodegenerative disease', *Alzheimers Dement*, 13: 828-38.
- Leacock, S. W., A. N. Basse, G. L. Chandler, A. M. Kirk, D. Rakheja, and J. F. Amatruda. 2012. 'A zebrafish transgenic model of Ewing's sarcoma reveals conserved mediators of EWS-FLI1 tumorigenesis', *Dis Model Mech*, 5: 95-106.

- Lee, J. A., A. Damianov, C. H. Lin, M. Fontes, N. N. Parikshak, E. S. Anderson, D. H. Geschwind, D. L. Black, and K. C. Martin. 2016. 'Cytoplasmic Rbfox1 Regulates the Expression of Synaptic and Autism-Related Genes', *Neuron*, 89: 113-28.
- Li, H., W. Xu, Y. Huang, X. Huang, L. Xu, and Z. Lv. 2012. 'Genistein demethylates the promoter of CHD5 and inhibits neuroblastoma growth in vivo', *Int J Mol Med*, 30: 1081-6.
- Li, J., and P. Yu. 2018. 'Genome-wide transcriptome analysis identifies alternative splicing regulatory network and key splicing factors in mouse and human psoriasis', *Sci Rep*, 8: 4124.
- Li, L. C., J. R. Sheng, N. Mulherkar, B. S. Prabhakar, and M. N. Meriggioli. 2008. 'Regulation of apoptosis and caspase-8 expression in neuroblastoma cells by isoforms of the IG20 gene', *Cancer Res*, 68: 7352-61.
- Li, M., and Y. Fang. 2015. 'Histone variants: the artists of eukaryotic chromatin', *Sci China Life Sci*, 58: 232-9.
- Li, W., J. Wu, S. Y. Kim, M. Zhao, S. A. Hearn, M. Q. Zhang, M. L. Meistrich, and A. A. Mills. 2014. 'Chd5 orchestrates chromatin remodelling during sperm development', *Nature communications*, 5: 3812.
- Liang, Y., J. Song, D. He, Y. Xia, Y. Wu, X. Yin, and J. Liu. 2019. 'Systematic analysis of survival-associated alternative splicing signatures uncovers prognostic predictors for head and neck cancer', *J Cell Physiol*.
- Lieber, M. R. 2010. 'The mechanism of double-strand DNA break repair by the nonhomologous DNA end-joining pathway', *Annu Rev Biochem*, 79: 181-211.
- Liu, D., J. M. Brockman, B. Dass, L. N. Hutchins, P. Singh, J. R. McCarrey, C. C. MacDonald, and J. H. Graber. 2007. 'Systematic variation in mRNA 3'-processing signals during mouse spermatogenesis', *Nucleic Acids Res*, 35: 234-46.
- Liu, J., A. Geng, X. Wu, R. J. Lin, and Q. Lu. 2018. 'Alternative RNA Splicing Associated With Mammalian Neuronal Differentiation', *Cereb Cortex*, 28: 2810-16.
- Liu, Y., D. Luo, Y. Lei, W. Hu, H. Zhao, and C. H. Cheng. 2014. 'A highly effective TALEN-mediated approach for targeted gene disruption in *Xenopus tropicalis* and zebrafish', *Methods*, 69: 58-66.

- Lobert, V. H., D. Mouradov, and J. K. Heath. 2016. 'Focusing the Spotlight on the Zebrafish Intestine to Illuminate Mechanisms of Colorectal Cancer', *Adv Exp Med Biol*, 916: 411-37.
- Lorch, Y., and R. D. Kornberg. 2017. 'Chromatin-remodeling for transcription', *Q Rev Biophys*, 50: e5.
- Lowe, S. W., and A. W. Lin. 2000. 'Apoptosis in cancer', *Carcinogenesis*, 21: 485-95.
- Lu, J. W., W. Y. Yang, S. M. Tsai, Y. M. Lin, P. H. Chang, J. R. Chen, H. D. Wang, J. L. Wu, S. L. Jin, and C. H. Yuh. 2013. 'Liver-specific expressions of HBx and src in the p53 mutant trigger hepatocarcinogenesis in zebrafish', *PLoS One*, 8: e76951.
- Luco, R. F., Q. Pan, K. Tominaga, B. J. Blencowe, O. M. Pereira-Smith, and T. Misteli. 2010. 'Regulation of alternative splicing by histone modifications', *Science*, 327: 996-1000.
- Luger, K., A. W. Mader, R. K. Richmond, D. F. Sargent, and T. J. Richmond. 1997. 'Crystal structure of the nucleosome core particle at 2.8 Å resolution', *Nature*, 389: 251-60.
- Lutz, T., R. Stoger, and A. Nieto. 2006. 'CHD6 is a DNA-dependent ATPase and localizes at nuclear sites of mRNA synthesis', *FEBS Lett*, 580: 5851-7.
- Lyko, F., S. Foret, R. Kucharski, S. Wolf, C. Falckenhayn, and R. Maleszka. 2010. 'The honey bee epigenomes: differential methylation of brain DNA in queens and workers', *PLoS Biol*, 8: e1000506.
- Ma, D. K., M. C. Marchetto, J. U. Guo, G. L. Ming, F. H. Gage, and H. Song. 2010. 'Epigenetic choreographers of neurogenesis in the adult mammalian brain', *Nat Neurosci*, 13: 1338-44.
- Ma, L., and A. G. Hunt. 2015. 'A 3' RACE protocol to confirm polyadenylation sites', *Methods Mol Biol*, 1255: 135-44.
- Macadangang, B. R., A. Oberai, T. Spektor, O. A. Campos, F. Sheng, M. F. Carey, M. Vogelaer, and S. K. Kurdistani. 2014. 'Evolution of histone 2A for chromatin compaction in eukaryotes', *Elife*, 3.
- MacDonald, C. C. 2019. 'Tissue-specific mechanisms of alternative polyadenylation: Testis, brain, and beyond (2018 update)', *Wiley Interdiscip Rev RNA*: e1526.
- Malik, H. S., and S. Henikoff. 2003. 'Phylogenomics of the nucleosome', *Nat Struct Biol*, 10: 882-91.

- Mansfield, R. E., C. A. Musselman, A. H. Kwan, S. S. Oliver, A. L. Garske, F. Davrazou, J. M. Denu, T. G. Kutateladze, and J. P. Mackay. 2011. 'Plant homeodomain (PHD) fingers of CHD4 are histone H3-binding modules with preference for unmodified H3K4 and methylated H3K9', *J Biol Chem*, 286: 11779-91.
- Marfella, C. G., and A. N. Imbalzano. 2007. 'The Chd family of chromatin remodelers', *Mutat Res*, 618: 30-40.
- Maris, J. M., and K. K. Matthay. 1999. 'Molecular biology of neuroblastoma', *J Clin Oncol*, 17: 2264-79.
- Martin, G. R. 1981. 'Isolation of a pluripotent cell line from early mouse embryos cultured in medium conditioned by teratocarcinoma stem cells', *Proc Natl Acad Sci U S A*, 78: 7634-8.
- Martinez-Montiel, N., N. H. Rosas-Murrieta, M. Anaya Ruiz, E. Monjaraz-Guzman, and R. Martinez-Contreras. 2018. 'Alternative Splicing as a Target for Cancer Treatment', *Int J Mol Sci*, 19.
- Mattiroli, F., S. Bhattacharyya, P. N. Dyer, A. E. White, K. Sandman, B. W. Burkhardt, K. R. Byrne, T. Lee, N. G. Ahn, T. J. Santangelo, J. N. Reeve, and K. Luger. 2017. 'Structure of histone-based chromatin in Archaea', *Science*, 357: 609-12.
- Mavrich, T. N., C. Jiang, I. P. Ioshikhes, X. Li, B. J. Venters, S. J. Zanton, L. P. Tomsho, J. Qi, R. L. Glaser, S. C. Schuster, D. S. Gilmour, I. Albert, and B. F. Pugh. 2008. 'Nucleosome organization in the Drosophila genome', *Nature*, 453: 358-62.
- Mayes, K., Z. Qiu, A. Alhazmi, and J. W. Landry. 2014. 'ATP-dependent chromatin remodeling complexes as novel targets for cancer therapy', *Adv Cancer Res*, 121: 183-233.
- McBride, M. J., and C. Kadoch. 2018. 'Disruption of mammalian SWI/SNF and polycomb complexes in human sarcomas: mechanisms and therapeutic opportunities', *J Pathol*, 244: 638-49.
- McKnight, J. N., K. R. Jenkins, I. M. Nodelman, T. Escobar, and G. D. Bowman. 2011. 'Extranucleosomal DNA binding directs nucleosome sliding by Chd1', *Mol Cell Biol*, 31: 4746-59.
- Miura, P., S. Shenker, C. Andreu-Agullo, J. O. Westholm, and E. C. Lai. 2013. 'Widespread and extensive lengthening of 3' UTRs in the mammalian brain', *Genome Res*, 23: 812-25.

- Mollet, I. G., C. Ben-Dov, D. Felicio-Silva, A. R. Grosso, P. Eleuterio, R. Alves, R. Staller, T. S. Silva, and M. Carmo-Fonseca. 2010. 'Unconstrained mining of transcript data reveals increased alternative splicing complexity in the human transcriptome', *Nucleic Acids Res*, 38: 4740-54.
- Montague, T. G., J. M. Cruz, J. A. Gagnon, G. M. Church, and E. Valen. 2014. 'CHOPCHOP: a CRISPR/Cas9 and TALEN web tool for genome editing', *Nucleic Acids Res*, 42: W401-7.
- Morettini, S., M. Tribus, A. Zeilner, J. Sebald, B. Campo-Fernandez, G. Scheran, H. Worle, V. Podhraski, D. V. Fyodorov, and A. Lusser. 2011. 'The chromodomains of CHD1 are critical for enzymatic activity but less important for chromatin localization', *Nucleic Acids Res*, 39: 3103-15.
- Morra, R., T. Fessl, Y. Wang, E. J. Mancini, and R. Tuma. 2016. 'Biophysical Characterization of Chromatin Remodeling Protein CHD4', *Methods Mol Biol*, 1431: 175-93.
- Morra, R., B. M. Lee, H. Shaw, R. Tuma, and E. J. Mancini. 2012. 'Concerted action of the PHD, chromo and motor domains regulates the human chromatin remodelling ATPase CHD4', *FEBS letters*, 586: 2513-21.
- Morrison, M. A., M. W. Zimmerman, A. T. Look, and R. A. Stewart. 2016. 'Studying the peripheral sympathetic nervous system and neuroblastoma in zebrafish', *Methods Cell Biol*, 134: 97-138.
- Mueller, T., P. Vernier, and M. F. Wullimann. 2006. 'A phylotypic stage in vertebrate brain development: GABA cell patterns in zebrafish compared with mouse', *J Comp Neurol*, 494: 620-34.
- Murawska, M., M. Hassler, R. Renkawitz-Pohl, A. Ladurner, and A. Brehm. 2011. 'Stress-Induced PARP Activation Mediates Recruitment of Drosophila Mi-2 to Promote Heat Shock Gene Expression', *PLoS Genet*, 7: e1002206.
- Musselman, C. A., R. E. Mansfield, A. L. Garske, F. Davrazou, A. H. Kwan, S. S. Oliver, H. O'Leary, J. M. Denu, J. P. Mackay, and T. G. Kutateladze. 2009. 'Binding of the CHD4 PHD2 finger to histone H3 is modulated by covalent modifications', *Biochem J*, 423: 179-87.

- Musselman, C. A., J. Ramirez, J. K. Sims, R. E. Mansfield, S. S. Oliver, J. M. Denu, J. P. Mackay, P. A. Wade, J. Hagman, and T. G. Kutateladze. 2012. 'Bivalent recognition of nucleosomes by the tandem PHD fingers of the CHD4 ATPase is required for CHD4-mediated repression', *Proceedings of the National Academy of Sciences of the United States of America*, 109: 787-92.
- Naraparaju, K., V. Kolla, T. Zhuang, M. Higashi, R. Iyer, S. Kolla, E. R. Okawa, G. A. Blobel, and G. M. Brodeur. 2016. 'Role of microRNAs in epigenetic silencing of the CHD5 tumor suppressor gene in neuroblastomas', *Oncotarget*, 7: 15977-85.
- Narayanan, N. S., R. L. Rodnitzky, and E. Y. Uc. 2013. 'Prefrontal dopamine signaling and cognitive symptoms of Parkinson's disease', *Rev Neurosci*, 24: 267-78.
- Narlikar, G. J., R. Sundaramoorthy, and T. Owen-Hughes. 2013. 'Mechanisms and functions of ATP-dependent chromatin-remodeling enzymes', *Cell*, 154: 490-503.
- Nasiadka, A., and M. D. Clark. 2012. 'Zebrafish breeding in the laboratory environment', *ILAR J*, 53: 161-8.
- Neve, J., R. Patel, Z. Wang, A. Louey, and A. M. Furger. 2017. 'Cleavage and polyadenylation: Ending the message expands gene regulation', *RNA Biol*, 14: 865-90.
- Nishiyama, M., K. Oshikawa, Y. Tsukada, T. Nakagawa, S. Iemura, T. Natsume, Y. Fan, A. Kikuchi, A. I. Skoultchi, and K. I. Nakayama. 2009. 'CHD8 suppresses p53-mediated apoptosis through histone H1 recruitment during early embryogenesis', *Nat Cell Biol*, 11: 172-82.
- Nitarska, J., J. G. Smith, W. T. Sherlock, M. M. Hillege, A. Nott, W. D. Barshop, A. A. Vashisht, J. A. Wohlschlegel, R. Mitter, and A. Riccio. 2016. 'A Functional Switch of NuRD Chromatin Remodeling Complex Subunits Regulates Mouse Cortical Development', *Cell reports*, 17: 1683-98.
- Nodelman, I. M., K. C. Horvath, R. F. Levendosky, J. Winger, R. Ren, A. Patel, M. Li, M. D. Wang, E. Roberts, and G. D. Bowman. 2016. 'The Chd1 chromatin remodeler can sense both entry and exit sides of the nucleosome', *Nucleic Acids Res*, 44: 7580-91.
- Okada, M., K. Okawa, T. Isobe, and T. Fukagawa. 2009. 'CENP-H-containing complex facilitates centromere deposition of CENP-A in cooperation with FACT and CHD1', *Mol Biol Cell*, 20: 3986-95.

- Okuda, M., M. Horikoshi, and Y. Nishimura. 2007. 'Structural polymorphism of chromodomains in Chd1', *J Mol Biol*, 365: 1047-62.
- Oliver, S. S., C. A. Musselman, R. Srinivasan, J. P. Svaren, T. G. Kutateladze, and J. M. Denu. 2012. 'Multivalent Recognition of Histone Tails by the PHD Fingers of CHD5', *Biochemistry*, 51: 6534-44.
- Oliveros, J. C., M. Franch, D. Tabas-Madrid, D. San-Leon, L. Montoliu, P. Cubas, and F. Pazos. 2016. 'Breaking-Cas-interactive design of guide RNAs for CRISPR-Cas experiments for ENSEMBL genomes', *Nucleic Acids Res*, 44: W267-71.
- Ota, S., Y. Hisano, Y. Ikawa, and A. Kawahara. 2014. 'Multiple genome modifications by the CRISPR/Cas9 system in zebrafish', *Genes Cells*, 19: 555-64.
- Ota, S., Y. Hisano, M. Muraki, K. Hoshijima, T. J. Dahlem, D. J. Grunwald, Y. Okada, and A. Kawahara. 2013. 'Efficient identification of TALEN-mediated genome modifications using heteroduplex mobility assays', *Genes Cells*, 18: 450-8.
- Ota, S., and A. Kawahara. 2014. 'Zebrafish: a model vertebrate suitable for the analysis of human genetic disorders', *Congenit Anom (Kyoto)*, 54: 8-11.
- Pan, Q., O. Shai, L. J. Lee, B. J. Frey, and B. J. Blencowe. 2008. 'Deep surveying of alternative splicing complexity in the human transcriptome by high-throughput sequencing', *Nat Genet*, 40: 1413-5.
- Pang, S. C., H. P. Wang, Z. Y. Zhu, and Y. H. Sun. 2015. 'Transcriptional Activity and DNA Methylation Dynamics of the Gal4/UAS System in Zebrafish', *Mar Biotechnol (NY)*, 17: 593-603.
- Patel, A., J. N. McKnight, P. Genzor, and G. D. Bowman. 2011. 'Identification of residues in chromodomain helicase DNA-binding protein 1 (Chd1) required for coupling ATP hydrolysis to nucleosome sliding', *J Biol Chem*, 286: 43984-93.
- Patton, E. E., H. R. Widlund, J. L. Kutok, K. R. Kopani, J. F. Amatruda, R. D. Murphey, S. Berghmans, E. A. Mayhall, D. Traver, C. D. Fletcher, J. C. Aster, S. R. Granter, A. T. Look, C. Lee, D. E. Fisher, and L. I. Zon. 2005. 'BRAF mutations are sufficient to promote nevi formation and cooperate with p53 in the genesis of melanoma', *Curr Biol*, 15: 249-54.

- Paul, S., A. Kuo, T. Schalch, H. Vogel, L. Joshua-Tor, W. R. McCombie, O. Gozani, M. Hammell, and A. A. Mills. 2013a. 'Chd5 requires PHD-mediated histone 3 binding for tumor suppression', *Cell Rep*, 3: 92-102.
- . 2013b. 'Chd5 Requires PHD-Mediated Histone 3 Binding for Tumor Suppression', *Cell reports*, 3: 92-102.
- Pauli, S., N. von Velsen, P. Burfeind, M. Steckel, J. Manz, A. Buchholz, W. Borozdin, and J. Kohlhase. 2012. 'CHD7 mutations causing CHARGE syndrome are predominantly of paternal origin', *Clin Genet*, 81: 234-9.
- Pei, D., W. Luther, W. Wang, B. H. Paw, R. A. Stewart, and R. E. George. 2013. 'Distinct neuroblastoma-associated alterations of PHOX2B impair sympathetic neuronal differentiation in zebrafish models', *PLoS Genet*, 9: e1003533.
- Pensold, D., and G. Zimmer. 2018. 'Single-Cell Transcriptomics Reveals Regulators of Neuronal Migration and Maturation During Brain Development', *J Exp Neurosci*, 12: 1179069518760783.
- Perreault, M. L., A. Hasbi, B. F. O'Dowd, and S. R. George. 2014. 'Heteromeric dopamine receptor signaling complexes: emerging neurobiology and disease relevance', *Neuropsychopharmacology*, 39: 156-68.
- Persson, J., and K. Ekwall. 2010. 'Chd1 remodelers maintain open chromatin and regulate the epigenetics of differentiation', *Exp Cell Res*, 316: 1316-23.
- Phelps, M., and E. Chen. 2016. 'Zebrafish Rhabdomyosarcoma', *Adv Exp Med Biol*, 916: 371-89.
- Pisansky, M. T., A. E. Young, M. B. O'Connor, Gottesman, II, A. Bagchi, and J. C. Gewirtz. 2017. 'Mice lacking the chromodomain helicase DNA-binding 5 chromatin remodeler display autism-like characteristics', *Transl Psychiatry*, 7: e1152.
- Podhraski, V., B. Campo-Fernandez, H. Worle, P. Piatti, H. Niederegger, G. Bock, D. V. Fyodorov, and A. Lusser. 2010. 'CenH3/CID incorporation is not dependent on the chromatin assembly factor CHD1 in *Drosophila*', *PLoS One*, 5: e10120.
- Pointner, J., J. Persson, P. Prasad, U. Norman-Axelsson, A. Stralfors, O. Khorosjutina, N. Krietenstein, J. P. Svensson, K. Ekwall, and P. Korber. 2012. 'CHD1 remodelers regulate nucleosome spacing in vitro and align nucleosomal arrays over gene coding regions in *S. pombe*', *The EMBO journal*, 31: 4388-403.

- Polach, K. J., and J. Widom. 1995. 'Mechanism of protein access to specific DNA sequences in chromatin: a dynamic equilibrium model for gene regulation', *J Mol Biol*, 254: 130-49.
- Potts, R. C., P. Zhang, A. L. Wurster, P. Precht, M. R. Mughal, W. H. Wood, 3rd, Y. Zhang, K. G. Becker, M. P. Mattson, and M. J. Pazin. 2011. 'CHD5, a Brain-Specific Paralog of Mi2 Chromatin Remodeling Enzymes, Regulates Expression of Neuronal Genes', *PLoS ONE*, 6: e24515.
- Prakash, K., and D. Fournier. 2018. 'Evidence for the implication of the histone code in building the genome structure', *Biosystems*, 164: 49-59.
- Pray-Grant, M. G., J. A. Daniel, D. Schieltz, J. R. Yates, 3rd, and P. A. Grant. 2005. 'Chd1 chromodomain links histone H3 methylation with SAGA- and SLIK-dependent acetylation', *Nature*, 433: 434-8.
- Prykhozhij, S. V., V. Rajan, and J. N. Berman. 2016. 'A Guide to Computational Tools and Design Strategies for Genome Editing Experiments in Zebrafish Using CRISPR/Cas9', *Zebrafish*, 13: 70-3.
- Qiu, Y., R. F. Levendosky, S. Chakravarthy, A. Patel, G. D. Bowman, and S. Myong. 2017. 'The Chd1 Chromatin Remodeler Shifts Nucleosomal DNA Bidirectionally as a Monomer', *Mol Cell*, 68: 76-88 e6.
- Quan, J., G. Adelmant, J. A. Marto, A. T. Look, and T. Yusufzai. 2014. 'The Chromatin Remodeling Factor CHD5 Is a Transcriptional Repressor of WEE1', *PLoS ONE*, 9: e108066.
- Quan, J., and T. Yusufzai. 2014. 'The Tumor Suppressor Chromodomain Helicase DNA-binding Protein 5 (CHD5) Remodels Nucleosomes by Unwrapping', *J Biol Chem*, 289: 20717-26.
- Radman-Livaja, M., T. K. Quan, L. Valenzuela, J. A. Armstrong, T. van Welsem, T. Kim, L. J. Lee, S. Buratowski, F. van Leeuwen, O. J. Rando, and G. A. Hartzog. 2012. 'A key role for Chd1 in histone H3 dynamics at the 3' ends of long genes in yeast', *Plos Genetics*, 8: e1002811.
- Ramirez, J., C. Dege, T. G. Kutateladze, and J. Hagman. 2012. 'MBD2 and multiple domains of CHD4 are required for transcriptional repression by Mi-2/NuRD complexes', *Molecular and cellular biology*.

- Ran, F. A., P. D. Hsu, C. Y. Lin, J. S. Gootenberg, S. Konermann, A. E. Trevino, D. A. Scott, A. Inoue, S. Matoba, Y. Zhang, and F. Zhang. 2013. 'Double Nicking by RNA-Guided CRISPR Cas9 for Enhanced Genome Editing Specificity', *Cell*, 154: 1380-9.
- Ran, F. A., P. D. Hsu, J. Wright, V. Agarwala, D. A. Scott, and F. Zhang. 2013. 'Genome engineering using the CRISPR-Cas9 system', *Nat Protoc*, 8: 2281-308.
- Reddington, J. P., S. Pennings, and R. R. Meehan. 2013. 'Non-canonical functions of the DNA methylome in gene regulation', *Biochem J*, 451: 13-23.
- Reeve, J. N. 2003. 'Archaeal chromatin and transcription', *Mol Microbiol*, 48: 587-98.
- Ren, X., Z. Yang, J. Xu, J. Sun, D. Mao, Y. Hu, S. J. Yang, H. H. Qiao, X. Wang, Q. Hu, P. Deng, L. P. Liu, J. Y. Ji, J. B. Li, and J. Q. Ni. 2014. 'Enhanced specificity and efficiency of the CRISPR/Cas9 system with optimized sgRNA parameters in Drosophila', *Cell Rep*, 9: 1151-62.
- Reynolds, N., M. Salmon-Divon, H. Dvinge, A. Hynes-Allen, G. Balasooriya, D. Leaford, A. Behrens, P. Bertone, and B. Hendrich. 2012. 'NuRD-mediated deacetylation of H3K27 facilitates recruitment of Polycomb Repressive Complex 2 to direct gene repression', *The EMBO journal*, 31: 593-605.
- Rhee, H. S., and B. F. Pugh. 2012. 'Genome-wide structure and organization of eukaryotic pre-initiation complexes', *Nature*, 483: 295-301.
- Ribas, J., and J. Boix. 2004. 'Cell differentiation, caspase inhibition, and macromolecular synthesis blockage, but not BCL-2 or BCL-XL proteins, protect SH-SY5Y cells from apoptosis triggered by two CDK inhibitory drugs', *Exp Cell Res*, 295: 9-24.
- Ribas, J., J. Boix, and L. Meijer. 2006. '(R)-roscovitine (CYC202, Seliciclib) sensitizes SH-SY5Y neuroblastoma cells to nutlin-3-induced apoptosis', *Exp Cell Res*, 312: 2394-400.
- Ritchie, M. E., B. Phipson, D. Wu, Y. Hu, C. W. Law, W. Shi, and G. K. Smyth. 2015. 'limma powers differential expression analyses for RNA-sequencing and microarray studies', *Nucleic Acids Res*, 43: e47.
- Robinson, M. D., D. J. McCarthy, and G. K. Smyth. 2010. 'edgeR: a Bioconductor package for differential expression analysis of digital gene expression data', *Bioinformatics*, 26: 139-40.
- Roidl, D., and C. Hacker. 2014. 'Histone methylation during neural development', *Cell Tissue Res*, 356: 539-52.

- Rosen, J. N., M. F. Sweeney, and J. D. Mably. 2009. 'Microinjection of zebrafish embryos to analyze gene function', *J Vis Exp*.
- Rossi, A., Z. Kontarakis, C. Gerri, H. Nolte, S. Holper, M. Kruger, and D. Y. Stainier. 2015. 'Genetic compensation induced by deleterious mutations but not gene knockdowns', *Nature*, 524: 230-3.
- Roy, P., B. Kumar, A. Shende, A. Singh, A. Meena, R. Ghosal, M. Ranganathan, and A. Bandyopadhyay. 2013. 'A genome-wide screen indicates correlation between differentiation and expression of metabolism related genes', *PLoS One*, 8: e63670.
- Ryan, D. P., R. Sundaramoorthy, D. Martin, V. Singh, and T. Owen-Hughes. 2011. 'The DNA-binding domain of the Chd1 chromatin-remodelling enzyme contains SANT and SLIDE domains', *EMBO J*, 30: 2596-609.
- Sallinen, V., M. Sundvik, I. Reenila, N. Peitsaro, D. Khrustalyov, O. Anichtchik, G. Toleikyte, J. Kaslin, and P. Panula. 2009. 'Hyperserotonergic phenotype after monoamine oxidase inhibition in larval zebrafish', *J Neurochem*, 109: 403-15.
- Samarut, E., A. Lissouba, and P. Drapeau. 2016. 'A simplified method for identifying early CRISPR-induced indels in zebrafish embryos using High Resolution Melting analysis', *BMC Genomics*, 17: 547.
- Sanchez, A., and J. F. Amatruda. 2016. 'Zebrafish Germ Cell Tumors', *Adv Exp Med Biol*, 916: 479-94.
- Sander, J. D., and J. K. Joung. 2014. 'CRISPR-Cas systems for editing, regulating and targeting genomes', *Nat Biotechnol*, 32: 347-55.
- Sandman, K., and J. N. Reeve. 2006. 'Archaeal histones and the origin of the histone fold', *Curr Opin Microbiol*, 9: 520-5.
- Sanjana, N. E., O. Shalem, and F. Zhang. 2014. 'Improved vectors and genome-wide libraries for CRISPR screening', *Nat Methods*, 11: 783-84.
- Schmidt, R., U. Strahle, and S. Scholpp. 2013. 'Neurogenesis in zebrafish - from embryo to adult', *Neural development*, 8: 3.
- Schones, D. E., K. Cui, S. Cuddapah, T. Y. Roh, A. Barski, Z. Wang, G. Wei, and K. Zhao. 2008. 'Dynamic regulation of nucleosome positioning in the human genome', *Cell*, 132: 887-98.

- Schulte-Merker, S., and D. Y. Stainier. 2014. 'Out with the old, in with the new: reassessing morpholino knockdowns in light of genome editing technology', *Development*, 141: 3103-4.
- Schwartz, S., E. Meshorer, and G. Ast. 2009. 'Chromatin organization marks exon-intron structure', *Nat Struct Mol Biol*, 16: 990-5.
- Sertori, R., M. Trengove, F. Basheer, A. C. Ward, and C. Liongue. 2016. 'Genome editing in zebrafish: a practical overview', *Brief Funct Genomics*, 15: 322-30.
- Sharma, A., K. R. Jenkins, A. Heroux, and G. D. Bowman. 2011. 'Crystal structure of the chromodomain helicase DNA-binding protein 1 (Chd1) DNA-binding domain in complex with DNA', *J Biol Chem*, 286: 42099-104.
- Sharova, L. V., A. A. Sharov, Y. Piao, C. A. Stagg, T. Amano, Y. Qian, D. Dudekula, D. Schlessinger, and M. S. Ko. 2016. 'Emergence of undifferentiated colonies from mouse embryonic stem cells undergoing differentiation by retinoic acid treatment', *In Vitro Cell Dev Biol Anim*, 52: 616-24.
- Shen, B., W. Zhang, J. Zhang, J. Zhou, J. Wang, L. Chen, L. Wang, A. Hodgkins, V. Iyer, X. Huang, and W. C. Skarnes. 2014. 'Efficient genome modification by CRISPR-Cas9 nickase with minimal off-target effects', *Nat Methods*, 11: 399-402.
- Shen, Y., M. Devic, L. Lepiniec, and D. X. Zhou. 2015. 'Chromodomain, Helicase and DNA-binding CHD1 protein, CHR5, are involved in establishing active chromatin state of seed maturation genes', *Plant Biotechnol J*.
- Shim, Y. S., Y. Choi, K. Kang, K. Cho, S. Oh, J. Lee, S. I. Grewal, and D. Lee. 2012. 'Hrp3 controls nucleosome positioning to suppress non-coding transcription in eu- and heterochromatin', *The EMBO journal*, 31: 4375-87.
- Shrivastav, M., L. P. De Haro, and J. A. Nickoloff. 2008. 'Regulation of DNA double-strand break repair pathway choice', *Cell Res*, 18: 134-47.
- Siggins, L., L. Cordeddu, M. Ronnerblad, A. Lennartsson, and K. Ekwall. 2015. 'Transcription-coupled recruitment of human CHD1 and CHD2 influences chromatin accessibility and histone H3 and H3.3 occupancy at active chromatin regions', *Epigenetics Chromatin*, 8: 4.

- Simic, R., D. L. Lindstrom, H. G. Tran, K. L. Roinick, P. J. Costa, A. D. Johnson, G. A. Hartzog, and K. M. Arndt. 2003. 'Chromatin remodeling protein Chd1 interacts with transcription elongation factors and localizes to transcribed genes', *Embo J*, 22: 1846-56.
- Sims, J. K., and P. A. Wade. 2011. 'SnapShot: Chromatin remodeling: CHD', *Cell*, 144: 626-26 e1.
- Sims, R. J., 3rd, C. F. Chen, H. Santos-Rosa, T. Kouzarides, S. S. Patel, and D. Reinberg. 2005. 'Human but not yeast CHD1 binds directly and selectively to histone H3 methylated at lysine 4 via its tandem chromodomains', *J Biol Chem*, 280: 41789-92.
- Singleton, M. R., M. S. Dillingham, and D. B. Wigley. 2007. 'Structure and mechanism of helicases and nucleic acid translocases', *Annu Rev Biochem*, 76: 23-50.
- Sirinakis, G., C. R. Clapier, Y. Gao, R. Viswanathan, B. R. Cairns, and Y. Zhang. 2011. 'The RSC chromatin remodelling ATPase translocates DNA with high force and small step size', *The EMBO journal*, 30: 2364-72.
- Skene, P. J., A. E. Hernandez, M. Groudine, and S. Henikoff. 2014. 'The nucleosomal barrier to promoter escape by RNA polymerase II is overcome by the chromatin remodeler Chd1', *Elife*, 3: e02042.
- Smolle, M., S. Venkatesh, M. M. Gogol, H. Li, Y. Zhang, L. Florens, M. P. Washburn, and J. L. Workman. 2012. 'Chromatin remodelers Isw1 and Chd1 maintain chromatin structure during transcription by preventing histone exchange', *Nature structural & molecular biology*, 19: 884-92.
- Sokpor, G., Y. Xie, J. Rosenbusch, and T. Tuoc. 2017. 'Chromatin Remodeling BAF (SWI/SNF) Complexes in Neural Development and Disorders', *Front Mol Neurosci*, 10: 243.
- Sorlien, E. L., M. A. Witucki, and J. Ogas. 2018. 'Efficient Production and Identification of CRISPR/Cas9-generated Gene Knockouts in the Model System *Danio rerio*', *J Vis Exp*.
- Sperry, E. D., E. A. Hurd, M. A. Durham, E. N. Reamer, A. B. Stein, and D. M. Martin. 2014. 'The chromatin remodeling protein CHD7, mutated in CHARGE syndrome, is necessary for proper craniofacial and tracheal development', *Dev Dyn*, 243: 1055-66.
- St Pierre, R., and C. Kadoch. 2017. 'Mammalian SWI/SNF complexes in cancer: emerging therapeutic opportunities', *Curr Opin Genet Dev*, 42: 56-67.
- Su, C. H., D. D., and W. Y. Tarn. 2018. 'Alternative Splicing in Neurogenesis and Brain Development', *Front Mol Biosci*, 5: 12.

- Summer, H., R. Gramer, and P. Droge. 2009. 'Denaturing urea polyacrylamide gel electrophoresis (Urea PAGE)', *J Vis Exp*.
- Sundaramoorthy, R., A. L. Hughes, H. El-Mkami, D. G. Norman, H. Ferreira, and T. Owen-Hughes. 2018. 'Structure of the chromatin remodelling enzyme Chd1 bound to a ubiquitinated nucleosome', *Elife*, 7.
- Suster, M. L., G. Abe, A. Schouw, and K. Kawakami. 2011. 'Transposon-mediated BAC transgenesis in zebrafish', *Nat Protoc*, 6: 1998-2021.
- Swygert, S. G., and C. L. Peterson. 2014. 'Chromatin dynamics: interplay between remodeling enzymes and histone modifications', *Biochim Biophys Acta*, 1839: 728-36.
- Tahiliani, M., K. P. Koh, Y. Shen, W. A. Pastor, H. Bandukwala, Y. Brudno, S. Agarwal, L. M. Iyer, D. R. Liu, L. Aravind, and A. Rao. 2009. 'Conversion of 5-methylcytosine to 5-hydroxymethylcytosine in mammalian DNA by MLL partner TET1', *Science*, 324: 930-5.
- Tai, H. H., M. Geisterfer, J. C. Bell, M. Moniwa, J. R. Davie, L. Boucher, and M. W. McBurney. 2003. 'CHD1 associates with NCoR and histone deacetylase as well as with RNA splicing proteins', *Biochem Biophys Res Commun*, 308: 170-6.
- Talbert, P. B., and S. Henikoff. 2010. 'Histone variants--ancient wrap artists of the epigenome', *Nat Rev Mol Cell Biol*, 11: 264-75.
- . 2017. 'Histone variants on the move: substrates for chromatin dynamics', *Nat Rev Mol Cell Biol*, 18: 115-26.
- Talbot, J. C., and S. L. Amacher. 2014. 'A streamlined CRISPR pipeline to reliably generate zebrafish frameshifting alleles', *Zebrafish*, 11: 583-5.
- Termglinchan, V., T. Seeger, C. Chen, J. C. Wu, and I. Karakikes. 2017. 'Efficient Genome Editing in Induced Pluripotent Stem Cells with Engineered Nucleases In Vitro', *Methods Mol Biol*, 1521: 55-68.
- Thisse, B., and C. Thisse. 2014. 'In situ hybridization on whole-mount zebrafish embryos and young larvae', *Methods Mol Biol*, 1211: 53-67.
- Thisse, C., and B. Thisse. 2008. 'High-resolution in situ hybridization to whole-mount zebrafish embryos', *Nat Protoc*, 3: 59-69.
- Thompson, B. A., V. Tremblay, G. Lin, and D. A. Bochar. 2008. 'CHD8 is an ATP-dependent chromatin remodeling factor that regulates beta-catenin target genes', *Mol Cell Biol*, 28: 3894-904.

- Thompson, P. M., T. Gotoh, M. Kok, P. S. White, and G. M. Brodeur. 2003. 'CHD5, a new member of the chromodomain gene family, is preferentially expressed in the nervous system', *Oncogene*, 22: 1002-11.
- Tilgner, H., D. G. Knowles, R. Johnson, C. A. Davis, S. Chakraborty, S. Djebali, J. Curado, M. Snyder, T. R. Gingeras, and R. Guigo. 2012. 'Deep sequencing of subcellular RNA fractions shows splicing to be predominantly co-transcriptional in the human genome but inefficient for lncRNAs', *Genome Res*, 22: 1616-25.
- Torchy, M. P., A. Hamiche, and B. P. Klaholz. 2015. 'Structure and function insights into the NuRD chromatin remodeling complex', *Cell Mol Life Sci*, 72: 2491-507.
- Torigoe, S. E., A. Patel, M. T. Khuong, G. D. Bowman, and J. T. Kadonaga. 2013. 'ATP-dependent chromatin assembly is functionally distinct from chromatin remodeling', *Elife*, 2: e00863.
- Torrado, M., J. K. K. Low, A. P. G. Silva, J. W. Schmidberger, M. Sana, M. Sharifi Tabar, M. E. Isilak, C. S. Winning, C. Kwong, M. J. Bedward, M. J. Sperlazza, D. C. Williams, Jr., N. E. Shepherd, and J. P. Mackay. 2017. 'Refinement of the subunit interaction network within the nucleosome remodelling and deacetylase (NuRD) complex', *FEBS J*, 284: 4216-32.
- Touat-Todeschini, L., E. Hiriart, and A. Verdel. 2012. 'Nucleosome positioning and transcription: fission yeast CHD remodellers make their move', *EMBO J*, 31: 4371-2.
- Tran, H. G., D. J. Steger, V. R. Iyer, and A. D. Johnson. 2000. 'The chromo domain protein chd1p from budding yeast is an ATP-dependent chromatin-modifying factor', *Embo J*, 19: 2323-31.
- Tran, S., D. Chatterjee, and R. Gerlai. 2015. 'An integrative analysis of ethanol tolerance and withdrawal in zebrafish (*Danio rerio*)', *Behav Brain Res*, 276: 161-70.
- Trujillo, C. A., T. T. Schwindt, A. H. Martins, J. M. Alves, L. E. Mello, and H. Ulrich. 2009. 'Novel perspectives of neural stem cell differentiation: from neurotransmitters to therapeutics', *Cytometry A*, 75: 38-53.
- Tsukiyama, T., J. Palmer, C. C. Landel, J. Shiloach, and C. Wu. 1999. 'Characterization of the imitation switch subfamily of ATP-dependent chromatin-remodeling factors in *Saccharomyces cerevisiae*', *Genes Dev*, 13: 686-97.

- Uetake, H., K. Oka, and Y. Niki. 2011. 'Stable transformation and cloning mediated by piggyBac vector and RNA interference knockdown of *Drosophila* ovarian cell line', *In Vitro Cell Dev Biol Anim*, 47: 689-94.
- Urban, N., and F. Guillemot. 2014. 'Neurogenesis in the embryonic and adult brain: same regulators, different roles', *Front Cell Neurosci*, 8: 396.
- Urnov, F. D., E. J. Rebar, M. C. Holmes, H. S. Zhang, and P. D. Gregory. 2010. 'Genome editing with engineered zinc finger nucleases', *Nat Rev Genet*, 11: 636-46.
- van Dijk, E. L., H. Auger, Y. Jaszczyszyn, and C. Thermes. 2014. 'Ten years of next-generation sequencing technology', *Trends Genet*, 30: 418-26.
- Varshney, G. K., B. Carrington, W. Pei, K. Bishop, Z. Chen, C. Fan, L. Xu, M. Jones, M. C. LaFave, J. Ledin, R. Sood, and S. M. Burgess. 2016. 'A high-throughput functional genomics workflow based on CRISPR/Cas9-mediated targeted mutagenesis in zebrafish', *Nat Protoc*, 11: 2357-75.
- Varshney, G. K., R. Sood, and S. M. Burgess. 2015. 'Understanding and Editing the Zebrafish Genome', *Adv Genet*, 92: 1-52.
- Vejnar, C. E., M. A. Moreno-Mateos, D. Cifuentes, A. A. Bazzini, and A. J. Giraldez. 2016. 'Optimized CRISPR-Cas9 System for Genome Editing in Zebrafish', *Cold Spring Harb Protoc*, 2016: pdb prot086850.
- Venkatesh, S., M. Smolle, H. Li, M. M. Gogol, M. Saint, S. Kumar, K. Natarajan, and J. L. Workman. 2012. 'Set2 methylation of histone H3 lysine 36 suppresses histone exchange on transcribed genes', *Nature*, 489: 452-5.
- Vestin, A., and A. A. Mills. 2013. 'The tumor suppressor Chd5 is induced during neuronal differentiation in the developing mouse brain', *Gene Expr Patterns*, 13: 482-9.
- Vinogradov, A. E. 2005. 'Genome size and chromatin condensation in vertebrates', *Chromosoma*, 113: 362-9.
- Vuong, C. K., D. L. Black, and S. Zheng. 2016. 'The neurogenetics of alternative splicing', *Nat Rev Neurosci*, 17: 265-81.
- Walfridsson, J., P. Bjerling, M. Thalen, E. J. Yoo, S. D. Park, and K. Ekwall. 2005. 'The CHD remodeling factor Hrp1 stimulates CENP-A loading to centromeres', *Nucleic Acids Res*, 33: 2868-79.

- Walfridsson, J., O. Khorosjutina, P. Matikainen, C. M. Gustafsson, and K. Ekwall. 2007. 'A genome-wide role for CHD remodelling factors and Nap1 in nucleosome disassembly', *Embo J*, 26: 2868-79.
- Wang, E. T., R. Sandberg, S. Luo, I. Khrebtkova, L. Zhang, C. Mayr, S. F. Kingsmore, G. P. Schroth, and C. B. Burge. 2008. 'Alternative isoform regulation in human tissue transcriptomes', *Nature*, 456: 470-6.
- Wang, H., H. Yang, C. S. Shivalila, M. M. Dawlaty, A. W. Cheng, F. Zhang, and R. Jaenisch. 2013. 'One-step generation of mice carrying mutations in multiple genes by CRISPR/Cas-mediated genome engineering', *Cell*, 153: 910-8.
- Wang, L., S. He, Y. Tu, P. Ji, J. Zong, J. Zhang, F. Feng, J. Zhao, G. Gao, and Y. Zhang. 2013. 'Downregulation of chromatin remodeling factor CHD5 is associated with a poor prognosis in human glioma', *J Clin Neurosci*, 20: 958-63.
- Wang, T., J. J. Wei, D. M. Sabatini, and E. S. Lander. 2014. 'Genetic screens in human cells using the CRISPR-Cas9 system', *Science*, 343: 80-4.
- Wang, Y., P. A. Loomis, R. P. Zinkowski, and L. I. Binder. 1993. 'A novel tau transcript in cultured human neuroblastoma cells expressing nuclear tau', *J Cell Biol*, 121: 257-67.
- Wang, Z., B. Tang, Y. He, and P. Jin. 2016. 'DNA methylation dynamics in neurogenesis', *Epigenomics*, 8: 401-14.
- Watson, A. A., P. Mahajan, H. D. Mertens, M. J. Deery, W. Zhang, P. Pham, X. Du, T. Bartke, C. Edlich, G. Berridge, Y. Chen, N. A. Burgess-Brown, T. Kouzarides, N. Wiechens, T. Owen-Hughes, D. I. Svergun, O. Gileadi, and E. D. Laue. 2012. 'The PHD and Chromo Domains Regulate the ATPase Activity of the Human Chromatin Remodeler CHD4', *Journal of molecular biology*, 422: 3-17.
- White, R. J., J. E. Collins, I. M. Sealy, N. Wali, C. M. Dooley, Z. Digby, D. L. Stemple, D. N. Murphy, K. Billis, T. Hourlier, A. Fullgrabe, M. P. Davis, A. J. Enright, and E. M. Busch-Nentwich. 2017. 'A high-resolution mRNA expression time course of embryonic development in zebrafish', *Elife*, 6.
- Williams, C. J., T. Naito, P. G. Arco, J. R. Seavitt, S. M. Cashman, B. De Souza, X. Qi, P. Keables, U. H. Von Andrian, and K. Georgopoulos. 2004. 'The chromatin remodeler Mi-2beta is required for CD4 expression and T cell development', *Immunity*, 20: 719-33.

- Wolffe, A. P., F. D. Urnov, and D. Guschin. 2000. 'Co-repressor complexes and remodelling chromatin for repression', *Biochem Soc Trans*, 28: 379-86.
- Wong, R. R., L. K. Chan, T. P. Tsang, C. W. Lee, T. H. Cheung, S. F. Yim, N. S. Siu, S. N. Lee, M. Y. Yu, S. S. Chim, Y. F. Wong, and T. K. Chung. 2011a. 'CHD5 Downregulation Associated with Poor Prognosis in Epithelial Ovarian Cancer', *Gynecologic and obstetric investigation*, 72: 203-7.
- . 2011b. 'CHD5 Downregulation Associated with Poor Prognosis in Epithelial Ovarian Cancer', *Gynecol Obstet Invest*, 72: 203-7.
- Woodage, T., M. A. Basrai, A. D. Baxevanis, P. Hieter, and F. S. Collins. 1997. 'Characterization of the CHD family of proteins', *Proc Natl Acad Sci U S A*, 94: 11472-7.
- Woodard, L. E., and M. H. Wilson. 2015. 'piggyBac-ing models and new therapeutic strategies', *Trends Biotechnol*, 33: 525-33.
- Wu, H., J. Zhao, B. Fu, S. Yin, C. Song, J. Zhang, S. Zhao, and Y. Zhang. 2017. 'Retinoic acid-induced upregulation of miR-219 promotes the differentiation of embryonic stem cells into neural cells', *Cell Death Dis*, 8: e2953.
- Wu, X., Z. Zhu, W. Li, X. Fu, D. Su, L. Fu, Z. Zhang, A. Luo, X. Sun, and J. T. Dong. 2012. 'Chromodomain helicase DNA binding protein 5 plays a tumor suppressor role in human breast cancer', *Breast cancer research : BCR*, 14: R73.
- Wu, X., Z. Zhu, W. Li, X. Fu, D. Su, L. Fu, Z. Zhang, A. Luo, X. Sun, L. Fu, and J. T. Dong. 2012. 'Chromodomain helicase DNA binding protein 5 plays a tumor suppressor role in human breast cancer', *Breast Cancer Res*, 14: R73.
- Xiao, A., Z. Wang, Y. Hu, Y. Wu, Z. Luo, Z. Yang, Y. Zu, W. Li, P. Huang, X. Tong, Z. Zhu, S. Lin, and B. Zhang. 2013. 'Chromosomal deletions and inversions mediated by TALENs and CRISPR/Cas in zebrafish', *Nucleic Acids Res*, 41: e141.
- Xie, S. L., W. P. Bian, C. Wang, M. Junaid, J. X. Zou, and D. S. Pei. 2016. 'A novel technique based on in vitro oocyte injection to improve CRISPR/Cas9 gene editing in zebrafish', *Sci Rep*, 6: 34555.
- Xu, Q. 1999. 'Microinjection into zebrafish embryos', *Methods Mol Biol*, 127: 125-32.
- Xue, Y., J. Wong, G. T. Moreno, M. K. Young, J. Cote, and W. Wang. 1998a. 'NURD, a novel complex with both ATP-dependent chromatin-remodeling and histone deacetylase activities', *Mol Cell*, 2: 851-61.

- . 1998b. 'NURD, a novel complex with both ATP-dependent chromatin-remodeling and histone deacetylase activities', *Mol. Cell*, 2: 851-61.
- Yang, J., C. Wu, I. Stefanescu, and A. Horowitz. 2017. 'Analysis of Retinoic Acid-induced Neural Differentiation of Mouse Embryonic Stem Cells in Two and Three-dimensional Embryoid Bodies', *J Vis Exp*.
- Yao, B., K. M. Christian, C. He, P. Jin, G. L. Ming, and H. Song. 2016. 'Epigenetic mechanisms in neurogenesis', *Nat Rev Neurosci*, 17: 537-49.
- Yao, B., and P. Jin. 2014. 'Unlocking epigenetic codes in neurogenesis', *Genes Dev*, 28: 1253-71.
- Yildirim, O., R. Li, J. H. Hung, P. B. Chen, X. Dong, L. S. Ee, Z. Weng, O. J. Rando, and T. G. Fazio. 2011. 'Mbd3/NURD complex regulates expression of 5-hydroxymethylcytosine marked genes in embryonic stem cells', *Cell*, 147: 1498-510.
- Yin, L., L. E. Jao, and W. Chen. 2015. 'Generation of Targeted Mutations in Zebrafish Using the CRISPR/Cas System', *Methods Mol Biol*, 1332: 205-17.
- Yin, L., L. A. Maddison, and W. Chen. 2016. 'Multiplex conditional mutagenesis in zebrafish using the CRISPR/Cas system', *Methods Cell Biol*, 135: 3-17.
- Yu, C., Y. Zhang, S. Yao, and Y. Wei. 2014. 'A PCR based protocol for detecting indel mutations induced by TALENs and CRISPR/Cas9 in zebrafish', *PLoS ONE*, 9: e98282.
- Yusa, K. 2015. 'piggyBac Transposon', *Microbiol Spectr*, 3: MDNA3-0028-2014.
- Zentner, G. E., T. Tsukiyama, and S. Henikoff. 2013. 'ISWI and CHD Chromatin Remodelers Bind Promoters but Act in Gene Bodies', *Plos Genetics*, 9: e1003317.
- Zhang, D., Y. Jing, Z. Jiang, and R. Lin. 2014. 'The Chromatin-Remodeling Factor PICKLE Integrates Brassinosteroid and Gibberellin Signaling during Skotomorphogenic Growth in Arabidopsis', *Plant Cell*, 26: 2472-85.
- Zhang, H., B. Bishop, W. Ringenberg, W. M. Muir, and J. Ogas. 2012. 'The CHD3 Remodeler PICKLE Associates with Genes Enriched for Trimethylation of Histone H3 Lysine 27', *Plant Physiology*, 159: 418-32.
- Zhang, H., S. D. Rider, Jr., J. T. Henderson, M. Fountain, K. Chuang, V. Kandachar, A. Simons, H. J. Edenberg, J. Romero-Severson, W. M. Muir, and J. Ogas. 2008. 'The CHD3 remodeler PICKLE promotes trimethylation of histone H3 lysine 27', *J Biol Chem*, 283: 22637-48.

- Zhao, R., F. Meng, N. Wang, W. Ma, and Q. Yan. 2014. 'Silencing of CHD5 Gene by Promoter Methylation in Leukemia', *PLoS ONE*, 9: e85172.
- Zhao, R., N. Wang, H. Huang, W. Ma, and Q. Yan. 2014. 'CHD5 a tumour suppressor is epigenetically silenced in hepatocellular carcinoma', *Liver Int*, 34: e151-60.
- Zhao, R., Q. Yan, J. Lv, H. Huang, W. Zheng, B. Zhang, and W. Ma. 2012. 'CHD5, a tumor suppressor that is epigenetically silenced in lung cancer', *Lung cancer*, 76: 324-31.
- Zhou, C. Y., S. L. Johnson, N. I. Gamarra, and G. J. Narlikar. 2016. 'Mechanisms of ATP-Dependent Chromatin Remodeling Motors', *Annu Rev Biophys*, 45: 153-81.
- Zhu, D., J. Fang, Y. Li, and J. Zhang. 2009. 'Mbd3, a component of NuRD/Mi-2 complex, helps maintain pluripotency of mouse embryonic stem cells by repressing trophectoderm differentiation', *PLoS One*, 4: e7684.
- Zhu, S., J. S. Lee, F. Guo, J. Shin, A. R. Perez-Atayde, J. L. Kutok, S. J. Rodig, D. S. Neuberg, D. Helman, H. Feng, R. A. Stewart, W. Wang, R. E. George, J. P. Kanki, and A. T. Look. 2012. 'Activated ALK collaborates with MYCN in neuroblastoma pathogenesis', *Cancer Cell*, 21: 362-73.
- Zhu, S., and A. Thomas Look. 2016. 'Neuroblastoma and Its Zebrafish Model', *Adv Exp Med Biol*, 916: 451-78.
- Zhu, S., X. Zhang, N. Weichert-Leahey, Z. Dong, C. Zhang, G. Lopez, T. Tao, S. He, A. C. Wood, D. Oldridge, C. Y. Ung, J. H. van Ree, A. Khan, B. M. Salazar, E. Lummertz da Rocha, M. W. Zimmerman, F. Guo, H. Cao, X. Hou, S. J. Weroha, A. R. Perez-Atayde, D. S. Neuberg, A. Meves, M. A. McNiven, J. M. van Deursen, H. Li, J. M. Maris, and A. T. Look. 2017. 'LMO1 Synergizes with MYCN to Promote Neuroblastoma Initiation and Metastasis', *Cancer Cell*, 32: 310-23 e5.
- Zhuang, T., R. A. Hess, V. Kolla, M. Higashi, T. D. Raabe, and G. M. Brodeur. 2014. 'CHD5 is required for spermiogenesis and chromatin condensation', *Mech Dev*, 131: 35-46.

VITA

Education

2013-Present	Ph.D. Biochemistry, Purdue University
2013	B.S. Microbiology, with Honors, University of Rhode Island
2013	B.A. Chemistry, with Honors, University of Rhode Island

Research Experience

In my doctoral work, I use biochemistry, molecular biology, and bioinformatic techniques to investigate the contributions of chromatin remodelers to cancer and cell fate establishment. I primarily use zebrafish as a vertebrate model in my research, and I have built and maintained my own zebrafish facility that can house 1,500 fish. After obtaining my Ph.D., I plan to pursue research opportunities to study the mechanisms that drive neurogenesis and how the neural epigenome may serve as a therapeutic target in human diseases.

Publications

IN PROGRESS: Sorlien, E; et al. “The Chromatin Remodeler CHD5 is Required for Proper Splicing During Neural Differentiation.” TBD.

IN PROGRESS: Sorlien, E; et al. “CHD Remodelers in Multicellular Eukaryotes: Comparing and Contrasting the Contribution of CHDs to Chromatin-Based Processes.” BBA. (2019).

IN PROGRESS: Sorlien, E; et al. “transcriptomics reveals a role for the chromatin remodeler chd5 in neurogenesis in the developing zebrafish brain” TBD. (2019)

Sorlien, E; Witucki, M; Ogas, J. “Efficient production and identification of CRISPR/Cas9-generated gene knockouts in the model system *Danio rerio*.” JoVE. (2018).

Lucht, B.; Potvin, J.; Sorlien, E.; Hegner, J.; “Effect of NaCl on the conversion of cellulose to glucose and levulinic acid via solid supported acid catalysis.” Tetrahedron Letters 52.44 (2011): 5891-5893.

Awards and Honors

2019	Finalist, 3-Minute Thesis Competition	Purdue University Graduate School
2018	Chromatin, Epigenetics and Gene Expression Scientific Training Program	Cold Spring Harbor Laboratory, NY
	Helmsley Scholarship (\$2,000); Dr. Clint Chapple (Dept. of Biochemistry), Supporting Scholarship (\$1,500)	
2018	Outstanding Speaker Award	Cancer Institute Symposium, Purdue
2018	Bilsland Dissertation Fellowship	Purdue Department of Biochemistry
2015-18	Bird Stair Research Grants (\$24,000 tot.)	Purdue Department of Biochemistry
	Development of a zebrafish model to examine loss of the <i>chd5</i> tumor suppressor in <i>MYC</i> -driven neuroblastoma, development of a zebrafish research facility within the Dept. of Biochemistry.	
2018	Graduate Student Travel Award	Purdue Center for Cancer Research
2017	Beach Travel Award	Purdue Department of Biochemistry
2017	Summer Research Assistantship	Purdue College of Agriculture
2017	PRF Research Fellowship	Purdue Research Foundation
	One-year Research Assistantship funding from the Purdue Research Foundation	

2013 Ross Fellowship (One-year Assistantship) Purdue Department of Biochemistry

Conference Presentations

2018 Cancer Institute Symposium West Lafayette, IN
Analysis of the contribution of the chromatin remodeler *chd5* to neural differentiation and tumor suppression in *Danio rerio*

2018 Dept. of Biochemistry Retreat West Lafayette, IN
Transcript analysis reveals loss of the chromatin remodeler *chd5* leads to neural differentiation defects in *D. rerio*

Selected Conference Posters

2018 13th International Zebrafish Conference Madison, WI
The chromatin remodeler *chd5* contributes to neural development in zebrafish

2018 Midwest Chromatin and Epigenetics Meeting West Lafayette, IN
Analysis of the remodeler and tumor suppressor *chd5* to nerve sheath tumor formation

2017 Biochemistry Horizons Symposium West Lafayette, IN
Investigation of the role of the chromatin remodeler *chd5* in neuroblastoma in *Danio rerio*

2016 Midwest Chromatin and Epigenetics Meeting Grand Rapids, MI
Development of a zebrafish model to examine loss of the *chd5* tumor suppressor

2016 Center for Cancer Research Annual Retreat West Lafayette, IN
Targeted ablation of *chd5* in zebrafish to characterize its tumor suppressive role

Student Mentoring Experience

Graduate Rotation (8 wks) Students (10): Elia Farah, Colin Carlock, Lee Stunkard, Smriti Hoda, Gilbert Kayanja, Der-Shyang Kao, Kirsten Westerhouse, Jiaxin Long, Matthew Russon, Noah Danielson

Undergraduate Researchers (8): Mary Witucki (4 yrs), Daniela Martir, Abha Gokhale, Ellen Denning (3 yrs), Taylor Sabato (2 yrs), Eleanor Logue (2 yrs), Emily Overway, Lianne Rupp

Graduate Teaching Assistantships

2018 Intro. to Biochemistry for non-majors (BCHM307-online, Purdue University)

2017 Intro. to Biochemistry (BCHM100, Purdue University)

2017 Macromolecular machines (BCHM439, Purdue University)

2016 Introductory Biochemistry course for non-majors (BCHM307, Purdue University)

Departmental Service

2017-2018 Graduate Student Organization, Founder and President

2017-2018 Student Invited Seminar Committee

2016-2018 Graduate/Postdoc Seminar Series Coordinator

2016-2017 College of Ag Graduate Student Advisory Council, BCHM Representative

References

Dr. Joseph Ogas*
Associate Professor
Purdue Biochemistry
ogas@purdue.edu
(765)-496-3969

Dr. Emily Dykhuizen
Assistant Professor
Purdue MCMP
edykhui@purdue.edu
(765)-494-4706

Dr. Ann Kirchmaier
Associate Professor
Purdue Biochemistry
akirchma@purdue.edu
(765)-494-0977

Dr. Scott Briggs
Associate Professor
Purdue Biochemistry
sdbriggs@purdue.edu
(765)-494-7897

**Graduate Research Advisor*